Editors
Prof. Canan ÖZDEMİR, PhD.
Assoc. Prof. Ali ÖZDEMİR, Ph.D.

PIONEER AND CONTEMPORARY STUDIES IN NATURAL SCIENCE AND MATHEMATICS

PIONEER AND CONTEMPORARY STUDIES IN NATURAL SCIENCE AND MATHEMATICS

Editors

Prof. Canan ÖZDEMİR, PhD.,

Assoc. Prof. Ali ÖZDEMİR, Ph.D.

Pioneer and Contemporary Studies in Natural Science and Mathematics
Editors: Prof. Canan ÖZDEMİR, PhD., Assoc. Prof. Ali ÖZDEMİR, Ph.D.

Editor in chief: Berkan Balpetek
Cover and Page Design: Duvar Design
Printing : JUNE-2023
Publisher Certificate No: 49837
ISBN:978-625-6945-88-3

853 Sokak No:13 P.10 Kemeraltı-Konak/Izmir/ Turkey
Phone: 0 232 484 88 68
www.duvaryayinlari.com
duvarkitabevi@gmail.com

TABLE OF CONTENTS

Chapter 1

Thermotropic Main Chain Liquid Crystal Polymers and Their Current Applications

Hülya ELMALI GÜLBAŞ [1]

[1] Asst.. Prof. Dr. ; Usak University, Banaz Vocational School, Department of Chemistry and Chemical Processing Technologies, Chemical Tecnology Programme. hulya.elmali@usak.edu..tr ORCID No: 0000-0002-6041-6054

ABSTRACT

Liquid crystal polymers are used in many technological and industrial applications as high-tech materials due to their unique properties. In line with the increasing industrial and technological activities, the interest in materials such as liquid crystal and liquid crystal polymer, which has a high potential to be used in technological materials in many different fields, has increased in recent years. In the studies, the design, synthesis and determination of material properties (electro-optical, thermal, etc.) of liquid crystal polymer materials with different structures.

Designing, synthesizing, characterizing structure and material properties of liquid crystal polymer materials remains one of the most important areas of interest in modern materials science. Due to their unique material properties, liquid crystal polymers can easily take place in advanced technological systems in many different fields from energy to environment and biotechnology.

Although there are studies on main chain liquid crystal polymers and their various uses in the literature, there is no systematic study on these studies conducted in recent years. In this study, some main chain polymers in the literature are summarized. Thus, it is aimed to create a basic resource for researchers who may want to work on chain liquid crystal polymers.

Keywords: Liquid Crystal, Liquid Crystal Polymers, Main Chain Liquid Crystal Polymer, poly(ether-ketone) (PEKs), poly(ester-amide) (PEA), thermotropic main chain liquid crystal copolyesters,

INTRODUCTION

1. Liquid Crystal

It has been known since ancient times that matter has three basic phases: solid, liquid and gas. However, in 1888, Austrian botanist Freidrich Reinitzer, during his examination of cholesteryl benzoate, observed that this compound first melted at 145.5 °C and became a turbid liquid, then turned into a clear liquid at 178.5 °C when heating was continued. After the discovery of this different behavior, Reinitzer sent compound samples to German physicist Otto Lehman and as a result of Lehmann's investigations with polarization microscope, it was revealed that this state was a new phase of matter and he named this new phase Liquid Crystal [1-4] . This new phase is an intermediate phase between the solid and liquid phase of the substance due to its fluidity and anisotropic properties. For this reason, Friedel named the liquid crystals as the intermediate phase (mesophase) [5]. Liquid crystal compounds form mesophase with 2 different effects. If mesophase formation occurs with the effect of temperature during the transition from solid phase to liquid phase, it is called 'thermotropic liquid crystals', and if mesophase formation occurs with the effect of suitable solvent and heat, it is called 'lyotropic mesophase' [6]. In Figure 1. Liquid crystal phase transitions and forms of mesophase formation are given.

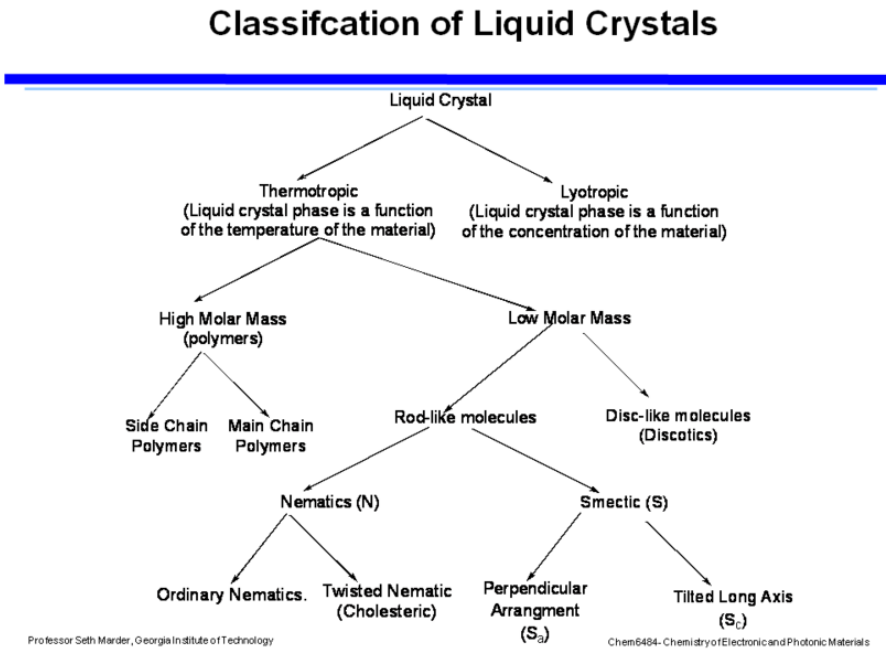

Figure 1. Phase transitions of liquid crystal compounds and forms of mesophase formation [6]

Liquid crystal materials show unusual behavior due to their properties. Liquid crystals are highly sensitive to external stimuli (thermal, electrical and magnetic). In addition, their ability to respond very quickly to these stimuli has made liquid crystal materials very important for materials science [7]. Figure 2. shows the visual showing liquid crystal materials and their applications [8].

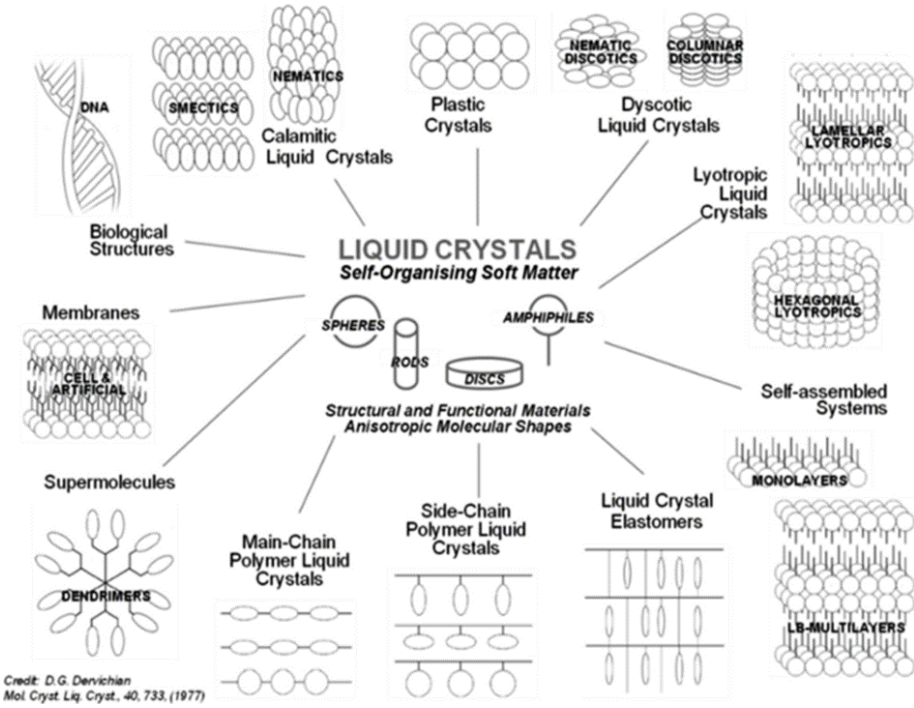

2. Liquid Crystal Polymers

Polymers that show liquid crystal properties under suitable conditions (pressure, temperature, concentration) are called Liquid Crystal Polymers [9]. In liquid liquid crystal polymers, liquid crystal mesogenic units are located in polymer chains. Due to the polymer chains in the structure of liquid crystal polymers, the polymer displays liquid crystal properties with the effect of mesogenic units. Liquid crystal polymer materials are a combination of both material properties. When examining the properties of liquid crystal materials, they are examined in 2 different dimensions in terms of polymer and liquid crystal material properties. Liquid crystal polymer materials are a very interesting field of study for materials science due to their high chemical resistance, inertness, stability in material unit arrangement, hardness, low thermal expansion coefficient and wide variety of material properties [10].

Figure 3. shows the visual showing the liquid crystal polymer and its applications.

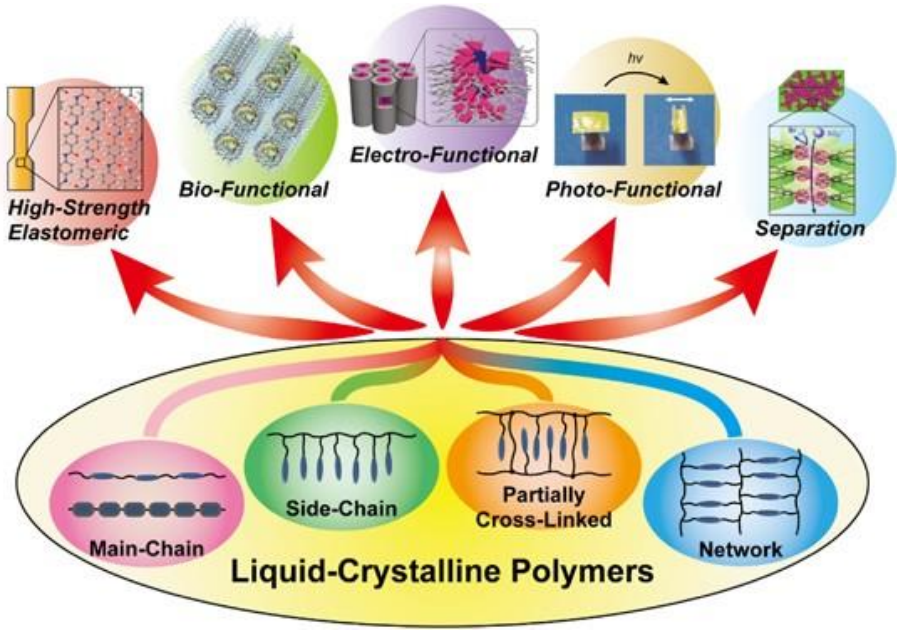

Figure 3. Liquid Crystal Polymer and Applications [11].

Liquid crystal polymers are used in many technological and industrial applications as high-tech materials due to their unique properties. In line with the increasing industrial and technological activities, the interest in materials such as liquid crystal and liquid crystal polymer, which has a high potential to be used in technological materials in many different fields, has increased in recent years. In the studies, the design, synthesis and determination of material properties (electro-optical, thermal, etc.) of liquid crystal polymer materials with different structures [12].

Designing, synthesizing, characterizing structure and material properties of liquid crystal polymer materials remains one of the most important areas of interest in modern materials science. Due to their unique material properties, liquid crystal polymers can easily take place in advanced technological systems in many different fields from energy to environment and biotechnology. [13].

The first synthesized liquid crystal polymer was polyamide 1 compound with lyotropic properties in 1960 [14]. Later in 1976, it was determined that aromatic polyester 2 compounds and polyazomethines showed thermotropic properties [15-16]. After these discoveries, a wide variety of polymer chains have been studied. Compounds 3 and 4, which are side chain liquid crystal

polymers, were synthesized in 1980 [17-19]. The molecular structures of these compounds are shown in Figure 4.

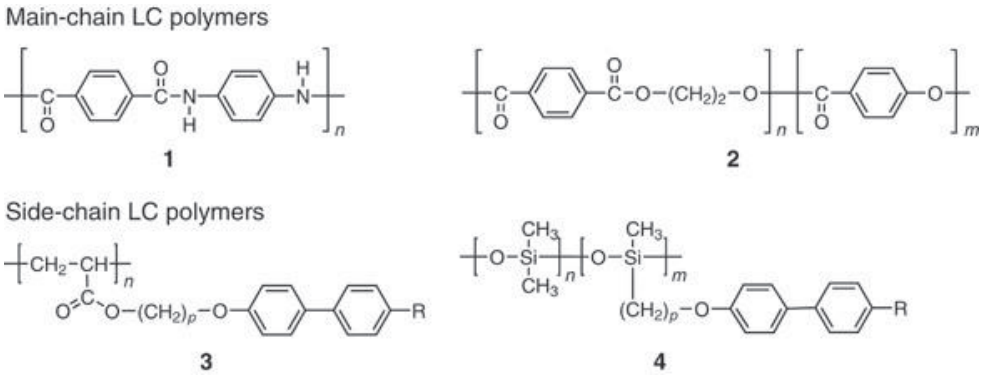

Figure 4. Molecular Structures of Compound 1,2,3,4 [11]

The emergence of liquid crystal character in liquid crystal polymer materials is provided by the mesogenic unit. The mesogenic units present in liquid crystal polymers can be thermotropic or lyotropic liquid crystals.

Liquid crystal polymer materials used in industrial and technological applications generally consist of thermotropic liquid crystals. [10].

Liquid crystal polymers are generally formed from low molecular weight liquid crystals. There are fixed or flexible mesogenic units in the polymer structure. These mesogenic units may be of calamitic (rod-like) or discotic molecular geometry. Mesogenic units in rod-like or discotic molecular geometry can be included in the polymer structure in many different ways. Mesogenic units are located in the main chain, side branches or in very different combinations in the polymer structure. The most commonly used liquid crystals as mesogenic units are calamitic (rod-like) liquid crystals [12-14]. The forms of mesogenic units in the polymer structure are shown in Figure 5.

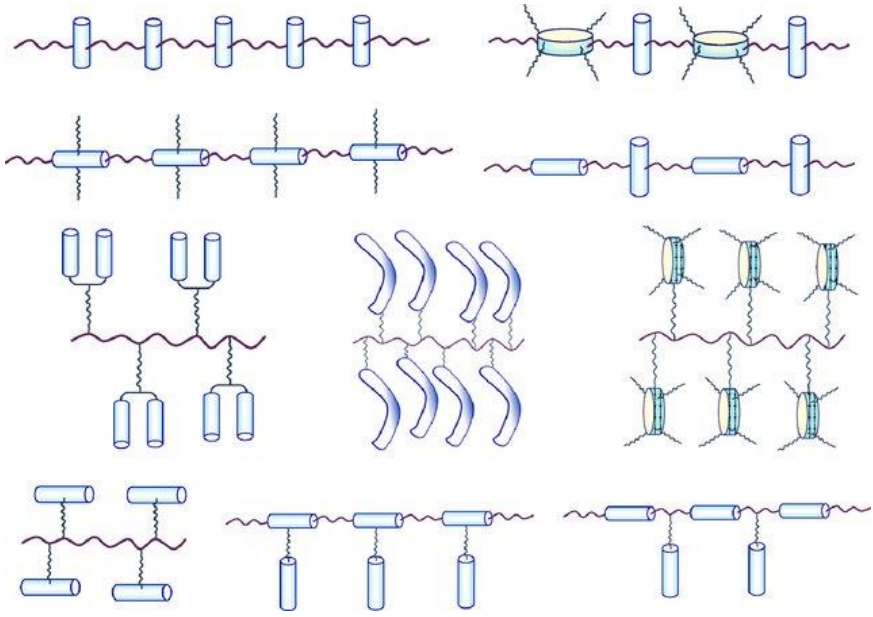

Figure 5. The forms of the mesogenic unit in the polymer structure [15].

In 1988, Brostow classified liquid crystal polymers. According to the location of the mesogenic unit in the polymeric structure, liquid crystal polymers can be classified in many different ways. Thermotropic liquid crystal polymers can be classified as main chain liquid crystal polymers in which the mesogenic unit is located in the main chain, or side chain liquid crystal polymers in which the mesogenic unit is attached to the main chain as a side group, and combined liquid crystal polymers consisting of a combination of both. [9,11] Figure 6. shows the general structure of the main chain and side chain polymers.

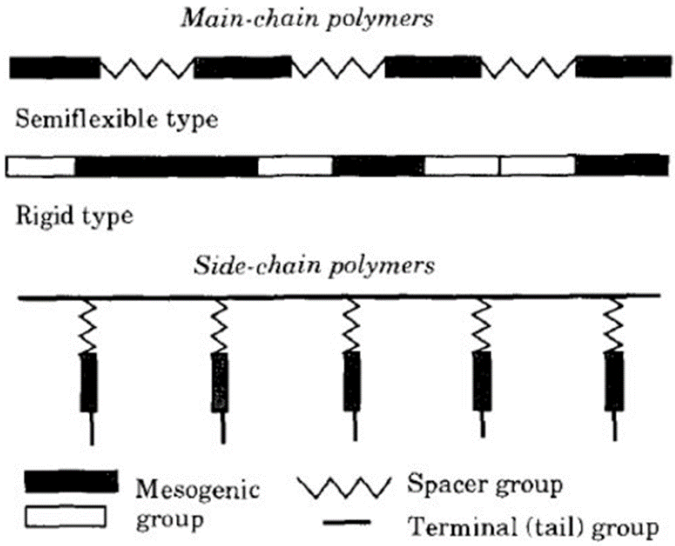

Figure 6. General structure of main chain and liquid crystal polymers [16].

3. Thermotropic Maın Chain Liquid Crystal Polymers and Their Current Applications

In the main chain liquid crystal polymers, the mesogenic units that enable the liquid crystal feature to emerge are located in the flexible polymer main chain. The first main chain liquid crystal polymer has been synthesized by Kuhfuss and Jackson [17].

Main chain liquid crystal polymers are divided into two according to the way the mesogenic units are attached to each other. These are semi-flexible polymers in which mesogenic units are bonded to each other through long and flexible units, and rigid polymers in which esogenic units are directly bonded to each other without any units in between. By arrangement of mesogenic units in the polymer chain, the polymeric and mesogenic behaviors of main chain polymers differ [18-19]. The general representation of the main chain polymers is shown in Figure 7. [20].

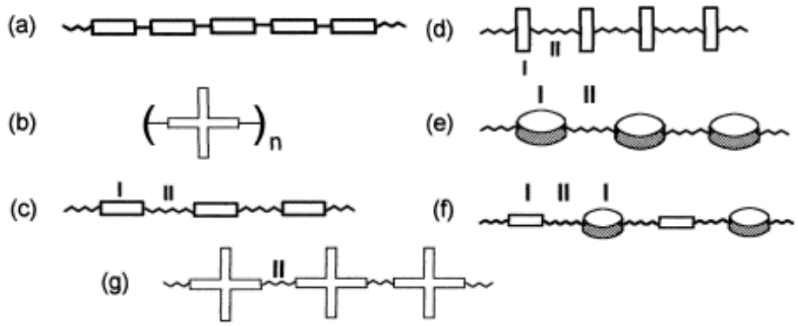

(I) Mesogenic Group
(II) Spacer Group

Figure 7. General representation of main chain polymers [20].

The first mesogenic unit synthesized in main chain liquid crystal polymers is liquid crystal monomers in calamitic structure. The structure of the first synthesized main chain liquid crystal is shown in Figure 8.

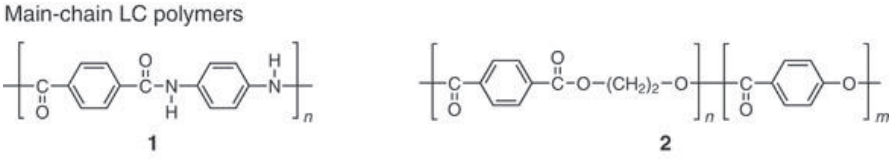

Figure 8. The molecular structure of the first synthesized main chain liquid crystal polymer [11].

Calamitic liquid-crystalline monomers generally consist of a large number of hard aromatic cores. Mesogenic units are usually linked to each other by ester and ether linker groups in main chain polymers [21]. In addition, amide, imine, urethane and carbonate linker groups may also be present in the structure. In addition, F, Cl, Br, CH_3, phenyl, alkyloxy or n-alkyl groups may be present on the aromatic core. The number and structure of aromatic nuclei in the mesogenic unit in main chain liquid crystal polymers are important because they restrict the movement of the polymer chain [22] .

In main chain liquid crystal polymers, flexibility to the polymer chain is provided by the separator group on the mesogenic units. Polyethylene, polymethylene, polyoxyethylene, polysiloxane etc. as flexible separating group. groups can be used [23].

Monomer units showing mesomorphic properties in main chain polymers are bifunctional. For example, such mesogenic monomers can be given as

monomers with a carboxylic acid at one end and an amine at the other. For example, mesogenic monomers in this structure form liquid crystal polyamide polymers, which are formed by sequential bonding of mesogenic units as a result of condensation reaction. The first synthesized main chain liquid crystal polymer is a polyamide polymer consisting of a monomer with an acid and an amine end, as in the example given above [11-13].

In recent years, considerable progress has been made in the synthesis of thermotropic main chain liquid crystal polymers. In the main chain liquid crystal polymers, hard main chain polymers are formed by directly connecting the mesogenic structure to the main chain. This situation causes situations such as high melting point and dissolution difficulty, which makes it difficult to use in material applications. For this reason, various synthesis methods have been developed for the synthesis of thermotropic main chain polymers with lower melting points, which may have higher potential to be used as materials [24-26].

In the studies carried out, main chain liquid crystal polymers with different properties such as electron conductivity and luminescence properties were synthesized [27-28].

There are studies on thermotropic main chain liquid crystal polymers in the literatur but there is no systematic study on current studies. In this study, some current thermotropic main chain liquid crystal polymer compounds in the literature are summarized. Thus, it is aimed to create a basic resource for researchers who may want to work on thermotropic main chain liquid crystal polymers.

4.Some Current Thermotropic Main Chain Liquid Crystalline Compounds in the Literature

In the study of Alkskas et al., a series of poly(ether-ketone) (PEKs), 3,5-bis(3-ethoxy-4-hydroxybenzyldehyde)-1-benzyl having a thermally stable 1-benzy-4-piperidone group -4-piperidone and various dibromo alkynes were successfully synthesized using the solution polycondensation method and the material properties were characterized. As a result of thermal analyzes and POM examinations, it was determined that PEKs with 4 and 8 separating groups were liquid crystals [21]. PEKs III molecular structure and synthesis scheme are given in Figure 9.

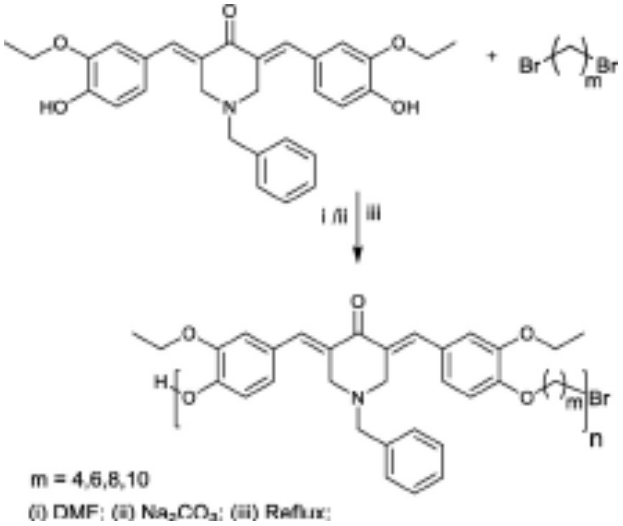

Figure 9. Synthesis of PEKs III [21].

In the study by Wei et al., the thermal degradation and pyrolysis behavior of three thermotropic main chain liquid crystal copolyesters containing fully aromatic phosphorus were investigated. 10-(2,5- Dihydroxypheny)-10 h-9-oxa-10-phospha-phe-nanthrene- It was observed that those containing 10-oxide (DOPO-HQ) were more thermally stable. According to the results of micro-scale combustion calorimetry (MCC) and limiting oxygen index (LOI), it was determined that copolyesters have excellent flame retardant properties and the LOI value increases monotonically with the increase of DOPO-HQ content, and the maximum value reaches 73.8%. . In the general study, according to the data obtained, it was determined that thermo-tropic liquid crystal copolyesters containing phosphorus exhibit excellent thermal stability and flame retardant properties [29]. The structure and mass fragmentation products of the copolyester are given in Figure 10.

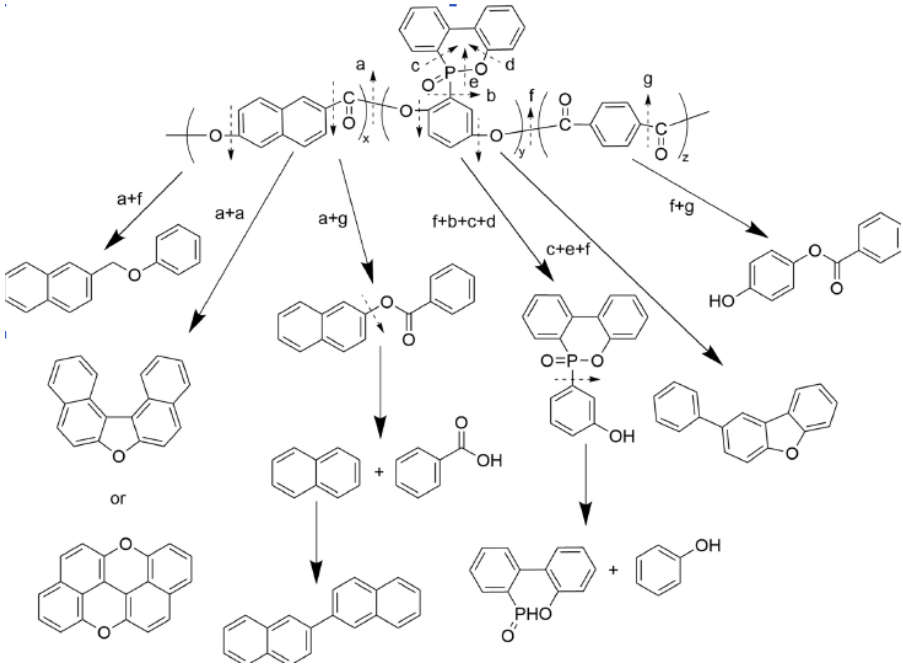

Figure 10. The structure and mass fragmentation products of the copolyester [29].

In the study of Jasmine et al., 4 random copolyesters chalcone diol 3-(4-hydroxy-3methoxyphenyl)-1-(4-hydroxyphenyl)prop-2-en-1-one (HMPP) and 4,40-oxybis(benzoic acid) and polycondensation of terephthalic acid and isophthalic acid and 2 diols 1,4-dihydroxyanthraquinone and 1,5-dihydroxyanthraquinone have been successfully synthesized and characterized. The chalcone diol was synthesized by acid-catalyzed Claisen-Schmidt reaction. Copolyesters were observed to exhibit nematic phase without methylene-flexible spacers in the polymeric chain. It has been reported for the first time that the synthesis and characterization of a series of novel photosensitive liquid crystal chalcone polymers without intermediate chains has been carried out in the study [30]. The synthesis scheme of the monomer is shown in Figure 11 and the synthesis scheme of the copolymer is shown in Figure 12.

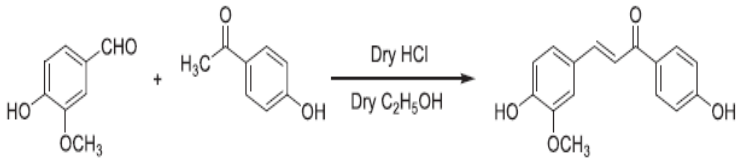

Figure 11. Synthesis reaction of the monomer [30].

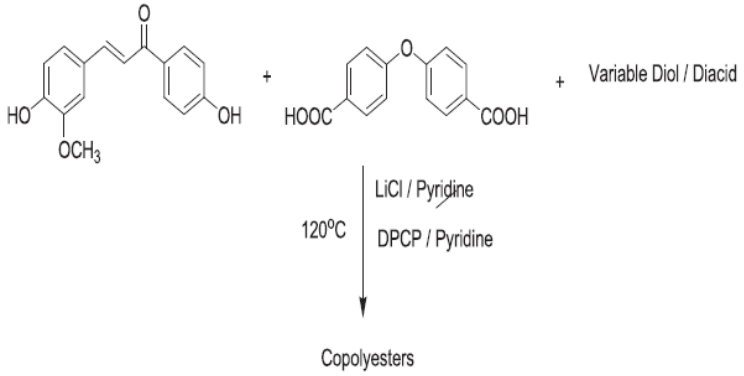

Figure 12. Synthesis reaction of the copolyesters [30].

In the study of Zhang et al., advanced photoactuators from a high-molecular-weight main-chain azo crystalline poly(ester-amide) (PEA) were synthesized with the Michael Addition reaction. It has been determined that azo PEA polymer can be easily formed into films with reversible light-induced bending/non-bending due to both the cross-linked, uniaxially oriented fibers in its structure and high mechanical strength at room temperature. In this study, it has been determined that the presence of both amide unit-induced hydrogen bonding and crystalline domains of the polymer in such films and fibers have dynamic and stable cross-linking points that allow the polymeric material to be easily three-dimensional (3D) reprogrammed under tension at room temperature. It has also been determined that the polymers are recyclable and recyclable from solution at room temperature [31]. The synthesis scheme and fiber structures of the polymer PEA-4 are shown in Figure 13.

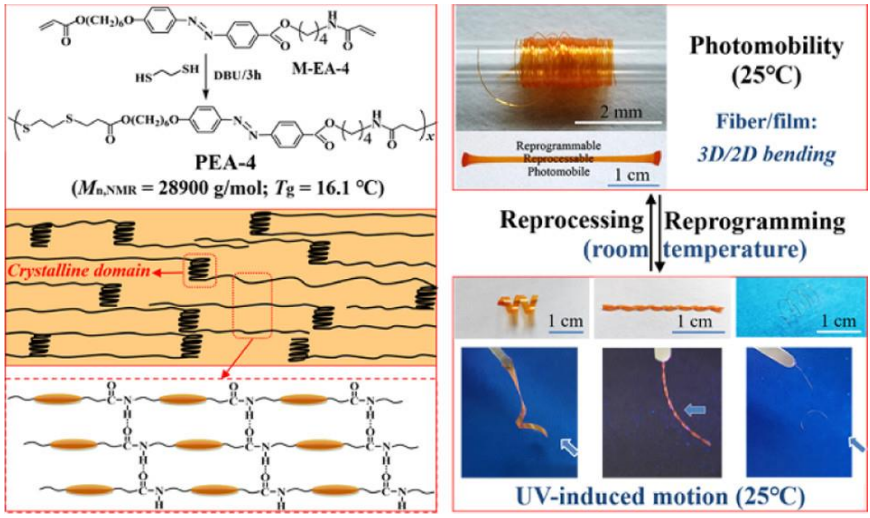

Figure 13.]. The synthesis scheme and fiber structures of the polymer PEA-4

5. CONCULUSION

In our study, some current thermotropic main chain liquid crystal polymers in the literature and their material behavior were investigated. Liquid crystal polymers have been studied intensively by different researchers due to their photophysical, electro-optical, electronic and thermal properties, but there is a wide field to carry out studies on the synthesis, characterization and examination and development of material properties of main chain polymers. It is quite possible to synthesize a new liquid crystalline main chain polymer by derivatizing the mesogenic units that take place as monomers in the thermotropic main chain polymer structure. Due to the existence of many different parameters affecting the material character, such as examining the structure-mesogenity relationship in liquid crystal materials, derivatizing the mesogenic properties with structure-dependent groups, examining the material properties in terms of liquid crystal and polymeric character, the properties of the material are directly related to the molecular structure of the monomer and polymer. Synthesis of thermotropic main chain liquid crystal polymers will continue to create an interesting field in the coming years.

REFERENCES

[1] Reinitzer, F., (1888). Monatsch. Chem., 9:421-441.
[2] Lehmann, O.Z., (1889). Phys. Chem. 4: 462-472.
[3] Lehmann, O.Z., (1890). Phys. Chem. 5: 427-435.
[4] Lehmann, O.Z., (1904). Flüssige Kristalle, Engelman, Leipzing.
[5] Friedel, G., (1922). Ann. Phys., 18 (2):273-474.
[6] Demus, D., Goodby, J., Gray, G.W., Spiess, H.W., Vill, V., (1998). Handbook of Liquid Crystals Fundamentals, Volume 1, First Edition, Wiley-VCH, Weinheim.
[7] Castello, J. A., (2005). Liquid Gold, The Story of Liquid Crystal Display and The Creation of an Indystry, 1. Baskı, World Scientific , London.
[8] Rey, A.D., Herrera-Valencia, E.E., Aguilar Gutierrez, O.F. (2020). Liquid Crystalline Polymers: Structure and Dynamics. In: Zhu, L., Li, C. (eds) Liquid Crystalline Polymers. Polymers and Polymeric Composites: A Reference Series. Springer, Cham
[9] Whang, X., Zhou, Q., (2004). Liquid Crystalline Polymers, World Scientific Publishing, Singapore.
[10] Baron, M., Stepto, R.F.T., (2002). "Defenitions of Basic Terms Relating to Polymer Liquid Crystals ", Pure Appl. Chem., 74 (3):493-509.
[11] Polymer Journal (2018) 50, 149–166; doi:10.1038/pj.2017.55
[12] Shibaev, V. P., Lam, L., (1994). Liquid Crystalline and Mesogenic Polymers,Springer.
[13] Blumstein, A., (1985). Polimeric Liquid Crystals, Volume 28, First Edition, Plenum Press, New York and Londra.
[14] Shibaev, V.P., Bobrovsky, A., Boiko, N., (2003). "Photoactive Liquid Crystalline Polymer Systems with Light-controllable Structure and Optical Properties", Progress in Polymer Science, 28:729-836.
[15] Shibaev V., Liquid Crystalline Polymers. In: Saleem Hashmi (editor-in-chief), Reference Module in Materials Science and Materials Engineering. Oxford: Elsevier; 2016. pp. 1-46.
[16] Gedde, U. W., Polymer Physics. 1995: Springer.
[17] Kuhfuss, H. F., Eastman Kodak Co., (September 1972), B. P. 1,435,021, USA.
[18] Palsule, A., (2006). "Morphological hierarchy in liquid crystalline polymers",Morphology of Complex Materials, Winter.
[19] Shibaev, V.P., Bobrovsky, A., Boiko, N., (2003). "Photoactive Liquid Crystalline Polymer Systems with Light-controllable Structure and Optical Properties", Progress in Polymer Science, 28:729-836.
[20] Baron, M., Stepto, R.F.T., (2002). "Defenitions of Basic Terms Relating to Polymer Liquid Crystals ", Pure Appl. Chem., 74 (3):493-509.

[21] Ismail A. Alkskas, Suade M. Almadani , Faizul Azam,″ Synthesis and characterization of liquid crystalline poly(ether-ketone)s containing 1-benzyl-4-piperidone moiety as a pendent group', Journal of Molecular Structure 1257 (2022) 132550.

[22] M. Pytlarczyk, P. Kula, Synthesis and mesomorphic properties of 4,4”-dialkynyl-2’,3’-difluoro-p-terphenyls –the influence of C = C acetylene linking bridge, Liq. Cryst. 46 (2019) 618–628,

[23] J. Herman, P. Kula, Design of new super-high birefringent isothiocyanatobistolanes–synthesis and properties, Liq. Cryst. 44 (2017) 1462–1467, doi: 10. 1080/02678292.2017.1282548.

[24] M. Iqbal, S.J. Picken, T.J. Dingemans, Synthesis and properties of aligned all-romatic liquid crystal networks, High Perform. Polym. 26 (2014) 381–391.

[25] G.T. Park, J.H. Chang, A.R. Lim, Thermotropic liquid crystalline polymers with arious Alkoxy Side Groups: thermal properties and molecular dynamics, Polymers 11 (2019) 992 (Basel).

[26] R.W. Lenz, Synthesis and properties of thermotropic liquid crystal polymers with main chain mesogenic units, Polym. J. 17 (1985) 105–115.

[27] O’Neill, M. & Kelly, S. M. Ordered materials for organic electronics and photonics. Adv. Mater. 23,566–584 (2011).

[28] McCulloch, I., Heeney, M., Bailey, C., Genevicius, K., MacDonald, I., Shkunov, M. Sparrowe, D., Tierney, S., Wagner, R., Zhang, W., Chabinyc, M. L., Kline, R. J., McGehee, M. D. & Toney, M. F. Liquid-crystalline semiconducting polymers with high charge-carrier mobility. Nat. Mater. 5,328–333 (2006).

[29] Peng Wei, Jinfei Yan, Longlong Li , Hejuan Lou, Yifeng Zhang, Keqian Hao, Yumin Xia, Yanping Wang, Yimin Wang, ‘Thermal degradation and pyrolysis behavior of wholly aromatic phosphorus-containing thermotropic liquid crystal copolyesters, ournal of Analytical and Applied Pyrolysis 164 (2022) 105524.

[30] S. Jasmine, J. Sidharthan, D. Reuben Jonathan, Rajadurai Vijay Solomon, Cheriyan Ebenezer, D. Roopsingh, ‘UV-A and UV-B banning highly soluble photocrosslinkable thermotropic liquid crystalline copolyesters with ether linkage in the backbone’, Materials Today: Proceedings 66 (2022) 2411–2421.

[31] Yan Zhou, Lei Wang, Shengkui Ma, and Huiqi Zhang,’ Fully Room-Temperature Reprogrammable, Reprocessable, and Photomobile Soft Actuators from a High-Molecular-Weight Main-Chain Azobenzene Crystalline Poly(ester-amide), ACS Appl. Mater. Interfaces 2022, 14, 3264−3273.

Chapter 2

Osteological Comparison of Hemidactylus turcicus (Linnaeus, 1758) (Sauria: Lacertilia: Gekkonidae) Populations Distributed in Ayvacık and Bozcaada (Çanakkale)

Didem KURTUL [1]

Çiğdem GÜL[2]

[1] Çanakkale Onsekiz Mart University, School of Graduate Studies, Department of Biology. didemkurtul17@gmail.com ORCID No: 0000-0003-0778-5966

[2] Prof. Dr.; Çanakkale Onsekiz Mart University, Faculty of Sciences, Department of Biology. gulcigdem@comu.edu.tr ORCID No: 0000-0003-4736-2677

ABSTRACT

Morphological and osteological characteristics are a great guide in the systematic and taxonomic classification of species. Osteological features reveal important distinguishing characters for both detailed knowledge and description of the species.

Species distributed on the island and the mainland may differ in terms of speciation. For this reason, in this study, it was aimed to determine the similarities and differences between the populations by examining the osteological characteristics of the Ayvacık (Mainland) and Bozcaada (Island) populations of the *Hemidactylus turcicus* species distributed in Çanakkale. The double transparent stained skeleton method was used in the osteological analysis of the samples belonging to *Hemidactylus turcicus* populations. Cranial and postcranial features were analysed in detail, both qualitatively and quantitatively. Comparisons between Ayvacık and Bozcaada populations were made and statistically evaluated.

As a result of osteological analyses conducted between Bozcaada and Ayvacık populations, statistically significant differences were determined that three of the qualitative characteristics of cranial and postcranial between both populations. In quantitative characteristics, three measurements and four ratios of the cranial, five measurements of the postcranial and two ratios were statistically difference between populations. As summary, according to result of the study, osteological variations were detected more in the *Hemidactylus turcicus* populations of Bozcaada, and it was concluded that there was no significance difference at the subspecies level between the Ayvacık and Bozcaada populations.

Keywords: Hemidactylus turcicus, Osteology, Ayvacık, Bozcaada.

INTRODUCTION

As with most groups of vertebrates, the preferred osteological studies for reptile classification are usually determined at the ordo levels, but they are also determined within families, genus, species and subspecies. In phylogenetic studies, characters that undergo the least change during the evolutionary process are preferred. For this reason, osteological characters are one of the most suitable markers for predicting interspecies kinship relationships and are of great importance in evolutionary explanations (Özeti, 1970). Like other methods, osteological studies is frequently used to determine the kinship relationships of species (Presch, 1969; Özeti, 1970; Arnold, 1983; Fraser, 1988; Gow, 1972; Cadwell, 1997; Müller, 2001; Caputo, 2004; Arnold et al., 2007; Evans, 2008; Arribas et al., 2013; Yıldırım et al., 2017).

The Gekkonidae family, one of the largest groups of lizards, is a group with a wide species richness that includes more than about 1460 species (Uetz et al., 2021). There are 158 species described to the genus *Hemidactylus*, Oken 1817 one of the largest genus of the Gekkonidae family, and they are distributed in tropical and subtropical regions of the world (Carranza and Arnold, 2006; Sindaco and Jeremcenko, 2008). The wide distribution areas have increased the diversity in habitat choices and caused many morphological adaptations (Koppetsch et al., 2020). It is stated that there is a direct relationship between the differences in their external morphology and their osteology (Rothier et al., 2017).

The *Hemidactylus turcicus* (Linnaeus, 1758) species of the *Hemidactylus* genus is commonly associated with countries around the Mediterranean Basin throughout the world. *Hemidactylus turcicus* is distributed in the southeastern part of Portugal, Southern and Eastern Spain, Southern France, Italy, Slovenia, Croatia, Bosnia-Herzegovina and the coastal parts of Albania and most of Greece in the European continent (Agasyan et al., 2009; Altunışık, 2017; Baran et al., 2021). In Türkiye, this species is usually found in the Aegean, Mediterranean, Black Sea and Southeastern Anatolia Regions (Yıldız et al., 2007; Altunışık, 2017). *H. turcicus* is a nocturnal species that is generally found in houses, exterior walls of houses, forest edges, stony and rocky areas (Das et al., 2014). The only known subspecies of *Hemidactylus turcicus* in our country is the nominate subspecies *Hemidactylus turcicus turcicus* (Başoğlu and Baran, 1977; Baran and Gruber, 1982).

It has been shown in many studies that the species distributed on the island and mainland differs in terms of speciation (Jesus et al., 2001; Algar and Losos, 2011). There are no osteological studies conducted on reptile species that have become widespread in Ayvacık and Bozcaada belonging to the province of

Çanakkale. Therefore, the aim of this study is to determine the osteological characteristics of the *H. turcicus* populations distributed in Ayvacık representing the mainland and Bozcaada representing the island for the first time in detail, and to reveal the differences and similarities.

MATERIALS AND METHODS

In this study, a total of 20 specimens, 10 (5♂♂,5♀♀) Ayvacık and 10 (5♂♂,5♀♀) from Bozcaada, were used from museum material specimens preserved in Çanakkale Onsekiz Mart University Department of Biology Zoology Museum (Baycan and Tosunoğlu, 2017). For the procedures, necessary permissions were obtained from the Animal Experiments Ethics Committee of Çanakkale Onsekiz Mart University, numbered 2021/01-05. The sexes were determined by the presence or absence of the preneal pore located anterior to the anal cleft.

Osteological Examinations

The painting of the cartilage and bone elements that make up the skeletal system in different colors by using different dyes are called double skeletal staining (McLeod, 1980). There are many osteological studies in which the double skeletal staining method was used (McLeod, 1980; Taylor and Dyke, 1985; Sunay, 2005; Depew, 2008; Gül and Tosunoğlu, 2011; El bakry et al., 2013; Yıldırım et al., 2017). For this reason, transparent stained skeletons formed the essence of the present study as well. The osteological analyses performed according to the transparent stained skeleton method were prepared by changing the method of Wassersug (1976).

In the osteological analyses of *H. turcicus* from Ayvacık and Bozcaada populations, cranial and postcranial bones were dissected and examined. Cranial and postcranial qualitative and quantitative characteristics were determined as reference studies (Worthy, 1987; Mohammed, 1988; Daza et al., 2008; El Bakry et al., 2013; Rothier et al., 2017; Villa et al., 2018). Quantitative features of cranial and postcranial were measured with using digital caliper (Mitutoyo, 0.01 mm). Qualitative features were examined under an Olympus SZ2-ILST microscope.

Statistical Analyses

SPSS 26.0 package program was used for statistical evaluation of measurements and ratios obtained from osteological analyses of the specimens. Kolmogorov Smirnov test of normality was applied to all data within and between populations. As a result of the test, it was determined that it did not show normal

distribution and nonparametric Mann Whitney-U test was applied. Discriminant analysis was performed to determine the levels of difference between populations. The stepwise method was used to detect characters that discriminated between populations (F for entry: 3.84; F for removal: 2.71).

RESULTS

For Ayvacık and Bozcaada populations, 40 qualitative and 12 quantitative parameters of the cranial; 17 qualitative and 22 quantitative parameters of the postcranial were determined and comparisons were made between populations.

Cranial Skeleton

In the Ayvacık and Bozcaada populations, the dorsal surfaces of the skulls were in the form of scattered and rough pits, and there was no difference detected between the two populations.

Nasals, The nasals are a pair of bones that articulate with the premaxilla anteriorly, the frontal posteriorly, the maxilla anterolaterally, and the prefrontals posterolaterally. In Ayvacık populations, there was 70% no contact between the nasals and the prefrontal, and 30% contact. On the other hand, in Bozcaada populations, there was no contact at the rate of 80%, there was contact at the rate of 20%. The margins of the nasals were concave in both populations. The frontal inputs of the posterior ends of the nasals were triangular in the entire Ayvacık population (100%). The population of Bozcaada was 50% triangular in shape and 50% round in shape. They showed intra-population variation.

Suborbital fenestra, There was no difference between the two populations and it was determined as small oval shaped cavity in all of the specimens.

Frontal, The bone is the only bone that articulates with the nasal anteriorly, the anterolaterally prefrontal, the posterolaterally the postfrontal, and the posteriorly the parietal. In the Ayvacık population, the anterior margins of the frontal were 70% V-shaped and 30% straight. It was V-shaped in all specimens from Bozcaada population. In both populations, the posterior end of the frontal was 1.5 to 2 times larger than the anterior end. In the Ayvacık population, the shapes of posterior margins of frontal was both straight (50%) and slightly concave (50%). On the other hand, in Bozcaada population, it was slightly concave at the rate of 70% and in the form of a straight line at the rate of 30%. The end of the frontal anterolateral triangular process was mostly round (90%) and rarely pointed (10%) in the Ayvacık population, and completely pointed (100%) in the Bozcaada population. In terms of this feature, a difference was determined between the two populations (Figure 1).

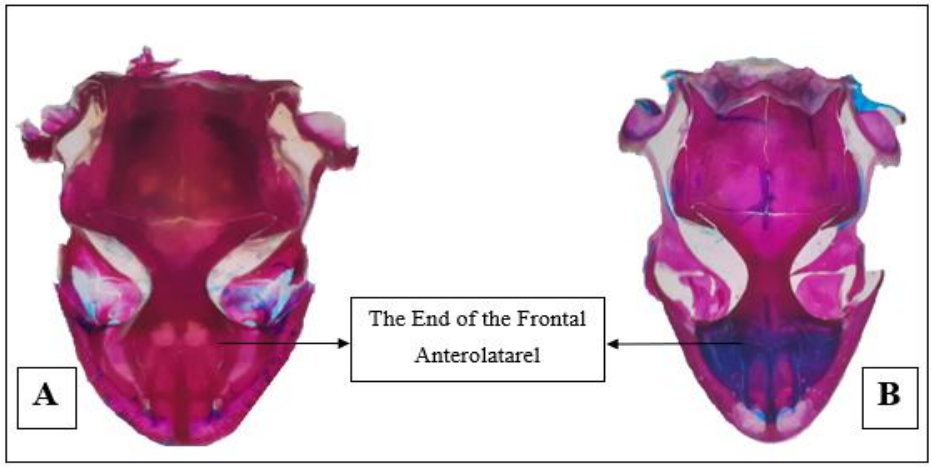

Figure 1. Comparison of the ends of frontal anterolateral triangular process of the dorsal skull in *H. turcicus* populations from Ayvacık and Bozcaada (A: Ayvacık, Round End; B: Bozcaada, Pointed End).

Prefrontal, The prefrontal is connected anteroventrally with the prefrontal maxilla, laterally with the lacrimale, anterodorsally with the nasal. Variations were detected in the connection with the frontal in the prefrontal dorsal. While it was 70% pointed and 30% round in Ayvacık population; in the Bozcaada population it was 90% pointed and 10% rounded. It was found that the prefrontal frontal entered 1/3 in both populations.

Postorbitofrontal, The postorbitofrontal is located anterolaterally on the dorsal of the skull. It is a bipartite bone that is in contact with the postorbital anterolateral, the parietal dorsolaterally, and the squamosum postlaterally. It has a connection with the frontal. The postorbitofrontal was boomerang-shaped in both populations. Anterior processes were shorter than posterior processes. Variations at the end of the posterior processes were detected in both populations. While the shape of postorbitofrontal was 60% round and 40% pointed in Ayvacık population; it was 50% pointed, 10% square and 40% round in the Bozcaada population.

Parietal, The parietal is the widest bone of the skull with a rectangular shape. There were two posterior projections at their posteromedial corners, and variations were identified in both populations. In Ayvacık population, square ends were seen in 90% of the population and a round end in 10%, while in the Bozcaada population square ends were seen in 80% and a round end in 20%. Postparietal processes were narrow and pointed in both populations. It was seen that it articulates anterolaterally with the postfrontal bones, laterally with the

postorbital bones, postlaterally with the squamosum, and anteriorly with the frontal bones.

Jugal, The jugal is in contact with the postorbital dorsally and with the maxilla anteriorly. The shape of the jugal was in contact with half of the maxilla at a rate of 80% in Ayvacık populations and started from the end of the maxilla at a rate of 20%. In all of the Bozcaada populations, it was in contact with half of the maxilla. It was determined that while the shape of tip of the jugal was 30% round and 70% pointed in Ayvacık populations; in Bozcaada populations, it was 90% round and 10% pointed.

Vomer, The vomer is the bone located between the premaxilla and the palatines. The posterior end of the vomer was 80% rounded and 20% square in Ayvacık populations, and it was 50% rounded or 50% square in Bozcaada populations. The lateral process of the vomer was found to be concave in the medial direction in *H. turcicus* populations of Ayvacık and Bozcaada.

Palatine, The palatine is a bone in contact with the vomer anteriorly, the pterygoid posteriorly, and the maxilla laterally. It was determined that the maxillary protuberance of the palatine was small, thin and triangular (100%) in Ayvacık population, while it was usually small, thin and triangular (90%) and rarely rounded and not indented (10%) in Bozcaada population. Palatine teeth were not present in both populations.

Pterygoid, The pterygoid is two separate bones consisting of a pyriform cavity. It was determined that *H. turcicus* specimens does not carry pterygoid teeth in both populations. While its connection with the pterygoid palatine was 80% straight and 20% pointed in Ayvacık population, it was flat in all specimens from Bozcaada population.

Squamosal, The squamosal was laterally in contact with the quadrate in Ayvacık and Bozcaada populations.

Sphenoid, The shape of the sphenoid was rectangular in both populations.

Prootic, Prootic forms the anterolateral part of the braincase. It is in contact with the sphenoid anteroventrally, with the supra-occipital in the posterodorsal and with the auto-occipital in the postroventrally. In Ayvacık population, the prootic was 90% round at the distal tip and 10% pointed. In Bozcaada population, no variation was observed and it was round in all specimens (100%).

Quadrate, The quadrate is the bone to which the lower jaw articulates, located on the posterolateral sides of the skull. The anterodorsal margins of the quadrat were 70% long and 30% narrow in Ayvacık population, and narrow in the entire Bozcaada population (100%).

Basioccipital, The basioccipital is located in front of the occipital condyl in the posterior part of the brain sheath and posterior of the parasphenoid. It was

determined that the basioccipital prootic was in contact in Ayvacık and Bozcaada populations.

Supraoccipital, The supraoccipital is located between the parietal and occipital condyl. In terms of dorsal shape of the supraoccipital, pointed tubercules were seen in 70% of Ayvacık population, while 30% of them do not have. In Bozcaada population, it was determined that pointed tubercles were seen in all of the specimens (100%).

Premaxilla, The premaxilla is in contact with the nasal dorsally and the maxilla laterally. While the margins of the nasal process of the premaxilla were pointed, long and narrow in all specimens from Ayvacık population; it was 90% pointed, long and narrow, and 10% blunt in Bozcaada population. The nasal connection of the premaxilla enters 2/3 of all Ayvacık and Bozcaada populations.

Maxillae, The maxilla forms the anterolateral part of the upper jaw. While the posterodorsal margins of the maxilla were 50% round or 50% pointed in Ayvacık population; it was 90% pointed and 10% round in Bozcaada population. The anterior process of the maxilla was 50% upright and vertical, 50% steep and forward sloping in Ayvacık population, while it was 70% steep and forward-sloping, 30% steep and vertical in Bozcaada population. When the Ayvacık and Bozcaada samples were examined together, the medial and lateral processes of the maxilla were completely rough.

Coronoid, The coronoid is a small triangular bone located lateral to the dentale between the mandibular row of teeth and the surangular bone. Posteromedial process of coronoid is 80% round, 20% long, thin and pointed in Ayvacık population. In Bozcaada *H. turcicus* specimens are 90% long, thin and pointed and 10% round.

Hyoid apparatus, The hyoid contains a total of 3 pairs of arms, 1 entoglossus protrusion, first and second branchial arms. The regions of the hyoid apparatus are cartilaginous. No significant difference was found in hyoid apparatus between Ayvacık and Bozcaada populations.

Quantitative measurements and ratios of the cranial were evaluated between the Ayvacık and Bozcaada populations were given in Table 1. When all characteristics were examined, statistically significant differences were found between the two populations for SH, SW, PMW measurements and SSVL/SL, SSVL/SW, SL/SW, PML/PMW ratios ($p<0,05$).

Table 1. Quantitative osteological measurements and ratios of the cranial in *H. turcicus* populations from Ayvacık and Bozcaada.

CRANIAL QUANTITATIVE FEATURES	AYVACIK (N: 10)				BOZCAADA (N: 10)				P
	Min	Max	Mean	SE	Min	Max	Mean	SE	
SL	12,03	15,40	13,69	0,329	10,85	15,67	12,95	0,424	0,12
SW	5,84	7,78	6,95	0,227	7,15	10,33	8,85	0,323	**0,00**
SH	3,01	5,04	3,89	0,176	4,05	5,65	4,92	0,149	**0,00**
ML	5,85	8,40	7	0,274	3,74	7,69	6,68	0,363	0,70
DL	11,09	13,58	12,69	0,309	10,10	13,50	12,16	0,344	0,24
FML	4,31	5,71	5,04	0,165	3,92	5,14	4,76	0,114	0,22
FMW	1,00	1,66	1,34	0,076	0,97	1,47	1,29	0,052	0,47
PML	3,65	4,50	4,14	0,077	2,89	4,55	4,08	0,146	0,94
PMW	3,97	4,75	4,25	0,085	3,09	4,51	3,83	0,125	**0,00**
PTL	4,67	6,81	6,04	0,187	4,85	6,70	5,71	0,184	0,14
OLL	2,80	4,64	3,71	0,174	2,90	4,53	3,70	0,187	1,00
OVL	3,24	4,86	4	0,170	2,59	4,26	3,60	0,196	0,120
SSVL/SL	3,39	3,78	3,59	0,042	3,25	3,69	3,46	0,043	**0,04**
SSVL/ SW	6,60	7,82	7,09	0,115	4,86	5,41	5,07	0,057	**0,00**
SL/SW	1,75	2,13	1,97	0,040	1,33	1,58	1,46	0,028	**0,00**
SL/ML	1,62	2,38	1,97	0,061	1,77	2,90	1,98	0,107	0,22
FML/FMW	3,19	4,42	3,80	0,129	3,29	4,09	3,70	0,084	0,49
PML/PMW	0,88	1,08	0,97	0,024	0,91	1,19	1,06	0,028	**0,01**
OLL/OVL	0,65	1,41	0,94	0,065	0,78	1,56	1,05	0,076	0,36

*SL: Skull Length, SW: Skull Width, SH: Skull Height, ML: Maxilla Length, DU: Dentale Length, FML: Frontal Medial Length, FMW: Frontal Medial Width, PML: Parietal Medial Length, PMW: Parietal Medial Width, PTL: Pterygoid Medial Length, OLL: Lateral Length of Orbit, OVL: Vertical Length of Orbit. SSVL/SL: Skeleton Vent Length/ Skull Length, SSVL/SW: Skeleton Snout Vent Length / Skull Width, SL/SW: Skull Length / Skull Width, SL/ML: Skull Length / Maxilla Length, FML/FMW: Frontal Medial Length / Frontal Medial Width, PML/PMW: Parietal Medial Length / Parietal Medial Width, OLL/OVL Lateral Length of Orbit / Vertical Length of Orbit.

*N: Number of Samples, Min- Max: Minimum- Maximum, SE: Standart Error.

Postcranial Skeleton

Vertabrae, *H. turcicus* have procoel type vertebrae. The spine is divided into 4 regions: cervical, dorsal, sacral, and caudal. In *H. turcicus* from Ayvacık and Bozcaada populations, 26 vertebrae including atlas and axis vertebrae (not including sacral vertebrae) and 22 of them were found to have ribs. While the average number of vertebrae linked to the sternum was 6-8 in Ayvacık population, it was 8 in Bozcaada population. The number of sacral vertebrae was equal for both populations and there were 2 sacral vertebrae.

Clavicle, The clavicle is a bone structure that expands laterally. While the distal end of the clavicle was articulated with the notch in the entire Ayvacık population, it was not attached with a notch (70%) in the majority of the Bozcaada

population, but was rarely articulated with a notch (30%). There were differences between the two populations in terms of this feature. In Ayvacık population, it was found that the clavicles merged with the cartilage in the midline (100%), while the clavicles do not merge with the cartilage at a rate of 90%, but at a rate of 10% in Bozcaada population. In terms of this feature, a difference was found between the two populations (Figure 2).

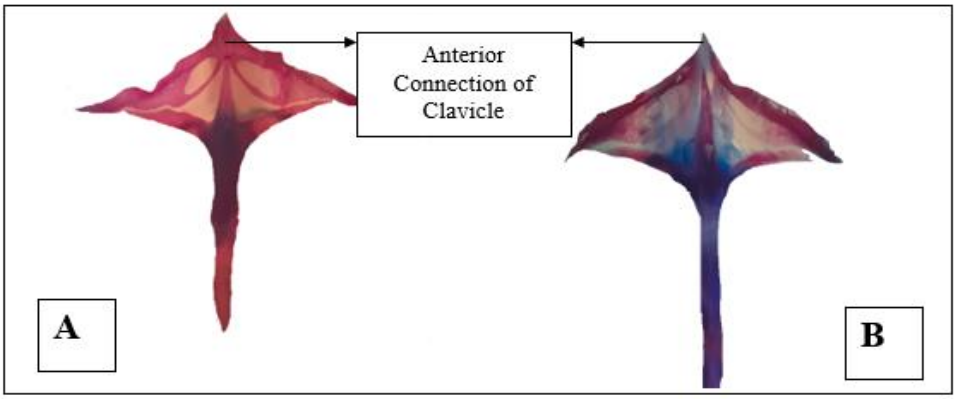

Figure 2. Comparison of midline clavicula of Ayvacık and Bozcaada *H. turcicus* populations (A: Ayvacık, B: Bozcaada).

Interclavicle, The interclavicle is bony structure. When the Ayvacık and Bozcaada populations were examined together, the shape of the interclavicle was dagger-shaped.

Fore and hind limbs, It was determined that the epiphyses of the phalanxes in the fore and hind limbs were calcified in the Ayvacık and Bozcaada *H. turcicus* populations. Paraphalangeal elements are located at the distal end of the extremities. The ulnar patella was present in both populations. It was found that Tarsus tarsalia consists of 1-3-4 in Ayvacık and Bozcaada populations. In Ayvacık and Bozcaada populations, the tarsus consists of proximal tarsal elements. In the Ayvacık and Bozcaada populations, the tibia was found to have a large surface. Femur, tibia, fibula, phalanx and the ends of the distal tarsals were cartilaginous in Ayvacık and Bozcaada populations. Fibular patella was present in both populations.

Postcranial quantitative characteristics of *H. turcicus* populations distributed in Ayvacık and Bozcaada were given in detail in Table 2.

Table 2. Postcranial quantitative osteological measurements and rates in *H turcicus* populations distributed in Ayvacık and Bozcaada.

POSTCRANIAL QUANTITATIVE FEATURES	AYVACIK (N: 10)				BOZCAADA (N:10)				P
	Min	Max	Mean	SE	Min	Max	Mean	SE	
SSVL	41,84	53,41	49,21	1,280	36,31	51,08	44,82	1,356	**0,03**
HL	5,96	7,47	6,81	0,123	4,94	7,39	6,46	0,244	0,29
UL	3,91	5,51	4,93	0,200	3,78	6,28	5,02	0,263	0,76
RL	4,61	6,51	5,15	1,193	4,48	6,58	5,38	0,211	0,32
FPW	1,46	3,34	2,68	0,195	1,20	3,75	2,80	0,245	0,49
FPL	0,97	2,32	1,56	0,115	1,48	2,87	2,27	0,146	**0,00**
FTPL	1,08	3,96	2,08	0,261	1,91	2,80	2,39	0,099	0,11
FFPL	0,83	4,32	1,96	0,329	2,07	3,27	2,71	0,127	**0,01**
FFthPL	0,67	2,81	1,61	0,222	,85	3,04	1,99	0,200	0,10
FL	11,05	13,26	11,96	0,230	9,42	13,53	11,85	0,394	0,94
TL	4,76	6,35	5,56	0,130	4,17	6,17	5,47	0,181	0,94
FIL	4,99	5,76	5,38	0,090	4,42	6,75	5,90	0,195	**0,00**
FL	7,73	9,60	8,49	0,208	6,51	8,93	7,85	0,280	0,07
HPL	1,510	2,80	2,32	0,111	2,23	3,93	3,04	0,161	**0,00**
HPW	1,97	4,26	3,20	0,228	2,23	3,96	3,02	0,176	0,47
HFPL	1,97	5,57	3,13	0,351	1,93	4,99	3,44	0,248	0,29
HFthW	0,98	3,34	2,04	0,274	1,17	3,59	1,73	0,263	0,22
HL	12,68	15,35	14,05	0,251	10,79	14,47	13,33	0,407	0,21
SSVL / HL	6,21	7,91	7,22	0,146	6,60	7,99	6,95	0,136	0,08
SSVL/TL	7,27	9,74	8,88	0,275	7,40	8,96	8,21	0,190	**0,03**
SSVL / FL	5,35	6,48	5,80	0,115	5,28	6,42	5,72	0,110	0,59
HL/ FFthPL	2,50	10,04	5,13	0,856	2,25	7,40	3,73	0,590	0,06
RL/UL	0,83	1,29	1,05	0,050	0,82	1,39	1,09	0,062	0,70
FPL / HPL	0,39	1,22	0,69	0,073	0,50	1,03	0,76	0,061	0,40
FPW / HPW	0,53	1,51	0,86	0,083	0,45	1,19	0,92	0,067	0,25
FFPL / FPL	0,37	2,52	1,30	0,210	0,90	1,91	1,23	0,087	0,94
TL/FIL	0,88	1,17	1,03	0,027	0,83	1,09	0,93	0,022	**0,01**
FL/ HFthL	2,64	7,88	4,82	0,590	2,44	6,86	5,12	0,477	0,49
FL/ TL	1,21	1,67	1,53	0,047	1,24	1,65	1,44	0,047	0,19

* SSVL: Skeleton Snout Vent Length, HL: Humerus Length, UL: Ulna Length, RL: Radius Length, FPW: Forelimb Palm Width, FPL: Forelimb Palm Length, FTPL: Forelimb Third Phalanx Length, FFPL: Forelimb Fourth Phalanx Length, FFthPL: Forelimb Fifth Phalanx Length, FL: Forelimb Length, TL: Tibia Length, FIL: Fibula Length, FL: Femur Length, HPL: Hindlimb Palm Length, HPW: Hindlimb Palm Width, HFPL: Hindlimb Fourth Phalanx Length, HFthL: Hindlimb Fifth Phalanx Length, HL: Hindlimb Length, SSVL / HL: Skeleton Vent Length / Humerus Length, SSVL/TL: Skeleton Vent Length / Tibia Length, SSVL / FL: Skeleton Snout Vent Length / Femur Length, HL/ FFthPL: Humerus Length / Forelimb Fifth Phalanx Length, RL/UL: Radius Length / Ulna Length, FPL / HPL: : Forelimb Palm Length / Hindlimb Palm Length, FPW / HPW: Forelimb Palm Width / Hindlimb Palm Width, FFPL / FPL: Forelimb Fourth Phalanx Length / Forelimb Palm Length, TL/FIL: Tibia Length / Fibula Length, FL/ HFthL: Femur Length / Hindlimb Fifth Phalanx Length, FL/ TL: Femur Length / Tibia Length.

*N: Number of Samples, Min- Max: Minimum- Maximum, SE: Standart Error.

Osteological measurement and Discriminant analysis were applied to the ratios obtained from these measurements in Ayvacık and Bozcaada populations (Figure 3). As a result of this analysis, it was determined that the *H. turcicus* samples in Bozcaada and Ayvacık populations were separated from each other. The first function formed because of the discriminant analysis explained 99.9% of the total variance and the p value was statistically significant (p= 0,000). While the second function formed explained 1% of the variance, the p value was not statistically significant (p=0,773).

In the last step of the analysis (Stepwise procedure), the ratios that best differentiated the two populations were found to be Skull Length/ Skull Width (SL/SW) (F= 43.00; p=0.000) and Skeleton Snout Vent Length/ Skull Length (SSVL /SL) (F=24.46; p=0.000).

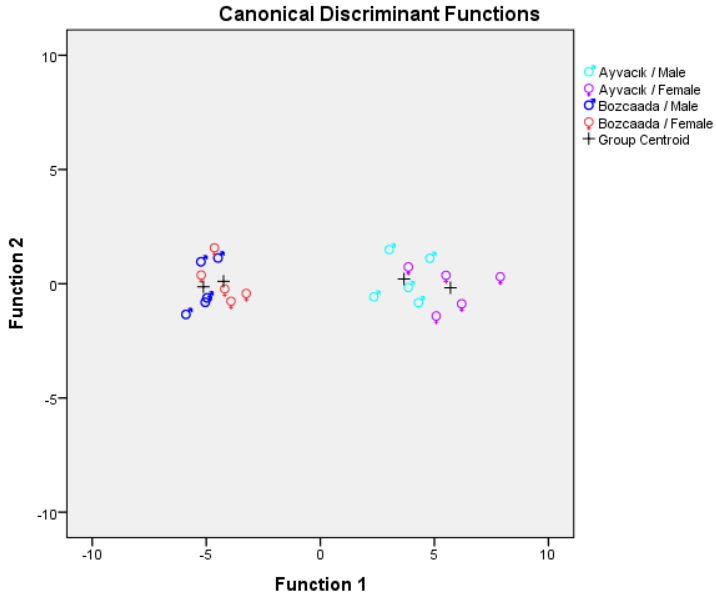

Figure 3. Differential osteological measurements of *H. turcicus* samples from Ayvacık and Bozcaada populations and Discriminant Analysis according to the ratios obtained from these measurements.

DISCUSSION

General osteological studies on *H. turcicus* populations are very few, and information on the detailed postcranial skeleton is limited (Worthy, 1987; Daza et al., 2008; El Bakry et al., 2013; Rothier et al., 2017; Villa et al., 2018).

Due to the size, shape and location, the skull bones are the most important and complex element of the lizard skeleton (Yıldırım et al., 2017). Cranial features of

Hemidactylus turcicus were examined by comparing them with different European gecko species (Daza et al., 2008; Villa et al., 2018).

The frontal entrance of the posterior margins of the nasals was triangular in Ayvacık population, while it was triangular and rounded in Bozcaada population. Villa et al. (2018) were reported in their study that the posterior margins of the nasals were slightly concave for the *H. turcicus* species. Daza et al. (2008) were stated that the shape of the suborbital fenestra in *Sphaerodactylus roosevelti*, which is one of the geckonid species, was D-shaped. However, in Ayvacık and Bozcaada *H. turcicus* populations, the shape of the suborbital fenestra was small and oval. Villa et al. (2018) were reported that the posterior shape of the frontal was a straight line in *H. turcicus* species in the European population. The posterior shape of the frontal was determined as both straight line and slightly concave in Ayvacık population, while it was slightly concave in Bozcaada population. When our findings were compared with the literature, it was determined that there was variation in the Ayvacık population and a difference in the Bozcaada population. Villa et al. (2018) were reported that the anterior process of the postorbitofrontal was longer than the posterior process in the European *H. turcicus* population. The anterior and posterior processes of the postorbitofrontal were found to be shorter than the anterior process in both *H. turcicus* populations. The postparietal process of the parietal was narrow and pointed when the Ayvacık and Bozcaada *H. turcicus* populations were evaluated together. Villa et al. (2018) were reported that for the *H. turcicus* species, the postparietal corners of the parietals end with square ends. The shape of the jugal end was observed as round or pointed in both Ayvacık and Bozcaada populations. Daza et al. (2008) were reported in their research that the jugal end was round in some gecko species (*Sphaerodactylus roosevelti*). The distal end of the prootic is usually round in both populations of *H. turcicus*. In terms of this feature, Villa et al., (2018) were stated in their study that the distal end of the protic was pointed. In our findings, there were variations in this feature in the Ayvacık and Bozcaada *H. turcicus* populations. The posteromedial process of the coronoid was generally round, rarely long, thin and pointed in both Ayvacık and Bozcaada populations. Villa et al. (2018) were reported in their study that the posteromedial process of the coronoid was long, thin and pointed.

Postcranial osteology of *H. turcicus* was examined qualitatively and quantitatively by El-Bakry et al. (2013). When the findings of previous studies were examined, the data obtained from present study are consistent with the literature predominantly. Among the postcranial osteological characters, the humerus and femur were the least modified (El-Bakry et al., 2013). Since the island and the mainland were compared in our study, changes in the movement

mechanisms according to the habitats can be seen in the anterior and posterior extremities. For this reason, some ratios were studied in detail for the first time. TL/FIL ratio was statistically different between populations and this ratio was higher in Ayvacık population.

CONCLUSIONS

The characteristics of the cranial and postcranial bones of *H. turcicus* populations from Ayvacık and Bozcaada were examined in detail, both qualitatively and quantitatively, for the first time. As a result, differences in cranial qualitative characteristics were found in the end of the frontal anterolateral triangular process, coronoid and clavicle bones between *H. turcicus* populations distributed in the mainland and the island. Among the cranial quantitative characteristics, statistically significant differences between populations were determined in the measurements of skull width, skull height, medial width of the parietal, and the ratio of skeleton snout vent length to skull length and skull width, the ratio of skull length to skull width, the ratio of medial parietal length to medial width of the parietal. Differences in postcranial qualitatively characteristics were found in the anterior connection of clavicle bones between *H. turcicus* populations distributed in the mainland and the island. Among the postcranial quantitative features, statistically significant differences were found between the two populations for the skeleton snout vent length, forelimb palm length, forelimb fourth phalanx length, fibula length and hindlimb palm length the ratio of skeleton snout vent length to tibia length, and the ratio of tibula length to fibula length. As a result, *H. turcicus* populations distributed in Bozcaada were found to have variations in both morphological and osteological characters from the mainland populations, and it was determined that the island population differed from the mainland, but there was no difference at the subspecies level. Both populations were found to be included in the subspecies *Hemidactylus turcicus turcicus*. In this study, the total body osteology of the *H. turcicus* distributed on the mainland and the island, was presented in detail for the first time.

Funding: This study was financially supported by Canakkale Onsekiz Mart University Scientific Research Projects Commission (FYL-2021-3717).

Acknowledgements: This study is a part of Master's Thesis, Canakkale Onsekiz Mart University, School of Graduate Studies.

REFERENCES

Agasyan, A., Avci, A., Tuniyev, B., Isailovic, J. C., Lymberakis, P., Andrén, C., Cogalniceanu, D., Wilkinson, J., Ananjeva, N., Üzüm, N., Orlov, N., Podloucky, R, Tuniyev, S., Kaya, U., Vogrin, M., Corti, C., Pérez-Mellado, V., Sá-Sousa, P., Cheylan, M., Pleguezuelos J, Baha El Din S. and Tok, C. V. (2009). *Hemidactylus turcicus*. The IUCN Red List of Threatened Species 2009: [Consulta: 11 noviembre 2015].

Algar, A. C. and Losos, J. B. (2011). Evolutionary assembly of island faunas reverses the classic island–mainland richness difference in Anolis lizards. J. Biogeogr. 38, 1125–1137.

Altunışık, A. (2017). Geniş parmaklı keler (*Hemidactylus turcicus*)'e ait bir populasyonunda yaşam öyküsü özellikleri.

Arnold, E.N., Arribas, O.J. and Carranza, S. (2007): Systematics of the Palaearctic and Oriental lizard tribe Lacertini (Squamata: Lacertidae: Lacertinae), with descriptions of eight new genera. *Zootaxa*, 1430: 1 – 86.

Arnold, S.J. (1983). Morphology, performance and fitness. *American Zoologists*, 23: 347 – 361.

Arribas, O.J. Ilgaz, Ç., Kumlutaş, Y., Durmuş, S.H., Avcı, A. and Üzüm, N. (2013): External morphology and osteology of *Darevskia rudis* (Bedriaga, 1886), with a taxonomic revision of the Pontic and Small-Caucasus populations (Squamata: Lacertidae). *Zootaxa*, 3626(4): 401 – 428.

Baran, İ. and Gruber, U. (1982). Taxonomische Untersuchungen an Türkischen Gekkoniden. *Spixiana*, 5 (2): 109-138.

Baran, İ., Avcı, A., Kumlutaş, Y., Olgun, K. and Ilgaz, Ç. (2021). *Türkiye amfibi ve sürüngenleri*. Ankara: Palme Publishing, 230 pp.

Başoğlu, M. and Baran, İ. (1977). *Türkiye Sürüngenleri*, Kısım 1. Kaplumbağa ve Kertenkeleler. Ege Üniversitesi Fen Fakültesi Kitaplar Serisi No. 76, İlker Matbaası, Bornova- İzmir, 272s.

Baycan, B. and Tosunoğlu, M. (2017). The Catalog of Amphibia and Reptilia Specimens in the Çanakkale Onsekiz Mart University Zoology Museum (COMU-ZM). *Turkish Journal of Bioscience and Collections*, *1*(1), 38-55.

Budak, A., and Göçmen, B. (2014). *Herpetoloji*. (s. 115). Ege Üniversitesi Yayınları Fen Fakültesi Yayın No. 194: Bornova- İzmir.

Caldwell, M. W. (1997). Limb osteology and ossification patterns in Cryptoclidus (Reptilia: Plesiosauroidea) with a review of sauropterygian limbs. *Journal of Vertebrate Paleontology*, *17*(2), 295-307.

Caputo, V. (2004). The cranial osteology and dentition in the scincid lizards of the genus Chalcides (Reptilia, Scincidae). *Italian Journal of Zoology*, *71*(S2), 35-45.

Carranza, S. and Arnold, E. N. (2006). Systematics, biogeography, and evolution of *Hemidactylus* geckos (Reptilia: Gekkonidae) elucidated using mitochondrial DNA sequences. *Molecular phylogenetics and evolution*, *38*(2), 531-545.

Das, M., Bhattacharjee, P. C., Biswa, B. and Purkayastha, J. (2014). Effect of Light and Dark Phase on Dorsum Colour And Pattern in *Hemidactylus Sp*. Of Assam. *Northeast Journal of Contemporary Research*, *1*, 1-7.

Daza, J. D., Abdala, V., Thomas, R., and Bauer, A. M. (2008). Skull anatomy of the miniaturized gecko *Sphaerodactylus roosevelti* (Squamata: Gekkota). *Journal of Morphology*, *269*(11), 1340-1364.

Depew, M. J. (2009). Analysis of skeletal ontogenesis through differential staining of bone and cartilage. *Molecular Embryology: Methods and Protocols*, 37-45.

El-Bakry A. M., Abdeen A. M. and Abo-Eleneen, R. E. (2013). Comparative study of the osteology and locomotion of some reptilian species. *International J. of Biol. and Biol. Sci*, *2*(3), 40-58.

Evans, S. (2008). *The skull of lizards and tuatara*. In: Gans, C., Gaunt AS, Adler K, editors. Biology of the Reptilia, Vol. 20. New York, Society for the Study of Amphibians and Reptiles, 1 – 344 pp.

Fraser, N. C. (1988). The osteology and relationships of Clevosaurus (Reptilia: Sphenodontida). *Philosophical Transactions of the Royal Society of London. B, Biological Sciences*, *321*(1204), 125-178.

Gow, C. E. (1972). The osteology and relationships of the Millerettidae (Reptilia: Cotylosauria). *Journal of Zoology*, *167*(2), 219-264.

Jesus, J., Brehm, A. and Harris, D.J. (2001). Relationships of *Hemidactylus* (Reptilia: Gekkonidae) from the Cape Verde islands: what mito-chondrial DNA data indicate. *J. Herpetol.* 35, 672–675.

Koppetsch, T., Böhme, W., Büsse, S., ve Gorb, S. N. (2020). Comparative epidermal microstructure anatomy and limb and tail osteology of eyelid geckos (Squamata: Eublepharidae): implications of ecomorphological adaptations. *Zoologischer Anzeiger*, *287*, 45-60.

McLeod, M. J. (1980). Differantial staining of cartilage and bone in whole Mouse fetuses by alcian blue and alizarin red S. *Teratology* 22, 299-301.

Müller, J. (2001). Osteology and relationships of *Eolacerta robusta*, a lizard from the Middle Eocene of Germany (Reptilia, Squamata). *Journal of Vertebrate Paleontology*, *21*(2), 261-278.

Özeti, N. (1970). *Anadolu Dağ Kurbağaları ve Bunlara Yakın Bazı Türlerin Karşılaştırmalı Osteolojisi*. Ege Üniv. Fen Fak. Kitap. Ser. No:104.

Presch, W. (1969). Evolutionary osteology and relationships of the horned lizard genus *Phrynosoma* (family Iguanidae). *Copeia*, 250-275.

Rothier, P. S., Brandt R. and Kohlsdorf, T. (2017). Ecological associations of autopodial osteology in Neotropical geckos. *Journal of morphology*, *278*(3), 290-299.

Sindaco, R., Jeremčenko, V. K., Venchi, A. and Grieco, C. (2008). *The reptiles of the Western Palearctic: Annotated checklist and distributional atlas of the turtles, crocodiles, amphisbaenians and lizards of Europe, North Africa, Middle East and Central Asia* (p. 589). Latina: Edizioni Belvedere.

Sunay, F. B. (2005). İkili iskelet boyamaları. *Uludağ Üniversitesi Tıp Fakültesi Dergisi*, *31*(2), 119-126.

Taylor, W. R. (1985). Revised procedures for staining and clearing small fishes and other vertebrates for bone and cartilage study. *Cybium*, *9*, 107-121.

Uetz, Peter, Koo, M. S., Aguilar, R. O. C. Í. O., Brings, Elizabeth, Catenazzi, Alessandro, Chang, A. T., and Wake, D. B. (2021). A quarter century of reptile and amphibian databases. *Herpetological review*, *52*(2), 246-255.

Villa, A., Daza, J. D., Bauer, A. M. and Delfino, M. (2018). Comparative cranial osteology of European gekkotans (Reptilia, Squamata). *Zoological Journal of the Linnean Society*, *184*(3), 857-895.

Wassersug, R. J. (1976). A procedure for differential staining of cartilage and bone in whole formalin-fixed vertebrates. *Stain technology*, *51*(2), 131-134.

Worthy, T. H. (1987). Osteological observations on the larger species of the skink Cyclodina and the subfossil occurrence of these and the gecko *Hoplodactylus duvaucelii* in the North Island, New Zealand. *New Zealand journal of zoology*, *14*(2), 219-229.

Yıldırım, E., Kumlutaş, Y., Candan, K., and Ilgaz, Ç. (2017). Comparative skeletal osteology of three species of Scincid lizards (Genus: Ablepharus) from Turkey. *Vertebrate Zoology*, *67*(2), 251-259.

Chapter 3

New Natural Inventions Against Hair Loss (Alopecia)

Hülya ÇELİK ONAR[1]

Hasniye YAŞA[2]

[1] Assoc.Prof. Hülya ÇELİK ONAR İstanbul University-Cerrahpaşa, Engineering Faculty, Chemistry Department, Organic Chemistry Devision Avcılar, İstanbul, Turkey ORCID: 0000-0003-2573-5751. E mail: hcelik@iuc.edu.tr

[2] Assoc.Prof. Hasniye YAŞA İstanbul University-Cerrahpaşa, Engineering Faculty, Chemistry Department, Organic Chemistry Devision Avcılar, İstanbul, Turkey ORCID: 0000-0003-3171-9096.

ABSTRACT

A filament known as hair is primarily made up of keratinized, dead cells. The two elements that make up the structure of hair are the hair follicle and the hair shaft. Bulb and peribulbar are located in the lower part of the hair root, and infundibulum and isthmus are located in the lower part. Together, the dermal papilla, which is composed of specialized fibroblasts, blood arteries, and nerve endings, and the hair matrix, which is composed of keratinocytes that are reproducing quickly, create the hair bulb. The subcutis is where scalp hair follicles are anchored and they go through repeated growth cycles. The cuticle, cortex, and medulla are the three layers that make up the hair shaft. The farthest part of the hair visible on the skin is called the medulla. The root sheath, which is a defensive layer, surrounds it (Scheme 1).

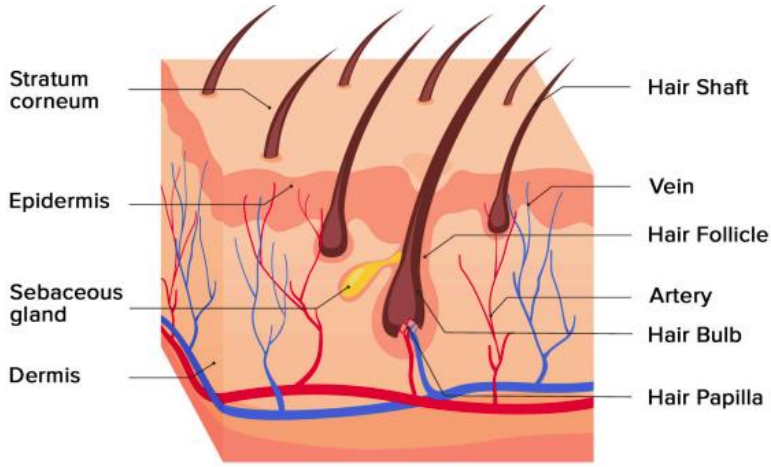

Scheme 1. Structure of Hair

Different hormones have a significant effect on the hair cycle and the development of the hair follicle. Androgens like testosterone (T), dihydrotestosterone (DHT), and their prohormones dehydroepiandrosterone sulfate (DHEAS) and androstenedione (A) are the principal causes of terminal hair growth. The intracellular enzyme 5-alpha reductase is required for most hair follicles to convert testosterone to DHT. Affecting the activity of the aromatase enzyme, which binds to estrogen receptors and converts androgen to DHT, estradiol can drastically alter the growth and turnover of hair follicles (Grymowicz et al., 2020:5342).

Hair care and treatment have changed dramatically over time as a result of ongoing research into new formulations to try to suit the demand in the cosmetic and pharmaceutical industries. Modern hair treatments are mainly concerned with preventing hair loss problems, and enhancing hair follicle

qualities. Hair washing, which aims to maintain and clean the hair, as well as hair colouring and bleaching formulas for hair decoration, are considered standard hair care operations.

Alopecia or hair loss can occur temporarily or permanently as a result of hereditary factors, hormonal changes, diseases or aging. Hair loss can only have negative effects on mental health, it has no other negative effects on the body (Znidaric et al., 2021:435). One of the most common causes of hair loss, seen in 53% of men and 30% of women, is androgenic alopecia (AGA) (Lolli et al., 2017:9; Rossi et al., 2019:E279; Norwood, 2001:53; Lee and Lee, 2012:243). Some people choose to let their hair loss progress naturally without treatment or camouflage. The vast majority use one of the treatments offered to stop hair loss or stimulate growth. The most popular drugs for the treatment of AGA are; Minoxidil, a topical hair growth stimulant, finasteride, a 5α-reductase inhibitor, and Diclofenac, an anti-inflammatory drug. However, they all have some limitations. For example, minoxidil has been associated with skin irritants such as stinging and itching, while finasteride has been associated with erectile dysfunction in men after long-term use (Sakr et al., 2013:413; Kiguradze et al., 2016:221) Therefore, there is a pressing need to develop new therapies that can successfully encourage hair regrowth and are also biocompatible.

Due to rising beauty awareness and increasing demand for skin care, cosmetics and beauty products, the global cosmetics industry is expanding rapidly. With the growth of this lucrative industry, a new consumer preference for natural, environmentally friendly and sustainably derived cosmetics has developed over synthetic products, fueling growth in the global herbal extracts market. Plants have traditionally been an important source of bioactive substances with a variety of applications. They offer antioxidants, UV radiation protection, anti-aging, anti-wrinkle, anti-cancer and skin-altering (soothing, moisturizing or whitening) qualities, among other proven health and wellness benefits (Georgiev et al., 2018:779). Therefore, there is a pressing need to create new treatments that may effectively encourage hair regrowth and are also biocompatible.

One of the most popular beverages consumed worldwide is undoubtedly coffee. Colombia and Vietnam are the next-largest producers of coffee after Brazil. Coffee is a good source of income, especially for developing countries. In addition to the use of coffee as a beverage, its applicability has expanded in many industrial sectors, including the beauty industry. Consuming it has been linked to several health advantages, including a reduced risk of type II diabetes and protection against neurodegenerative diseases (Wu et al., 2022:101373; Ludwig et al., 2014: 1695). These benefits are largely attributed to the presence

of two main bioactive groups, phenolic compounds and alkaloids. These substances also have dermocosmetic properties related to hair care, skin health and beauty (Herman and Herman, 2013:8; Saewan, 2022:66). Each year, the amount of waste from the use and production of coffee, such as waste coffee grounds, damaged or immature coffee beans, leaves, husks, pulp, silver bark and greens, is enormous. Evaluation of coffee by-products, which contain abundant phenolic compounds, caffeine, fatty acids, diterpenes, tocopherols and other beneficial components, is essential for the economy and society. Bioactive substances found in coffee and its by-products have been proven to have anti-inflammatory, antibacterial, emollient, antioxidant, UV protective, antityrosinase, anticollagenase, antielastase, anti-inflammatory and antilipogenic activities. Because it contains phenolic chemicals like caffeine and chlorogenic acids, coffee is used as a cosmetic ingredient. Due to its abilities to prevent aging and photodamage and its lipolytic effects on cellulite and hair regeneration, caffeine is commonly employed in cosmetic formulations. Powerful antioxidants with anti-aging and photoprotective properties are chlorogenic acids (Rodrigues et al., 2023:12). Coffee beans and their byproducts are used as ingredients in a variety of compositions, including creams, lotions, shampoos, soaps, essences, and serums. These by-products include pulp, leaves, silver bark, and discarded coffee grounds. These compositions claim anti-aging, moisturizers, sun protection, hair growth, anti-dandruff and other properties and are primarily for use on non-specific skin areas, eye areas, scalp and lip skin. In conclusion, coffee and its by-products are promising ingredients that can be added to topical formulations to guarantee skin health benefits and reduce their environmental impact (de Mello et al., 2023:1).

In this study, the plant Ulmus davidiana (UD), which has a wide variety of medicinal uses, was used. The mechanism of supercritical fluid extract residues of Ulmus davidiana extract against hair loss was investigated through the control of cytokine production and hormone activity in human dermal follicle papilla cells. In addition, it was investigated how H2O2-mediated cytokines, dihydrotestosterone hormone synthesis and anti-apoptosis effects were modulated. The findings show that the extracted Ulmus davidiana supercritical fluid extraction residues contain functional compounds and are promising candidates for baldness treatment (Kwon et al., 2022:1419).

In another study, the effect of Connarus semidecandrus Jack plant, which is used as a folk remedy in tropical locations to treat fever, against hair loss was investigated. The anti-androgenic alopecia effect of Connarus semidecandrus Jack (Cs-EE) ethanol extract was revealed in this study in terms of hair-skin

ratio, hair type density and hair thickness. After Cs-EE treatment, it has been shown to restore hair growth and promote hair growth in the area of the thickened hair population (Jang et al., 2022:4086).

It has been demonstrated that oleanolic acid from food and plants, as well as its isomer ursolic acid, exhibit various biological activities for skin-related disorders. The ability of these phytochemicals found in foods and plant materials to eliminate dysregulation brought on by inflammatory or oxidative stress pathways, as well as other mechanisms, was examined in several in vitro and in vivo research emphasized in this review. Androgenic alopecia, acne vulgaris, and skin aging, including the development of wrinkles and hyperpigmentation, are the most common skin-related problems. These disorders have oxidative and inflammatory pathways as their primary targets. Oleanolic and ursolic acids are intriguing candidates for application in cosmeceutical products, according to the studies that were analyzed (Mejía-Valdez et al., 2023:576).

Banana flowers contain a large number of bioactive substances. However, no studies have been conducted on hair with this herb. In this study, it was examined how banana flower extracts can strengthen hair follicles and stop hair loss. This study discovered that, in vitro, the expression of genes associated with hair growth was increased by banana flower extracts, while the expression of ROS and DHT was decreased. In the clinical study, participants who took banana flower extracts saw reduced scalp redness and hair loss. It contains antioxidant flavonoids and phenolic compounds that promote healthy hair growth in patients taking banana flower extract supplements. In this study, antioxidant activity of banana flowers (Musa paradicicus) from various cultivars such as Kathali, Bichi, Shinapuri, Kacha, Champa and Kalabou were investigated. The Kacha variety showed the highest total antioxidant capacity (TAC), DPPH scavenging activity and free radical scavenging activity, as well as the highest concentration of polyphenols and flavonoids. (Liang et al., 2023:1917).

A class of therapeutic plants known as adaptogens has the potential to broadly improve human resistance. Although the majority of plant adaptogens have useful applications in dermatology, there are presently few investigations on their specific actions and cooperative mechanisms when applied topically to the skin. We discovered that atopic dermatitis, acne, allergic contact dermatitis, psoriasis, eczema, and androgenetic alopecia are the key skin conditions that plant adaptogens have an impact on. Anti-aging and antiphotoaging, anti-bacterial and anti-fungal, anti-inflammatory, whitening, and hair loss prevention are the key effects on skin health. Additionally, based on the findings of the

patent study, it is discovered that the effects of plant adaptogens on skin primarily center on delaying the onset of aging. Terpenoids, phenolic compounds, and flavonoids are the principal phytochemical components of plant adaptogens that have dermatological effects, and they are found primarily in the Fabaceae Lindl., Araliaceae Juss., and Lamiaceae Martinov. families of plants (Liu et al., 2023: 341).

Due to the negative consequences of chemically manufactured components, natural products are becoming more popular in skin and hair treatments. The purpose of this study is to examine the cosmeceutical benefits of Equisetum debile (horsetail) extracts in relation to tyrosinase-mediated inhibition of hyperpigmentation, matrix metalloproteinase-mediated inhibition of wrinkle formation, and 5α-reductase-mediated inhibition of androgenic alopecia. Total phenolic content in the ethylacetate fraction was found to be 39.24 ± 0.72 mg gallic acid/g, while anti-tyrosinase activity was found to be 583.33 ± 23.59 mg kojic acid/g. It was also stated that the IC50 inhibitions of collagenase for MMP-1 and MMP-2 were 0.82 ± 0.09 and 0.94 ± 0.11 mg/mL, respectively. All extracts showed significant inhibition of 5α-reductase, while the dichloromethane fraction showed the best activity with a value of 83.07 ± 3.46%. In conclusion, E. debile extracts have potential as cosmeceuticals. According to this research, the ethyl acetate fraction of E. debile may be a potential substance for the natural treatment of hyperpigmentation and the prevention of skin aging. As a result, dichloromethane fraction (horsetail) of Equisetum debile was given as an option that can be used effectively instead of the recommended 1 mg/day Finasteride against hair loss (Thammarat et al., 2023:1336).

Trace elements are very important in the formation of immune cells and healthy hair follicles (Almohanna et al., 2019:51). Zn^{2+}, for example, is one of the most important essential components in hair follicles (Almohanna et al., 2019:51; Finner, 2013:167). In addition to Zn^{2+}, Cu^{2+} is also important for the health of hair follicles, as it can be combined with the human tripeptide glycyl-l-histidyl-L-lysine to further enlarge the hair follicle and prevent hair loss (Pickart, 2008:969; Makowska et al., 2018:80; Pickart and Margolina, 2018:1987). In light of this knowledge, a nanocomposite microneedle (ZCQ/MN) patch was created as part of this study as a combined therapy for androgenic alopecia (AGA). The patch contains quercetin (ZCQ) loaded copper/zinc doped mesoporous silica nanoparticles. Following skin penetration, the biodegradable microneedle slowly disintegrates and releases the ZCQ nanoparticles. Quercetin (Qu), copper (Cu^{2+}), and zinc ions (Zn^{2+}) are released by ZCQ nanoparticles subcutaneously to collectively enhance hair follicle

regeneration. This study shows the effectiveness of systematic intervention targeting several pathophysiological connections of AGA by the combination of organic medicines and bioactive metal ions, laying the theoretical groundwork for the creation of biomaterial-based anti-hair loss therapy (Zhang et al., 2023:81).

The organ most vulnerable to the effects of the exposome is the skin. It safeguards interior organs through the epidermis' barrier function since it is situated at the point where the external environment meets the body. It must adjust to the results of solar radiation's negative effects, the numerous chemical pollutants in the atmosphere, and wounds brought on by mechanical damage, such as inflammation, cytotoxicity, oxidation and other conditions. In this biological setting, the ability to respond to the many pressures brought on by the exposome is crucial; otherwise, more or less significant problems, such as accelerated aging, pigmentation disorders, atopy, psoriasis, and skin malignancies, may emerge. At this level, Nrf2-controlled pathways are crucial. A transcription factor called Nrf2 regulates the genes that defend against oxidative stress and detoxify pollutants. It has been shown to contribute to the prevention of UV damage, control of inflammation throughout the healing process, epidermal differentiation for barrier function, and hair growth. This is intriguing given the scarcity of published information. In these experiments, it was discovered that the triterpenoid RTA-408, an activator of Nrf2, significantly accelerated the regrowth of mouse hair exposed to X-rays (Reisman et al., 2014:512; Haslam et al., 2017:295). Sulforaphane can activate Nrf2 in the hair follicle, which offers defense against stressors like menadione or hydrogen peroxide treatment. Numerous cosmetic products on the market, primarily skin care products for anti-aging, skin protection, and recovery from external stressors, but also some hair care products for things like anti-hair loss and even some nutraceuticals, have been reported to act on Nrf2 (Li et al., 2016:39336). The majority of the time, marketed ingredients aren't pure tiny molecules; instead, they're a mixture of natural substances or one or more plant extracts. This also satisfies customers' growing need for naturalness (Frantz et al., 2023:32).

Common hair irregularities that impair physical appearance and lead to psychological issues include alopecia and gray hair. Chemical therapies produce painful side effects yet only partially heal hair abnormalities. Instead of pharmaceutical agents with high adverse consequences, active plant substances represent interesting sources of new therapeutic medicines. Bue Bang 3 CMU (BB3CMU) and Bue Bang 4 CMU (BB4CMU) rice varieties grown in northern Thailand were used in this study. The effects of rice husk (H), defatted rice bran

extract (DFRB) and Rice bran oil (RBO) obtained from rice varieties on hair regeneration were evaluated in terms of melanin production, steroid 5α-reductase inhibition and nitric oxide (NO) secretion. BB4CMU-RBO was the variety that showed the best activity with high iron, zinc and free fatty acid concentrations and it was suggested that it could be a candidate for hair revitalizing compound (Ruksiriwanich et al., 2023:653).

The goal of the current study was to create and improve caffeine-loaded nanostructured lipid carriers (NLCs) for the topical treatment of alopecia. The solubility of several excipients with drugs was tested. To optimize NLCs, the 23 complete factorial design was used. The independent variables were lipid type, surfactant type, and medication concentration. The chosen responses were entrapment efficiency (EE), particle size, polydispersity index (PDI), and percent drug release (Makky et al., 2021:1).

In a different investigation, niosome formulations enriched with pumpkin seed oil (PSO) were created to improve skin penetration and hair follicle accumulation. The effectiveness of PSO-loaded niosomes in preventing hair loss by inhibiting 5α-reductase and lowering inflammation caused by interleukin-6 (IL-6) inhibition was assessed (Teeranachaideekul et al., 2022:930).

Acanthus ebracteatus Vahl's 95% ethanol extract (AE) and verbascoside (VB), a biomarker of AE extract, were used in this investigation. Using the MTT test and flow cytometry, the effects of these extracts on cell viability and the cell cycle were examined. In in vitro experiments held at different doses, it was discovered that AE extract and VB stimulated dermal papilla cell proliferation by detecting the increase in cell number in S and G2/M stages. It was emphasized that AE extract at 250 g/mL concentration or VB extract at 62.50 g/mL concentration statistically significantly reduced testosterone-induced cell death. In addition, it was also noted that the release of proinflammatory cytokines from dermal papilla cells was significantly reduced by both AE extract and VB. Based on these findings, it was suggested that Acanthus ebracteatus Vahl extracts used in the study are effective components for anti-hair loss treatments (Wisuitiprot et al., 2022:1491).

The current study sought to determine whether coffee berry extract (CBE) has any anti-aging effects on human dermal fibroblast (HDF) and hair follicle dermal papilla (HFDP) cells. 50% ethanol was used to extract the coffee berry, and HPLC analysis was used to identify its chemical components. By using the MTT assay, the extract's cytotoxicity was evaluated in both cell types. In HFDP cells, the effects of anti-hair loss qualities were examined by taking into account growth factor expression, cell proliferation, and 5α-reductase inhibition (5AR).

The findings demonstrated that coffee berry extract (CBE) has anti-aging effects on both skin and hair cells and suggested that it might have uses in cosmeceuticals (Saewan, 2022:66).

In this work, the ability of the mountain plant Edelweiss, Leontopodium alpinum var. Helvetia, to regulate hair follicle (HF) growth ex vivo, inhibit hair loss, and promote hair regeneration in vivo has been examined. The results of the study showed that the selected plant extract inhibited early catagen induction by stimulating dermal papilla inducibility, which proved that this plant extract can be used both to prevent hair loss due to aging and as an adjuvant treatment for hair loss disorders (Campiche et al., 2022:363).

Finasteride and minoxidil both play an important part in reversing and delaying hair loss, but they each have unique side effects and efficacy restrictions. In this study, the results of Trust tonic solution containing 1% w/w Capixyl, 1% w/w Procapil, 0.5% rosemary extract were compared with the results of minoxidil compound at 2% concentration. Experiment results revealed that this mixture could be an alternative to Minoxidil (Eslahi et al., 2022:346).

In another study, Ethanol extracts of Acacia concina (Wild.) DC., Acanthus ebracteatus Vahl, Bridelia ovata Decne, Cleome viscosa L., Cocos nucifera L., Hibiscus subdariffla L., Oryza sativa L., Terminalia chebula Retz., Tinospora Crisp investigated against hair loss. Only Acanthus ebracteatus Vahl plant extract has been reported to be active in this regard (Wisuitiprot et al., 2022:6109).

In another study, it was stated that Watercress extract (WCE) has a strong anti-androgenic effect and can be used against hair loss (Hashimoto et al., 2022:154).

In this study, a lotion called SERUM THICKER was tried against hair loss for a period of 6 months. A lotion called SERUM THICKER has 97% botanical components, including 5% Capixyl®. A biomimetic signal peptide with red clover extract that is high in biochanin A is called Capixyl®.Neither a significant effect on hair thickness nor a change in hair shedding was seen during the wash test (Fanian et al.2022:51).

Another study was done with "Trimax-360 Serum" for androgenic alopecia. This serum is herbal and contains organic Argan oil, Jojoba oil, grape seed oil, tocotrienols and capric/caprylic triglycerides. As a result of this study, it was observed that 100% of users of the product had decreased bald areas after using, enhanced hair growth over time, and a minor rise in the amount of visible new hair (Chew et al., 2022:4536).

In this clinical investigation, alopecia patients' use of a shampoo containing salicylic acid (0.2%), panthenol (0.2%), and niacinamide (0.1%) to prevent hair loss was examined. According to this study, shampoo therapy may be able to stop hair loss in alopecia patients (Kim et al., 2022:173).

Without any supporting scientific data, shallot (Allium ascalonicum L.) was used in Thai folk medicine to promote hair growth. In this study, it was aimed to determine the bioactive compounds in shallot extract and to evaluate their hair growth promoting activities. The findings show that the main components of the methanolic shallot extract are phenolic compounds, specifically quercetin, rosmarinic, and p-coumaric acids. These results show that shallot extract enhances the promotion of hair growth through the downregulation of androgen gene expression and may be further developed as nutraceutical, nutricosmetic, and cosmeceutical preparations for the treatment of AGA (Ruksiriwanich et al., 2022:1499).

In this work, the possible impact of cucurbitacin on hair development and the expression of FGF18 in mice were investigated. According to the study's findings, cucurbitacin, which is derived from plants in the Cucurbitaceae family and has a variety of pharmacological effects and potential for treating skin conditions, can be thought of as a fresh and useful ingredient for the creation of anti-hair loss products (Guo et al., 2022:1104).

In this work, native Thai red (Sang-Yod-SY and Mun-Poo-MP) and black (Black sticky-BG and Hom-Nil-HN) pigmented rice (Oryza sativa L.) extracts were used to examine hair development. According to the findings, SY red rice extract had considerably higher 5α-reductase inhibitory activity (18.5±9.0 mgFEA/g extract) and had a large amount of proanthocyanidin (1.50±0.16 mgECE/g extract). This study indicates the potential of SY red pericarp extract as a 5α-reductase inhibitor and natural hair growth promoter (Thitipramote et al., 2022:111).

The well-known tropical tree known as the guava (Psidium guajava L.) is commonly cultivated for its fruit in tropical regions. In this study, the ethanol extract of P. guajava leaves examined for hair loss. It has been suggested that this extract could be further developed as alternative products or therapeutic adjuvants to treat AGA and other androgen-related diseases (Ruksiriwanich et al., 2022:3514).

In a different study, the hair-growth capabilities of boehmite (Aluminum hydroxide) were examined in vitro and in vivo, and it was found that hDPCs (Human dermal papilla cells) proliferated in a dose-dependent manner in vitro and that hair regrowth occurred in a mouse model (Bak et al., 2020:341).

REFERENCES

Almohanna, H.M., Ahmed, A.A., Tsatalis, J.P., and Tosti, A. (2019). The role of vitamins and minerals in hair loss: A review. Dermatologic Therapy, 9 (1), 51–70.

Bak, D.H., Lee, E., and Lee, B.C. (2020). Boehmite enhances hair follicle growth via stimulation of dermal papilla cells by upregulating β-catenin signalling. Experimental Dermatology, 29, 341–348.

Campiche, R., Le Riche, A., Edelkamp, J., Botello, A.F., Martin, E., and Gempeler, M. (2022). An extract of Leontopodium alpinum inhibits catagen development ex vivo and increases hair density in vivo. International Journal of Cosmetic Science, 44, 363–376.

Chew, S.K., Gajjar, T., and Sethi, S. (2022). Safety and efficacy of Trimax-360 serum in healthy adult subjects with mild to moderate alopecia of scalp. Journal of Cosmetic Dermatology, 21, 4536–4544.

de Mello, V., de Mesquita Júnior, G.A., Alvim, J.G.E., Costa, J.C., and Vilela F.M.P. (2023). Recent patent applications for coffee and coffee by-products as active ingredients in cosmetics. International Journal of Cosmetic Science, 1–21.

Eslahi, E., Hashemi, N., and Shamaei, S. (2022). Effectiveness of the active ingredients (Capixyl, Procapil, and rosemary extract) of the Trust® tonic for the treatment of androgenetic alopecia in comparison to minoxidil. Our Dermatology Online, 13(4), 346-351.

Fanian, F., Meunier, P., Bumbea, D., Dahel, K. and Humbert, P. (2022) Efficacy and Safety of a Botanical Topical Serum on Male and Female Androgenetic Alopecia. Journal of Cosmetics, Dermatological Sciences and Applications, 12, 51-66.

Finner, A.M. (2013). Nutrition and hair deficiencies and supplements. Dermatologic Clinics, 31(1), 167–172.

Frantz, M.C., Rozot, R., and Marrot, L. (2023). NRF2 in dermo-cosmetic: From scientific knowledge to skin care products. BioFactors, 49(1), 32–61.

Georgiev, V., Slavov, A., Vasileva, I., and Pavlov, A. (2018). Plant Cell Culture as Emerging Technology for Production of Active Cosmetic Ingredients. Engineering in Life Sciences, 18, 779–798.

Grymowicz, M., Rudnicka, E., Podfigurna, A., Napierala, P., Smolarczyk, R., Smolarczyk, K., and Meczekalski, B. (2020). Hormonal Efects on Hair Follicles. International Journal of Molecular Sciences, 21, 5342-5355.

Guo, K., Wang, L., Zhong, Y., Gao, S., Jing, R., Ye, J., Zhang, K., Fu, M., Hu, Z., Zhao, W., and Xu, N. (2022). Cucurbitacin promotes hair growth in

mice by inhibiting the expression of fibroblast growth factor 18. Annals of Translational Medicine, 10(20), 1104-1114.

Hashimoto, M., Kawai, Y., Masutani, T., Tanaka, K., Ito, K., and Iddamalgoda, A. (2022). Effects of watercress extract fraction on R-spondin 1-mediated growth of human hair. International Journal of Cosmetic Science, 44, 154–165.

Haslam, I.S., Jadkauskaite, L., Szabo, I.L., Staege, S., Hesebeck-Brinckmann, J., and Jenkins, G. (2017). Oxidative damage control in a human (mini-) organ: Nrf2 activation protects against oxidative stress-induced hair growth inhibition. Journal of Investigative Dermatology, 137, 295–304.

Herman, A., and Herman, A.P. (2022). Caffeine's mechanisms of action and its cosmetic use. Skin Pharmacol. Physiol. 2013, 26, 8–14.

Jang, W.Y., Kim, D.S., Park, S.H., Yoon, J.H., Shin, C.Y., Huang, L., Nang, K., Kry, M., Byun, H.W., and Lee, B.H. (2022). Connarus semidecandrus Jack Exerts Anti-Alopecia Effects by Targeting 5α-Reductase Activity and an Intrinsic Apoptotic Pathway. Molecules, 27, 4086-4102.

Kiguradze, T., Temps, W.H., Kantor, R., Lyon, S., West, D.P., and Belknap, S.M. (2016). Evaluation of risk of SSRI-associated impotence and low libido in men exposed to finasteride. Journal of the American Academy of Dermatology, 74(5), AB221-AB221.

Kim, H.T., Park, H.S., Kim, Y.M., Lee, I.C., Lee, S.J. and Choi, J.S. (2022). Double-blind randomized placebo-controlled study of the efficacy and safety of hair loss prevention shampoo containing salicylic acid, panthenol, and niacinamide in alopecia patients. Toxicology and Environmental Health Sciences, 14, 173–185.

Kwon, Y.E., Choi, S.E., and Park, K.H. (2022). Regulation of Cytokines and Dihydrotestosterone Production in Human Hair Follicle Papilla Cells by Supercritical Extraction-Residues Extract of Ulmus davidiana. Molecules, 27, 1419-1430.

Lee, W.S. and Lee, H.J. (2012). Characteristics of androgenetic alopecia in Asian. Annals of Dermatology, 24(3), 243–252.

Li, J., Liu, D., Wu, J., Zhang, D., Cheng, B., and Zhang, Y. (2016). Ginsenoside Rg1 attenuates ultraviolet B-induced glucocortisides resistance in keratinocytes via Nrf2/HDAC2 signalling. Scientific Reports, 6, 39336-39346.

Liang, C.H., Lin, Y.H., Lin, Y.K., and Chiang, C.F. (2023). Hair growth-promotion effects and antioxidant activity of the banana fl ower extract HappyAngel®: double-blind, placebo-controlled trial. Food Science and Human Wellness, 12, 1917-1923.

Liu, X.X., Chen, C.Y., Li, L., Guo, M.M., He, Y.F., Meng, H., Dong, Y.M., Xiao, P.G., and Yi, F. (2023). Bibliometric Study of Adaptogens in Dermatology: Pharmacophylogeny, Phytochemistry, and Pharmacological Mechanisms. Drug Design, Development and Therapy, 341-361.

Lolli, F., Pallotti, F., Rossi, A., Fortuna, M.C., Caro, G., Lenzi, A., Sansone, A., and Lombardo, F. (2017). Androgenetic alopecia: a review. Endocrine, 57(1), 9–17.

Ludwig, I.A., Clifford, M.N., Lean, M.E., Ashihara, H., and Crozier, A. (2014). Coffee: Biochemistry and potential impact on health. Food and Function, 5, 1695–1717.

Makky, A., Sadddar, E., Gala, D., and Khattab, A. (2021). Skin Targeting of An Optimized Caffeine Nanostructured Lipid Carrier With Improved Efficiency Against Chemotherapy Induced Alopecia. Research Square, 1-27.

Makowska, J., Tesmar, A., Wyrzykowski, D., and Chmurzynski, L. (2018). Investigation of the binding properties of the cosmetic peptide argireline and its derivatives towards copper(II) ions. Journal of Solution Chemistry, 47 (1), 80–91.

Mejía-Valdez, D., Antunes-Ricardo, M., Martínez-Ávila, M. and Guajardo-Flores, D. (2023). Potential Role of Oleanolic and Ursolic Acids from Food and Plant Materials as Natural Ingredients for the Cosmetic Industry: A Review. ACS Food Science and Technology, 3, 4, 576–591.

Norwood, O.T. (2001). Incidence of female androgenetic alopecia (female pattern alopecia). Dermatologic Surgery, 27(1), 53–54.

Pickart, L. (2008). The human tri-peptide GHK and tissue remodeling. Journal of Biomaterials Science, Polymer Edition. 19 (8), 969–988.

Pickart, L., and Margolina, A. (2018). Regenerative and protective actions of the GHK-Cu peptide in the light of the new gene data. International Journal of Molecular Sciences, 19 (7), 1987-1999.

Reisman, S.A., Lee, C.Y., Meyer, C.J., Proksch, J.W., Sonis, S.T., and Ward, K.W. (2014). Topical application of the synthetic triterpenoid RTA 408 protects mice from radiation-induced dermatitis. Radiation Research, 181, 512–520.

Rodrigues, R., Oliveira, M.B.P.P., and Alves, R.C. (2023). Chlorogenic Acids and Caffeine from Coffee By-Products: A Review on Skincare Applications. Cosmetics, 10, 12-27.

Rossi, A., D'Arino, A., Pigliacelli, F., Caro, G., Muscianese, M., Fortuna, M.C., and Carlesimo, M. (2019). The diagnosis of androgenetic alopecia

in children: considerations of pathophysiological plausibility. Australasian Journal of Dermatology, 60(4), E279–E283.

Ruksiriwanich,W., Khantham, C., Muangsanguan, A., Phimolsiripol, Y., Barba, F.J., Sringarm, K., Rachtanapun, P., Jantanasakulwong, K., Jantrawut, P., and Chittasupho, C. (2022). Guava (Psidium guajava L.) Leaf Extract as Bioactive Substances for Anti-Androgen and Antioxidant Activities. Plants, 11, 3514-3527.

Ruksiriwanich,W., Khantham, C., Muangsanguan, A., Chittasupho, C., Rachtanapun, P., Jantanasakulwong, K., Phimolsiripol, Y., Sommano, S.R., Sringarm, K., and Ferrer, E. (2022). Phytochemical Constitution, Anti-Inflammation, Anti-Androgen, and Hair Growth-Promoting Potential of Shallot (Allium ascalonicum L.) Extract. Plants, 11, 1499-1512.

Ruksiriwanich,W., Linsaenkart, P., Khantham, C., Muangsanguan, A., Sringarm, K., Jantrawut, P., Prom-u-thai, C., Jamjod, S., Yamuangmorn, S., Arjin, C. (2023). Regulatory Effects of Thai Rice By-Product Extracts from Oryza sativa L. cv. Bue Bang 3 CMU and Bue Bang 4 CMU on Melanin Production, Nitric Oxide Secretion, and Steroid 5-Reductase Inhibition. Plants, 12, 653-668.

Saewan, N. (2022). Effect of coffee berry extract on anti-aging for skin and hair—In vitro approach. Cosmetics, 9, 66-85.

Sakr, F.M., Gado, A.M., Mohammed, H.R., and Adam, A.N.I. (2013). Preparation and evaluation of a multimodal minoxidil microemulsion versus minoxidil alone in the treatment of androgenic alopecia of mixed etiology: a pilot study. Drug Design, Development and Therapy, 7, 413–423.

Teeranachaideekul, V., Parichatikanond,W., Junyaprasert, V.B., and Morakul, B. (2022). Pumpkin Seed Oil-Loaded Niosomes for Topical Application: 5α-Reductase Inhibitory, Anti-Inflammatory, and In Vivo Anti-Hair Loss Effects. Pharmaceuticals, 15, 930-944.

Thammarat, P., Jiaranaikulwanitch, J., Phongpradist, R., Raiwa, A., Pandith, H., Sawangrat, K., and Sirilun, S. (2023). Cosmeceutical Potentials of Equisetum debile Roxb. Ex Vaucher Extracts. Applied Sciences, 13, 1336-1359.

Thitipramote, N., Imsonpang, S., Sukphopetch, P., Pradmeeteekul, P., Nimkamnerd, J., Nantitanon,W., Chaiyana, W. (2022). HealthBenefits and Safety of Red PigmentedRice (Oryza sativa L.): In Vitro,Cellular, and In Vivo Activities for Hair Growth Promoting Treatment. Cosmetics, 9, 111-122.

Wisuitiprot, V., Ingkaninan, K., Wisuitiprot, W., Srivilai, J., Chakkavittumrong, P., and Waranuch, N. (2022). Effects of some medicinal plant extracts on dermal papilla cells. Journal of Cosmetic Dermatology, 21, 6109–6117.

Wisuitiprot, V., Ingkaninan, K., Chakkavittumrong, P., Wisuitiprot, W., Neungchamnong, N., Chantakul, R., and Waranuch, N. (2022). Effects of Acanthus ebracteatus Vahl. extract and verbascoside on human dermal papilla and murine macrophage. Scientific Reports, 12, 1491-1503.

Wu, H., Gu, J., Bk, A., Nawaz, M.A., Barrow, C.J., Dunshea, F.R., and Suleria, H.A.R. (2022). Effect of processing on bioaccessibility and bioavailability of bioactive compounds in coffee beans. Food Bioscience, 46, 101373-101386.

Zhang, Z., Li, W., Chang, D., Wei, Z., Wang, E., Yu, J., Xu, Y., Que, Y., Chen, Y., Fan, C., Ma, B., Zhou, Y., Huan, Z., Yang, C., Guo, F., and Chang, J. (2023). A combination therapy for androgenic alopecia based on quercetin and zinc/copper dual-doped mesoporous silica nanocomposite microneedle patch. Bioactive Materials, 24, 81–95.

Znidaric, M., Zurga, Z.M., and Maver, U. (2021). Design of in vitro hair follicles for different applications in the treatment of alopecia-A review. Biomedicines, 9(4), 435-454.

Chapter 4

Human Mosquito-Borne Diseases, Their Vectors, and a Major Challenge in the Fight: Insecticide Resistance in the Vector Mosquito Populations of Türkiye

Sare İlknur YAVAŞOĞLU[1]

[1] Assist. Prof. Dr; Aydın Adnan Menderes University, Faculty of Science, Department of Biology, sarecihangir@adu.edu.tr; ORCID No: 0000-0002-9055-1556

ABSTRACT

Mosquitoes are capable of being vector of several dangerous infectious agents such as protozoa, viruses, bacteria and parasites. Mosquito-borne diseases leads mortality and morbidity among human and animal populations. Aedes, Anopheles and Culex mosquitoes rank among the most important global vectors of human diseases. Of these species, Anopheles sacharovi, Anopheles superpictus, Culex pipiens, Culex tritaeniorhynchus, Aedes caspius are widely distributed in Türkiye. Like these species, Aedes albopictus is another threatening mosquito species as it is highly invasive in all over the World as well as Türkiye. Anopheles sacharovi and Anopheles superpictus are vectors of malaria in Türkiye; Culex pipiens, Culex tritaeniorhynchus and Aedes caspius are capable of transmistting West Nile Virus and pose risk in terms of West Nile Virus in Türkiye. A highly invasive Aedes albopictus, transmit a wide range of human diseases including Zika, yellow fever, dengue, and chikungunya in the World. The range of these vectors has increased due to climate change, increased trade and tourism. Current control of mosquitoes is still heavily dependent upon the use of chemical insecticides but extensive spraying has also resulted in the development of resistance in mosquito populations around the world. The current book chapter focuses on the history of mosquito-borne diseases and their future risks for Türkiye. Insecticide resistance status of the populations of these six species are also discussed in this study as the knowledge of resistance levels of vector mosquito populations might be taken into consider for the effective vector control management.

Key words: West Nile Virus, Dengue, Malaria, Insecticide resistance, Anopheles, Culex, Aedes

1. INTRODUCTION

If we criticise vector-borne diseases in humans, several kind of dangerous pathogens that have been leading mortality and morbidity are transmitted by mosquitoes. Therefore, mosquitoes are considered to be one of the most important insect families from a medical and economical point of view (Wang et al., 2012:11). This has ensured that mosquito species have always been the primary target organism in vector insect control studies around the world. However, mosquitoes have many adaptive features such as being able to survive for a long time even in adverse environmental conditions, being able to be found in all zoogeographic regions of the world, rapid breeding ability, sucking blood from many living groups, breeding in almost all aquatic habitats, and quickly gaining resistance against insecticides which hardens the vector control managements. Furthermore, despite these adaptive features, vector mosquito species continue to cause serious problems in the area where they are distributed. Three important genera that are responsible for being vectors of very common and dangerous human diseases such as malaria, West Nile fever, yellow fever, Japanese encephalitis, Dengue fever and filarial diseases are *Culex, Anopheles and Aedes.* Vector mosquito species from these genera are also known to infect humans by being vectors of other mosquito-borne viruses such as Dengue fever (DENV), Sindbis, Snowshoe, Inkoo, Lednice, Sindbis, Tahyna, Usutu, Chikungunya (CHIKV) and Zika (ZIKV) (Brugman et al., 2018:9).

The World's almost half of the population was threatened by malaria in 2021. Totally, 247 million malaria cases and 619,000 deaths have been reported by World Health Organisation at the same year (WHO, 2022:372). Dengue fever is one of the most dangerous disease spreading fastly and more than 100 countries of the world is being affected. In 2022, 2,597,067 cases of dengue were reported worldwide (CDC, 2022). ZIKV, another emerging disease virus, is responsible of 500,000 cases per year, approximately (Franklinos et al., 2019:11). In the weeks when the epidemic increased in 2022, the USA reported 29,829 ZIKV cases 2022 in the USA alone (PAHO, 2022). A total of 2,474 ZIKV cases were reported from the European continent between 2015 and 2018 (ECDC, 2019a). CHIKV affects one-third to three-quarters of the human population in areas where the virus is circulating. Approximately 3 million suspected chikungunya cases were reported in the US in 2017 (CDC, 2017).

Mosquitoes can be easily localized all over the world except the poles as a result of their easy adaptability. In addition, due to the fact that they can complete their life cycles in a shorter time due to global warming and increasing temperatures, the number of larvae hatching from eggs and they can fly long

distances, they can easily carry the pathogenic microorganisms and other disease agents they carry to the places they go (Gould and Higgs, 2009:13). Due to the trade and travel interactions between countries on a global scale, the spread/settlement of vector mosquito species has become easier and increased in many parts of the world. As a result, the damage they cause to farm animals and human communities has gained importance day by day (Gould and Higgs, 2009:13).

Türkiye acts as a bridge between the Asian, European and African continents and is separated from Russia and Iran by mountain complexes. Its geological location and this geographical diversity are associated with the diversity of the climatic conditions in the country. In almost all regions except Northeast Anatolia, the precipitation period is limited between November and May and is mostly in the form of snow. Summer months are mostly dry except for the North part of the country, especially the Black Sea region. In addition to their climatic characteristics, the widespread presence of rivers, streams, deltas and lagoons makes these two regions suitable mosquito habitats in terms of being suitable mosquito breeding habitats. In addition, the intense human mobility due to tourism and industrialization makes these regions open to new mosquito species, arbovirus or other pathogenic microorganisms and disease agents, which were not previously found in the country, but may come from outside our country. As a natural consequence of this, it is faced with the threat of damage by mosquitoes (Günay, 2015:120).

Mosquito control managements basically depend on the chemical insecticides use: There are four classs of insectcides used: 1. Organochlorines (OC), 2. Carbamates (CB), 3. Organophosphates (OP), and 4. Pyrethroids (PYs) (WHO, 2011:41). Although, biological control agents such as *Bacillus thriungiensis israilensis* (*Bti*) and *Bacillus sphaericus* (*Bs*) are preferred both in Türkiye and other countries, chemical insecticides are in still use as they have several advantages such as cheapness (Lacey, 2007:11). However, increase in insecticide resistance in vector mosquito populations might harden the vector control efforts. That's why monitoring and surveillance of insecticide resistance status in vector populations might taken into consider before vector control managements (Labbe et al., 2017:28).

Surveillance of altered detoxification enzyme levels (Glutathion-S-transferase (GST), mixed function oxidases (MFO) and esterases (alpha esterase, beta esterase, acetylcholinesterase (AchE)) and allele frequencies of resistance genes (Knockdown resistance (kdr)-Voltage gated Sodium channel (VGSC) and Acetylcholinesterase (Ace-1)) that cause insecticide resistance are useful tools for resistance management. For this reason, it is necessary to know allele frequencies

such as *kdr* L1014F, L1014S, which cause knockdown resistance of populations, and *Ace-1* G119S, F290V, which cause Acetylcholinesterase insensitivity in addition, to GST, MFO and esterases (Hemingway et al.,2000:21).

From this point of view, the following three things are aimed in this book chapter:

1. To compile studies on malaria, West Nile fever and Dengue fever, which are mosquito-borne diseases that have been seen in Turkey until now and are even predicted to be at high risk of occurrence.

2. To give general information about *Anopheles sacharovi*, *An. superpictus, Culex pipiens*, *Cx. tritaeniorhynchus*, *Aedes caspius* and *Ae. albopictus*, which are the vectors of malaria, West Nile fever and dengue fever, respectively and spread in Turkey.

3. To compile the situation of insecticide resistance, which is a major obstacle in the fight against these 6 mosquito species, in the populations where these species are distributed.

2. MOSQUITO-BORNE HUMAN DISEASE IN TÜRKİYE

2.1. Malaria

Türkiye fought with malaria and its devastating effects for long years in the history. Reports indicates malaria and its effects dates back to the First World War (1914-1918) (Aksu, 1943:189). The first malaria campaign was launched between 1925-1945 when Turkish Republic is established (WHO, 2013:100). Draining swamps and destroying mosquito habitats were also some of the control methods of this period. Malaria case numbers increased dramatically during and after Second World War globally as well as Türkiye (1939-1945). The numbers were increased until 155.683 in 1940 (WHO, 2013:100).

With the implementation of the national malaria eradication program in 1957 and use of DDT as a new control method, significant successes were achieved and the case numbers were decreased until 2877 in 1974 (WHO, 2012:288). However, the final goal of eliminating local transmission was not yet achieved as a result of increased insecticide resistance in *Anopheles sacharovi* populations, a primary malaria vector of Türkiye. Case numbers reached until 115.512 in 1977 (WHO, 2012:288). After national malaria eradication program, malaria control programme was launched in 1983. Malaria case numbers decreased from 66.681 in 1983 to 8.680 in 1990 after the implementation of malaria control program. Unfortunately, as a result of uncontrolled migration from the Southeastern Anatolia Region where there is unplanned urbanization to city centers and migration from neighbouring countries to Türkiye, case numbers increased and peaked at 84.345 in 1994 (Özbilgin et al., 2011:9). Case numbers dramatically decreased between 1995-2005

by the effective malaria control programme. Türkiye signed Tashkent declaration in 2005 and malaria control programme replaced by 'Malaria Elimination Programme of Turkey' (WHO, 2013:100). By the effective work of the Turkish Ministry of Health, case numbers decreased from 796 in 2006 to 0 in 2012. There is no reported indigenous malaria cases since 2010. However, there are reported local cases derived from foreign cases that occurred in 2012 and 2014 in Turkey until 2022 (WHO, 2022:372).

2.2. West Nile fever

West Nile Virus (WNV) is a single-stranded positive-sense RNA virus with approximately 12,000 nucleotides in the Japanese encephalitis serocomplex belonging to the flavivirus genus of the flaviviridae family (Petersen et al., 2013:8). WNV completes its primary cycle among birds through the ornithophilic *Culex* mosquitoes. WNV hosts other mammals such as horses and humans by chance (Engler et al., 2013:27; Lustig et al., 2015:8). Mammals, especially horses and humans, are not involved in the transmission cycle and are therefore known as the dead-end hosts (Colpitts et al., 2012:14). To date, WNV has been obtained from 62 different mosquito species. However, infection in humans is primarily caused by vectors of *Culex pipiens* mosquitoes (Hannoun et al., 1964:3). Another important WNV vector is *Aedes albopictus*, and due to its highly invasive / invasive nature, it not only spread to large areas where it was not found before, but also caused it to be effective in these areas where disease agents were not previously found (Mayer et al., 2017:9). WNV infection in humans is not symptomatic, but leads a mild influenza-like sypmtoms as West Nile Fever illness in about 20% of cases. However, infection can lead to death in a minor rates of cases, especially in the elderly and immune-suppressive individuals (Hayes et al., 2005:6).

Until 2009, there was no record of WNV-related symptomatic disease in Türkiye, since it shows more asymptomatic behavior or its symptomatic features are very similar to other arboviral diseases, it is difficult to diagnose by laboratory methods, it is not well known by clinicians and it is not in the category of diseases that should be reported to the Turkish Ministry of Health. Since 2009, both epidemic and Central Nervous System associated with WNV diseases have been reported, especially in the west part of Anatolia (Özkul et al., 2013:6). In 2010, a total of 47 WNV fever disease records were reported and in 2011, a total of 5 cases of WNV fever were reported (Kalaycıoğlu et al., 2012:6). Although 40 of 47 cases seen in our country in 2010 were neuro-invasive, the disease resulted in death in 10 individuals (Kalaycıoğlu et al., 2012:6). In the following period, 7, 23 and 10 WNV cases were reported in Türkiye in 2017, 2018 and 2019, respectively (ECDC, 2018; 2019b; 2020).

Although there are spatial epidemiology studies in Türkiye, the number of these studies is quite limited. One of the field studies carried out is the study conducted with mosquito samples obtained from 23 localities in Edirne in 2012. In this study, WNV isolation was performed in *Cx. pipiens* (36.3%) and *Ae. caspius* (15.6%) samples obtained from western Türkiye for the first time in this study (Ergünay et al., 2013:9). Another field study was conducted in Şanlıurfa, in which the presence of WNV virus was investigated in mosquito samples containing *Cx. pipiens* and *Ae. caspius* as well as in human blood serum samples. In this study, nucleic acid belonging to WNV was not detected in any of the mosquito samples, but it was determined that 16% of the blood samples were positive for WNV by serological methods (Özer et al., 2007:5). Finally, in 2019, WNV was detected in 7.7% of *Ae. albopictus* or *Cx. pipiens* pools sampled from Artvin, Rize and Trabzon provinces (Akıner et al., 2019:18).

2.3. Dengue fever

Dengue virus is a flavivirus with four serotypes, which is found in tropical and subtropical regions and threats almost one third of the world's population (Bhatt et al., 2013:4). *Aedes aegypti* and in some areas *Ae. albopictus* are the main vectors of Dengue virus (Gomez et al., 2022:13).

The last severe dengue fever outbreak in Türkiye was reported in the late 1920s that infected more than 1 million and caused the death of nearly 1500 people (Schaffner and Mathis, 2014:10). Long years later, a total of 1074 serum sample has been obtained from people living in the Aegean Region in 1980 and seropositivity was determined as 12.6% by hemaglutination inhibition (HI) assay and it was reported that the most common serotype was DENV-1 (53.3%), followed by DENV-2 (2.1%) and DENV-4 (0.96%) (Serter, 1980:7). In recent years, antigens for DENV-1 and DENV-2 have been detected in serum samples obtanined from people living in Central Anatolia in 2010 (Ergünay et al., 2010:5). In 2014, 0.43% (4/920) of the blood samples taken from 920 individuals living in Mersin province were found to be DENV IgM positive. However, it was highly likely that the positivity observed against the virus emerged as a result of well-defined cross reactions that occured in serological tests of flaviviruses. This indicated that flaviviruses other than DENV, possibly with low virulence, were in the circulation (Tezcan et al., 2014:12). To date, there have been no detected indigenous DENV case in Türkiye. However, three exogenous dengue fever cases were reported in 2013, 2016 and 2019 (Uyar et al., 2013:8, Değirmenci et al., 2016:4, Özbay et al., 2019:4).

Although there has not been an indigenous dengue fever case in Türkiye to date, sero-epidemiological studies in which IgM gives positive results show that there

may be local cases in addition to imported cases. Additionally, this risk is being increased by the invasion of *Ae. albopictus* and *Ae. aegypti* in Türkiye.

Finally, mosquito based studies showed no positivity in terms of DENV as well as CHIKV, ZIKV and WNV in both *Ae. aegypti* and *Ae. albopictus* samples collected from the Black Sea Region of Türkiye (Coşgun et al., 2023:8).

3. VECTOR MOSQUITOES AND INSECTICIDE RESISTANCE STATUS OF THEIR POPULATIONS IN TÜRKİYE

3.1. *An. sacharovi*

Anopheles sacharovi has been reported in Italy, Sardinia, Corsica, Croatia, the former Yugoslav Republic of Macedonia, Albania, Greece, Bulgaria, Romania, Türkiye, Lebanon, Israel, Jordan, Syria, Iraq, Iran, Armenia and Cyprus (Becker et al., 2003:498; Schaffner et al., 2001; Yurttas and Alten, 2006:10; Merdic, 2004:6; Patsoula et al., 2007:8; Romi et al., 2002:5; Violaris et al., 2009:4).

An. sacharovi is an important vector of malaria throughout its range of distribution (Becker et al., 2003:498). It is a primary malaria vector of Türkiye (Kasap et al., 1981:10).

The activity of *An. sacharovi* adults usually peaks in July and August. Adult females hibernate in animal shelters (Becker et al., 2003:498). In warm regions, hibernation is not completed and their activity decreases in colder periods (Sinka et al., 2010:9). Adults can fly from 3-5 km to 14 km (Schaffner et al., 2001). *Anopheles sacharovi* is zoo-anthropophiles and endophiles (Yurttas and Alten, 2006:10) but can also feed on a wide variety of hosts, including sheep, goats, cattle, horses, birds, rabbits, rodents, and domestic animals (Boreham et al., 1973:10). They are found in warm shelters, houses and barns, where they suck blood from both humans and animals. They can suck blood during the winter and mate while flying (Alten and Çağlar, 1998:249). *Anopheles sacharovi* larvae prefer sunny areas with floating vegetation and typically live stagnant or slow-flowing, clean sunny waters with plenty of aquatic plants and high salt content (Merdivenci, 1984:340). In addition, it is found in swamps, lagoons, riverbanks, streams and water sources and pools (Becker et al., 2003:498). They can also be found in rice fields and other irrigated areas (Romi et al., 2002:5). Although primarily associated with stagnant water, *An. sacharovi* larvae are also tolerant of slowly flowing water such as streams and salinity up to 20% (Sinka et al., 2010:9; Özbilgin et al., 2011:9). Adults of *An. sacharovi* usually overwinter in warm shelters and can suck blood during the winter months (Merdivenci, 1984:340). Adults rest in animal shelters, houses, tree cavities and rock cavities (Becker et al., 2003:498).

Since *An. sacharovi* is a primary malaria vector in Türkiye, it has always been one of the primary targets of insecticides, and as a result, *An. sacharovi* populations

have encountered many types of insecticides in the past. After the Second World War, malaria incidence was decreased through the introduction of indoor residual spraying (IRS) with DDT. IRS was applied intensively in the transmission season in malaria endemic areas (Özbilgin et al., 2011:9).

After the occurrence of DDT resistance, lambda-cyhalothrin, alpha cypermethrin, chlorpyrifos methyl and deltamethrin had been used as IRS component. For larvicidal breeding sites, an organophosphate (OP) temephos, insect growth regulators (IGR) such as methoprene, pyriproxyfen, novaluron and finally biological control agents such as *Bti* was used as a control agent (Özbilgin et al., 2011:9).

Insecticide resistance status of *An. sacharovi* populations of Türkiye is listed in Table 1.

Ramsdale et al. (1980:9) reported that *An. sacharovi* Çukurova populations developed resistance to several kinds of organophosphate (OP) and carbamate (CB) due to extended use in agricultural pest control.

Hemingway et al. (1992:7), reported fenitrothion and propoxur resistance of *An. sacharovi* populations collected from the Çukurova plain of Adana. They also reported low level of DDT and bendiocarb resistance in this population. However, they had no evidence for primiphos-methyl resistance. Researchers reported correlation with AChE enzyme elevations with OP and CB resistance while GST levels correlated with DDT resistance.

Kasap et al. (2000:6), tested the resistance status of *An. sacharovi* populations collected from Adana, Adıyaman, Antalya, Aydın and Muğla against 12 different insecticides. Researchers reported that *An. sacharovi* populations from Adana and Antalya were only susceptible to malathion and pirimiphos-methyl. Specimen collected from Aydın were susceptible to both these insecticides as well as dieldrin, λ-cyhalothrin, etofenprox. Specimen collected from Muğla were susceptible to malathion and pirimiphos-methyl, dieldrin, fenitrothion, λ-cyhalothrin, cyfluthrin and etofenprox.

Lüleyap and Kasap (2000:24), reported malathion susceptibility in all *An. sacharovi* populations collected from Tabaklar, Herekli and Menekşe provinces of Adana in both the season October-April and May-September. Addirionally, researchers reported Asetylcholinesterase increase associated with malathion and propoxur resistance as well as GST activity increase associated with DDT an pyrethroid resistance.

Table 1. Insecticide resistance status of Turkish *Anopheles sacharovi* populations reported by researchers

Study	Study area	Insecticides tested	Resistance status		
			Resistant	Possible resistant	Susceptible
Ramsdale et al., 1980	Adana-Çukurova	Malathion, Fenitrothion, Fenthion Primiphos-methyl, Chlorphoxim, Phoxim, Parathion, Dianizon, İodofenphos, Mecabam, Bomyl Dimethoate, Propoxur, Carbaryl, Pyrolan, Dimetan, Dimetilan, İsopropoyl- phenyl, N-methyl-carbamate	Fenitrothion, Fenthion Parathion, Dianizon, İodofenphos, Mecabam Dimethoate, Propoxur Carbaryl, Dimetan Dimetilan, İsopropoyl-phenyl, N-methyl-carbamate	Chlorphoxim Phoxim Pyrolan	Malathion Primiphos-methyl Bomyl
Hemingway et al., 1992	Adana-Çukurova	DDT, Propoxur Bendiocarb, Fenitrothion Primiphos methyl	DDT, Propoxur Bendiocarb, Fenitrothion		Primiphos methyl
Lüleyap and Kasap (2000)	Adana-Karataş-Tabaklar (October-April)	DDT, Malathion Deltamethrin ,Permethrin Propoxur	DDT, Deltamethrin Permethrin, Propoxur		Malathion
	Adana-Karataş-Tabaklar (May-September)		DDT, Deltamethrin Permethrin, Propoxur		Malathion
	Adana- Ceyhan-Herekli (October-April)		DDT, Deltamethrin Permethrin, Propoxur		Malathion
	Adana- Ceyhan-Herekli (May-September)		DDT, Deltamethrin Permethrin, Propoxur		Malathion
	Adana-Menekşe-Merkez (October-April)		DDT, Deltamethrin Permethrin, Propoxur		Malathion
	Adana-Menekşe-Merkez (May-September)		DDT, Deltamethrin Permethrin, Propoxur		Malathion

Kasap et al., 2000	Adana	DDT, Dieldrin, Malathion Fenitrothion, Primiphos-methyl Bendiocarb,Propoxur Deltamethrin, Permethrin Lambda-cyhalothrin, Cyfluthrin Etofenprox	DDT, Dieldrin Fenitrothion, Bendiocarb Propoxur, Deltamethrin Permethrin, Lambda-cyhalothrin Cyfluthrin, Etofenprox		Malathion Primiphos-methyl
	Adıyaman		DDT, Dieldrin Fenitrothion, Bendiocarb Propoxur, Deltamethrin Permethrin, Cyfluthrin	Lambda-cyhalothrin	Malathion Primiphos-methyl Etofenprox
	Antalya		DDT, Dieldrin Fenitrothion, Bendiocarb Propoxur, Deltamethrin Permethrin, Lambda-cyhalothrin Cyfluthrin, Etofenprox		Malathion Primiphos-methyl
	Aydın		DDT Bendiocarb Propoxur, Deltamethrin Permethrin	Fenitrothion Cyfluthrin	Dieldrin, Malathion Primiphos-methyl Lambda-cyhalothrin Etofenprox
	Muğla		DDT, Bendiocarb Permethrin	Propoxur Deltamethrin	Dieldrin, Malathion Fenitrothion, Primiphos-methyl, Lambda-cyhalothrin Cyfluthrin, Etofenprox

3.2. *Anopheles superpictus*

Anopheles superpictus has been reported from Afghanistan, Albania, Algeria, Armenia, Azerbaijan, Bosnia and Herzegovina, Bulgaria, Croatia, Cyprus, Egypt, France, Georgia, Greece, India, Iran, Iraq, Israel, Italy, Jordan, Kazakhstan, Kyrgyzstan, Lebanon, Libya, Macedonia, Pakistan, Russia, Spain, Syria, Tajikistan, Tunisia, Türkiye, Turkmenistan, Uzbekistan, Serbia and Montenegro (Becker et al., 2003:498; Ramsdale and Snow, 2000:26; Azari-Hamidian et al., 2009:11; Habirov et al. 2012:9).

Anopheles superpictus is known to be a secondary malaria vector of Turkey. However, its vector ability may vary dependence on blood feeding behaviour since its exophilic and zoophilic behaviour differ based on location (Merdivenci, 1984:340). Females are both endophilic and exophilic Additionally, they have both zoophilic and antropohilic behaviour (Becker et al., 2003:498). *L*arvae are found in stagnant, warm and unpolluted waters such as riverside ponds and rice fields. They can tolerate salinity, but escape from muddy and eutrophic waters (Gutsevich et al. 1974:408).

Since *An. superpictus* is known as a secondary malaria vector in Türkiye, it has always been a primary target of insecticides similar to *An. sacharovi.* And again, IRS with DDT, chlorpyrifos methyl, alpha cypermethrin, lambda-cyhalothrin and deltamethrin had been used as IRS component. For larvicidal breeding sites, temephos, pyriproxyfen, methoprene, novaluron and diflubenzuron and *Bti* was used as a control agent (Özbilgin et al., 2011:9).

Insecticide resistance status of *An. superpictus* populations of Türkiye is listed in Table 2.

Yavaşoğlu et al. (2019:10) reported common resistance to DDT, malathion and propoxur in the Southeastern and Mediterranean populations of *An. superpictus*. Fortunately, most of the populations were susceptible to pyrethroids (permethrin, deltamethrin and etofenprox). Elevated oxidases and esterase levels were attributed to the OP, CB and DDT resistance in the *An. superpictus* populations of the study area.

Yavaşoğlu and Şimşek (2022:5) developed allele-specific primers to detect kdr related L1014F, L1014S and L1014C alleles in *An. superpictus*. Kdr L1014S mutation were detected in the Aegean *An. superpictus* populations for the first time, in this study.

Table 2. Insecticide resistance status of Turkish *Anopheles supepictus* populations reported by researchers

Study	Study area	Insecticides tested	Resistance status		
			Resistant	Possible resistant	Susceptible
Yavaşoğlu et al., 2019	Adıyaman-Kahta	DDT, Malathion, Propoxur, Permethrin, Deltamethrin, Etofenprox	DDT, Malathion, Propoxur		Permethrin Deltamethrin Etofenprox
	Batman-Hasankeyf		DDT, Malathion, Propoxur	Permethrin, Etofenprox	Deltamethrin
	Diyarbakır-Kapuzlu		DDT, Malathion, Propoxur		Permethrin Deltamethrin Etofenprox
	Gaziantep-Islahiye		DDT, Malathion, Propoxur		Permethrin Deltamethrin Etofenprox
	Gaziantep-Nizip		DDT, Malathion, Propoxur		Permethrin Deltamethrin Etofenprox
	Kilis-Musabeyli		DDT, Malathion	Propoxur	Permethrin Deltamethrin Etofenprox
	Kilis-Polateli		DDT, Malathion, Propoxur		Permethrin Deltamethrin Etofenprox
	Mardin-Savur		DDT, Malathion, Propoxur	Deltamethrin Etofenprox	Permethrin
	Mardin, Ömerli		DDT, Malathion, Propoxur		Permethrin Deltamethrin Etofenprox
	Şanlıurfa-Birecik		DDT, Malathion, Propoxur Etofenprox		Permethrin Deltamethrin
	Şanlıurfa-Siverek		DDT, Malathion, Propoxur		Permethrin Deltamethrin Etofenprox
	Adana-Kozan		DDT, Malathion, Propoxur		Permethrin Deltamethrin Etofenprox
	Adana-Tuzla		DDT, Malathion, Propoxur		Permethrin Deltamethrin Etofenprox
	Antalya-Aksu		DDT, Malathion, Propoxur	Permethrin Deltamethrin	Etofenprox
	Antalya-Manavgat		DDT, Malathion, Propoxur		Permethrin Deltamethrin Etofenprox
	Burdur-Bucak		DDT, Malathion, Propoxur		Permethrin Deltamethrin Etofenprox

	Hatay-Dörtyol		DDT, Malathion, Propoxur		Permethrin Deltamethrin Etofenprox
	Hatay-Kırıkhan		DDT, Malathion, Propoxur	Permethrin, Deltamethrin, Etofenprox	
	Isparta-Bağkonak		DDT, Malathion, Propoxur		Permethrin, Deltamethrin, Etofenprox
	Isparta-Sütçüler		DDT, Malathion, Propoxur		Permethrin Deltamethrin Etofenprox
	Mersin-Çamlıyayla		DDT, Malathion, Propoxur	Deltamethrin,	Permethrin Etofenprox
	Mersin-Huzurkent		DDT, Malathion, Propoxur		Permethrin Deltamethrin Etofenprox
	Kahramanmaraş-Andırın		DDT, Malathion	Propoxur	Permethrin Deltamethrin Etofenprox
	Kahramanmaraş-Göksun		DDT, Malathion, Propoxur		Permethrin Deltamethrin Etofenprox
	Kahramanmaraş-Türkoğlu		DDT, Malathion, Propoxur		Permethrin Deltamethrin Etofenprox
	Osmaniye-Düziçi		DDT, Malathion, Propoxur		Permethrin Deltamethrin Etofenprox
	Osmaniye-Kadirli		DDT, Malathion, Propoxur		Permethrin Deltamethrin Etofenprox
	Osmaniye-Sunbaş		DDT, Malathion	Propoxur	Permethrin Deltamethrin Etofenprox

3.3. *Culex pipiens*

Mosquitoes in the Pipiens complex are widely distributed in the holoarctic region and Eurasia (Vinogradova, 2000:250; Becker et al., 2003:498). The most common species in this complex are *Culex pipiens* Linnaeus, 1758 and *Culex quinquefasciatus* Say, 1823 and are relatively common in temperate and tropical regions. *Culex pipiens* includes two biotypes called *Culex pipiens pipiens* and *Culex pipiens molestus* which differ in their physiology and behaviour (Becker et al., 2003:498).

Culex pipiens is a vector of numerous viruses and disease pathogens that cause animal and human diseases, including WNV. (Turell et al., 2001:5). In addition, it is a vector of at least 10 more arboviruses (arthropod-derived viruses) of medical and veterinary importance such as CHIKV, DENV, Japanese Encephalitis virus (JEV), Batai virus, Usutu virus, Sindbis virus, Tahyna virus, Inkoo virus, Lednice virus, and Snowshoe virus (Brugman et al., 2018:9).

Culex pipiens larvae grow in stagnant and clean waters. In addition, they can develop in polluted waters with organic content. Larvae can be found from the beginning of April to November (Becker, 2003:498).

Culex pipiens pipiens requires blood for egg development (anotogeny) and usually prefers to feed on birds (ornithophilic). Adults enters diapause in winter (heterodynamic). Adults colonize only in above-ground habitats and mates in large, open areas (Vinagrodova, 2000:250).

Culex pipiens is one of the species that has been prioritized in control studies due to its vector potential and its prevalence in almost every province of Türkiye and the associated disturbances. Insecticide resistance status of *Cx. pipiens* populations of Türkiye is listed in Table 3.

Akıner et al. (2009:6) showed that *Cx. pipiens* popultions in Antalya, Ankara, Çankırı, Mersin, Hatay, Birecik and Viranşehir were still resistant to DDT. The Birecik, Viranşehir, Mersin, Ankara and Antalya populations were highly resistant to temephos and Birecik, Mersin, Çankırı and Antalya populations had an elevated fenthion resistance. While Ankara and Antalya populations were resistant to all adult insecticides, mortality rates were found to be quite high in other populations such as 97.5% malathion in Birecik and 97.5% deltamethrin in Hatay. Other populations were found to be in the surveillance (observation) category according to the WHO classification.

Akıner and Ekşi (2015:6) reported high DDT, permethrin and malathion resistance all *Cx. pipiens* populations in Mersin, Adana and Antalya provinces in the Mediterranean region of Turkiye while all of the populations were possible resistant and resistant in the study area. Biochemical analysis results

showed that MFOs and esterases were responsible for DDT, malathion and pyrethroid resistance.

Taşkın et al. (2015:13) reported middle or high to DDT, malathion, bendiocarb, dieldrin, permethrin and deltamethrin resistance in *Cx. pipiens* populations of Balıkesir, Çanakkale, Muğla, Aydın, İzmir. Researchers also reported low frequencies of ace-1 (G119S and F290V) and Rdl (A302S) mutations developed against malathion, bendiocarb and dieldrin. On the contrary, the frequencies of two kdr mutations (L1014F and L1014C) associated with DDT and pyrethroid insecticides were found to be quite high and show seasonal variation.

Guntay et al. (2018:8) reported middle or high insecticide resistance against deltamethrin, permethrin, α-cypermethrin and cyfluthrin in the İzmir-Menemen, Bornova and Çiğli *Cx. pipiens* populations. The only susceptible population against deltamethrin, permethrin and cypermethtrin was the Menemen population. Researchers also reported diverse effects of piperonyl-butoxide (PBO) on MFO detoxification enzymes.

Ser and Çetin (2019:16) reported wide permethrin susceptibility while possible resistance and/or resistance to deltamethrin reported in all of the populations. Most of the populations were still susceptible to etofenprox and lamda-cyhalothrin except for the Antalya-Alanya and Antalya-Kumluca populations.

Guz et al. (2020:21) reported high frequencies of Chitin synthase I gene mutations (I1043L and I1043M) associated with diflubenzuron resistance in five different *Cx. pipiens* populations of Muğla. Researchers also reported high L1014F mutation frequency associated with pyrethroid resistance.

Kılıçarslan et al. (2022:16) aimed to investigate the kdr (L1014L/F and L1014L/C) and ace-1 (G119S and F290V) mutation frequencies in Cx. Pipiens populations collected from the 33 locations from 9 provinces in central and eastern Black Sea Region of Türkiye. No L1014C mutation detected in any of the populations while L1014F mutation was characterised by three different silent mutations. G119S mutation was quite widespread along the populations while F290V lower. Researchers reported G119I and G119A mutations in the study area, for the first time.

Table 3. Insecticide resistance status of Turkish *Culex pipiens* populations reported by researchers

Study	Study area	Insecticides tested	Resistance status		
			Resistant	Possible resistant	Susceptible
Akiner et al., 2009	Şanlıurfa-Birecik	Temephos, Fenthion DDT, Malathion, Deltamethrin Permethrin	Temephos, Fenthion, DDT Permethrin, Deltamethrin	Malathion	
	Şanlıurfa-Viranşehir		Temephos , DDT, Permethrin, Deltamethrin, Malathion	Fenthion	
	Ankara-Akyurt		Temephos, DDT, Malathion Deltamethrin, Permethrin	Fenthion	
	Çankırı-Hacılar	Temephos, Fenthion Temephos, Fenthion	Fenthion	Temephos	
	Mersin-Erdemli		Temephos, Fenthion		
	Hatay-Merkez		DDT, Permethrin, Malathion	Deltamethrin	
	Antalya-Kundu		Temephos, Fenthion, DDT, Malathion, Deltamethrin, Permethrin		
Akıner and Ekşi, 2015	Adana-Kapıkaya	DDT, Permethrin, Deltamethrin Malathion	DDT, Permethrin, Malathion		Deltamethrin
	Mersin-Huzurkent		DDT, Permethrin, Malathion	Deltamethrin	
	Mersin- Center		DDT, Permethrin, Malathion		Deltamethrin
	Antalya-Aksu		DDT, Permethrin, Malathion		Deltamethrin
Taşkın et al., 2015	Çanakkale	DDT, Dieldrin, Malathion, Bendiocarb, Deltamethrin Permethrin	DDT (2012-I, 2012-II, 2013), Malathion (2012-I, 2012-II, 2013), Permethrin (2012-I, 2012-II), Bendiocarb (2012-II, 2013), Dieldrin (2012-II, 2013), Deltamethrin (2012-II)	Permethrin (2013) Bendiocarb (2012-I) Dieldrin (2012-I) Deltamethrin (2012-I, 2013)	
	Balıkesir		DDT (2012-I, 2012-II), Malathion (2012-I, 2012-II, 2013), Permethrin (2012-	DDT (2013), Permethrin (2013), Bendiocarb (2013),	

			I, 2012-II), Bendiocarb (2012-I, 2012-II), Dieldrin (2012-II), Deltamethrin (2012-II)	Dieldrin (2012-I, 2013), Deltamethrin (2012-I, 2013)	
	İzmir		DDT (2012-I, 2012-II, 2013) Malathion (2012-I, 2012-II, 2013), Permethrin (2012-I, 2012-II, 2013), Bendiocarb (2012-I, 2012-II, 2013), Dieldrin (2013), Deltamethrin (2012-II, 2013)	Dieldrin (2012-I, 2012-II), Deltamethrin (2012-I)	
	Aydın		DDT (2012-I, 2012-II, 2013) Malathion (2012-I, 2012-II, 2013), Permethrin (2012-I, 2012-II), Bendiocarb (2012-I, 2012-II, 2013), Dieldrin (2013),	Permethrin (2013), Dieldrin (2012-I, 2012-II), Deltamethrin (2012-I, 2012-II, 2013)	
	Muğla		DDT (2012-I, 2012-II, 2013) Malathion (2012-I, 2012-II, 2013), Permethrin (2012-I, 2012-II), Bendiocarb (2012-I, 2012-II, 2013), Dieldrin (2012-I), Deltamethrin (2012-II)	Permethrin (2013), Dieldrin (2012-II, 2013), Deltamethrin (2012-I, 2013)	
	Denizli		DDT (2012-I, 2012-II, 2013) Malathion (2012-I, 2012-II), Permethrin (2012-I, 2012-II), Bendiocarb (2012-I, 2012-II, 2013), Dieldrin (2013)	Malathion (2013), Permethrin (2013), Dieldrin (2012-I), Deltamethrin (2012-I, 2012-II, 2013)	Dieldrin (2012-II)
Guntay et al., 2018	İzmir-Menemen	Deltamethrin Permethrin α-	Cyfluthrin		Deltamethrin, Permethrin, α-

		Cypermethrin Cyfluthrin			Cypermethrin,
	İzmir-Çiğli		Deltamethrin Cyfluthrin	Permethrin, α-Cypermethrin	
	İzmir-Bornova		Deltamethrin, α-Cypermethrin, Cyfluthrin	Permethrin	
Ser and Çetin, 2019	Antalya-Alanya-Çıplaklı	Permethrin, Etofenprox, Deltamethrin, Lambda-cyhalothrin	Deltamethrin,	Etofenprox, Lambda-cyhalothrin	Permethrin
	Antalya-Alanya-Süleymanlar			Etofenprox, Deltamethrin	Permethrin, Lambda-cyhalothrin
	Antalya-Döşemealtı-Ilıca		Deltamethrin		Permethrin, Etofenprox, Lambda-cyhalothrin
	Antalya-Döşemealtı-Kilik			Deltamethrin	Permethrin, Etofenprox, Lambda-cyhalothrin
	Antalya-Kemer-Tekirova			Deltamethrin	Permethrin, Etofenprox, Lambda-cyhalothrin
	Antalya-Kumluca-Narenciye			Lambda-cyhalothrin, Deltamethrin	Permethrin, Etofenprox
	Antalya-Kumluca- Solid waste storage area		Deltamethrin		Permethrin, Etofenprox, Lambda-cyhalothrin
	Antalya-Manavgat-Çakış		Deltamethrin		Permethrin, Etofenprox, Lambda-cyhalothrin

3.4. *Culex tritaeniorhynchus*

Culex tritaeniorhynchus spreads in the Southeast Asia, most of Africa and the Middle East and is known as a is a very important vector mosquito species leading to several mosquito-borne diseases (Becker et al., 2003:498; Longbottom et al., 2017:8).

The distribution of *Cx. tritaeniorhynchus* in Türkiye is limited to Thrace subregion of the Marmara, Mediterranean and the Aegean regions (Ramsdale et al., 2001:11; Günay et al., 2015:9).

Females generally exhibit zoophilic behaviour and feed on many different vertebrates like cows, pigs and birds (Arunachalam et al., 2005:3). Its anthropophilic behaviour is also quite common and feed on humans (Wilson and Sevarkodiyone, 2015:8). As the females do blood-sucking intensively at night in open areas after sunset, they have nocturnal and exophagic behaviour. Adult emergence typically begins in the late afternoon and peaks in the evening. *Cx. tritaeniorhynchus* usually has a biphasic bite profile (Merdivenci, 1984:340)

Females lay their eggs in sun-drenched lakes and slowly flowing water shores (Merdivenci, 1984:340). Larvae use inundated areas like ditches, ponds, wells and fallow fields, as well as human related habitats such as water tanks (Kanojia et al., 2010:9).

Culex tritaeiorhynchus is an extremely widespread species. It can be found anywhere with an average annual temperature of 8.2-28.9°C and a maximum altitude of 838 m above sea level (Miller et al., 2012:9).

To date, there are limited reports regarding the insecticide resistance status and related resistance gene alleles of *Cx. tritaeniorhynchus* populations in Turkiye (Table 4).

Yavaşoğlu et al. (2022) reported wide DDT, malathion and propoxur resistance in *Cx. tritaeniorhynchus* populations of provinces of the Mediterranean region. Researchers also determined increasing resistance to permethrin and deltamethrin in some populations. Biochemical analysis showed altered esterase and GST levels in some populations. Molecular analysis indicated that kdr related L1014F frequency was too high in the Mediterranean populations.

Table 4. Insecticide resistance status of Turkish *Culex tritaeniorhynchus* populations reported by researchers

Study	Study area	Insecticides tested	Resistance status		
			Resistant	Possible resistant	Susceptible
Yavaşoğlu et al., 2022	Hatay - Erzin	DDT, Malathion, Propoxur, Permethrin, Deltamethrin	DDT, Malathion, Propoxur	Permethrin	Deltamethrin
	Hatay - Kırıkhan		DDT, Malathion, Propoxur	Permethrin, Deltamethrin	
	Antalya-Manavgat		DDT, Malathion	Propoxur Permethrin	Deltamethrin
	Mersin-Huzurkent		DDT, Malathion	Permethrin, Propoxur Deltamethrin	
	Mersin-Tarsus		DDT, Malathion	Permethrin, Propoxur, Deltamethrin	
	Osmaniye-Kadirli		DDT, Malathion, Propoxur		Permethrin Deltamethrin
	Osmaniye-Düziçi		DDT, Malathion	Propoxur, Permethrin	Deltamethrin
	Adana - Karatas		DDT, Malathion, Propoxur	Deltamethrin	Permethrin
	Adana-Yumurtalık		DDT, Malathion, Propoxur	Permethrin, Deltamethrin	
	Adana - Ceyhan		DDT, Malathion	Propoxur, Permethrin Deltamethrin	

3.5. *Aedes caspius*

The Palearctic populations of flood water mosquito, *Ae. caspius* are found in salty lakes and pools of the Mediterranean Region (Lambert et al., 1990:8), the coasts of England and the freshwater and salt marshes of the Europe, Russia, Northern Asia, North and North East Africa, Central Asia and in the Persian Sea (Bozizic-Lothtrop and Vujic, 1996:8; Cranston et al., 1987:152; Gabinaud, 1975:451).

Females are zoo-anthropophilic and feed on both day and night and both indoors and outdoors (Soliman et al., 2016:6).

Eggs are deposited in the mud along the pool and river banks, often 2 cm below the soil (Gabinaud, 1975:451). Salt tolerant *Ae. caspius* breeds on aquatic environments with varied salinity concentrations. E.g. salt marshes, rice fields, coastlands and swamps (Bellini et al. 1997:5).

Ae. caspius is demonstrated to be capable of carrying CHIKV, WNV, Tahyna virus and Usutu virus. *Ae. caspius* is also known as a primary vector of *Francisella tularensis*, a tularemia agent (Detinova and Smelova, 1973:17).

Aedes caspius has not epidemic history in Türkiye. However, several researchers identified insect related flaviviruses in *Ae. caspius* pools of the Aegean and Thrace (Ergünay et al., 2017:14). Similarly, a novel flavivirus were identified from *Ae. caspius* pools of the Thrace region (Öncü et al., 2018:10). These results demonstrate the active role of *Ae. caspius* in WNV and flavivirus transmissions.

Ae. caspius has not been targeted in mosquito control managements as it has not epidemic history. However, its larvae have been facing several insecticides that are used both for agricultural and mosquito control interventions. There are too restricted studies reporting the insecticide resistance status of *Ae. caspius* populations of Türkiye.

3.6. *Aedes albopictus*

Aedes albopictus spread worldwide especially after the second half of the 20th century and has been detected in all continents except Antarctica (Benedict et al., 2007:10; Kraemer et al., 2015:18). It was first detected in Albania in 1979 (Adhami and Murati, 1987:4) in Europe, later spread to many European regions, especially to Germany, France, Italy, Greece, Bosnia-Herzegovina, and Spain (Gratz, 2004:13; Benedict et al., 2007:10; Gatt et al., 2009:9; Schaffner & Mathis, 2014:10).

The first record in Turkey was given in 2013 at the Greek border line of the Thrace Region, but no resident population could be detected in this region (Oter et al., 2013:9). Akıner et al. (2016:5), determined the resident populations of *Ae. albopictus* for the first time in Artvin and Trabzon provinces. Then the Aegean

region populations have been reported from Aydın and Muğla (Yavaşoğlu, 2021:13).

Aedes albopictus mainly lives in forest border areas and breeds in small aquatic natural habitats where it accumulates in coconut shell pieces, bamboo trunks, tree cavities, and for this reason, it was previously considered as a rural vector mosquito species (Beaty and Marquardt, 1996:450; Bonizzoni et al., 2013:9).

As a result of its worldwide spread, it has adapted to use artificial habitats such as glass, plastic or tin containers associated with human beings that can accumulate, water collected in used tires, and animal drinkers as breeding grounds.

Aedes albopictus has a zoophilic behaviour and usually performs aggressive blood feeding attempts in outdoor areas during daylight hours. It also has strong anthropophilic tendency (Kamgang et al., 2012:5). *Ae. albopictus* produce eggs that can withstand the cold winter months and spend the winter in diapause (Becker et al., 2003:498). However, there is no diapause stage in its life cycle (Lambrechts et al., 2010:9).

A global struggle against the invasive *Ae. albopictus* has been carried out for many years. For this reason, populations of this species in many countries of the world have encountered different types of insecticides. However, data on insecticide resistance levels in Turkish populations are very limited (Table 6).

Yavaşoğlu, (2019:13) reported common DDT resistance in Aegean *Ae. albopictus* populations. However, wide susceptibility against bendiocarb, propoxur, fenitrothion has also been reported in this study. Additionally, the susceptibility was recorded against deltamethrin and permethrin in the Aydın-Didim and Muğla- Bodrum populations while possible resistance against permethrin was recorded in the Güzelçamlı and Kuşadası populations.

Pichler et al. (2022:7), reported the distribution of V1016G mutation in 69 *Ae. albopictus* populations from 19 European countries including Turkey. Researchers reported the low frequency of V106G mutation in the İstanbul and İğneada populations while V1016V frequency was 100% in the Aliaağa and Trabzon populations.

Table 6. Insecticide resistance status of Turkish *Aedes albopictus* populations reported by researchers

Study	Study area	Insecticides tested	Resistance status		
			Resistant	Possible resistant	Susceptible
Yavaşoğlu, 2021	Aydın-Kuşadası	DDT, Propoxur, Fenitrothion, Bendiocarb, Permethrin, Deltamethrin	DDT	Permethrin	Bendiocarb, Propoxur, Fenitrothion Deltamethrin
	Aydın-Güzelçamlı		DDT	Permethrin	Bendiocarb, Propoxur, Fenitrothion Deltamethrin
	Aydın-Didim			DDT, Propoxur Fenitrothion	Bendiocarb, Deltamethrin, Permethrin
	Muğla-Bodrum		DDT	Fenitrothion	Bendiocarb, Propoxur, Deltamethrin Permethrin

CONCLUSION

Turkey is situated in a suitable location for the maintenance of mosquito breeding areas due to reasons such as climatic characteristics, diversity of agricultural lands, changes in precipitation regime and increase in temperature due to global climate changes. In addition, due to its geopolitical location, it is in a region where there has been a large number of refugee movements as a result of the war in the Middle East in recent years. Accordingly, it is at risk from mosquito species that can come from both Africa, Asia and Europe, pathogens transmitted by mosquitoes, and therefore diseases. It has been observed that insecticide resistance levels have increased in many mosquito populations due to the use of insecticides for agricultural reasons as well as to prevent these mosquito-borne diseases. Conducting these studies is important both to draw attention to mosquito-borne disease and insecticide resistance in local population and to increase knowledge.

REFERENCES

Adhami, J., Murati, N. 2007. Presence of the mosquito Aedes albopictus in Albania. Rev. Mjekesore, 1: 13–16.

Akıner MM, Demirci B, Babuadze G, Robert V, Schaffner F (2016). Spread of the Invasive Mosquitoes Aedes aegypti and Aedes albopictus in the Black Sea Region Increases Risk of Chikungunya, Dengue, and Zika Outbreaks in Europe. Plos Neglected Tropical Diseases 10 (4): e0004664.

Akıner MM, Ekşi E. (2015) Evaluation of insecticide resistance and biochemical mechanisms of Culex pipiens L. in four localities of east and middle mediterranean basin in Turkey. *Int J Mosq Res*. 2(3): 39– 44.

Akıner MM, Öztürk M, Başer AB, Günay F, Hacıoğlu S, Brinkmann A, vd. (2019). Arboviral screening of invasive *Aedes* species in northeastern Turkey: West Nile virus circulation and detection of insect-only viruses. PLoS Negl Trop Dis, 13(5): e0007334.

Akıner MM, Şimşek FM, Çağlar SS. (2009) Insecticide resistance of Culex pipiens (Diptera: Culicidae) in Turkey. *J Pest Sci*. 34(4): 259– 264.

Aksu L, 1943. Malarya (Sıtma)-Tarihçe, Coğrafya, Türkiye'de Sıtma, Entomoloji, Bakteriyoloji, Biyoloji, Klinik, Patoloji, Tedavi, Mücadele ve Profilaksi, s.26, 34, 189.

Alten, B., Çağlar, S.S. 1998. Vektör Ekolojisi ve Mücadelesi. T.C. Sağlık Bakanlığı, Sıtma Savaşı Daire Başkanlığı, Ankara, 249 pp.

Arunachalam, N., Samuel, P.P., Hırıyan, J., Rajendran, R., Dash, A.P. 2005. Observations on the multiple feeding behavior of *Culex tritaeniorhynchus* (Diptera: Culicidae), the vector of Japanaese encephalitis in Kerala in Southern India. Am. J. Trop. Med. Hyg. 72(2): 198-200.

Azari-Hamidian, S., Yaghoobi-Ershadi, M. R., Javadian, E., Abai, M. R., Mobedi, I., Linton, Y. M., & Harbach, R. E. (2009). Distribution and ecology of mosquitoes in a focus of dirofilariasis in northwestern Iran, with the first finding of filarial larvae in naturally infected local mosquitoes. *Medical and veterinary entomology*, *23*(2), 111–121.

Beaty, B.J., Marquardt, W.C., 1996. The Biology of Disease Vectors. 450, University Press of Colorado, USA.

Becker, N., Petric, D., Zgomba, M., Boase, C., Dahl, C., Lane, J., Kaiser, A. 2003. Mosquitoes and Their Control. Kluwer Academic, Plenum publishers, USA, 498pp.

Bellini R, Veronesi R, Draghetti S, Carrieri M. 1997. Study on the flying height of Aedes caspius and Culex pipiens females in the Po Delta area, Italy. J Am Mosq Control Assoc. 13:356–360.

Benedict MQ, Levine RS, Hawley WA, Lounibos LP (2007). Spread of the tiger: global risk of invasion by the mosquito Aedes albopictus. Vector Borne Zoonotic Diseases 7:76–85.

Bhatt, S.; Gething, P.W.; Brady, O.J.; Messina, J.P.; Farlow, A.W.; Moyes, C.L.; Drake, J.M.; Brownstein, J.S.; Hoen, A.G.; Sankoh, O. The global distribution and burden of dengue. Nature 2013, 496, 504–507.

Bonizzoni, M., Gasperi, G., Xioaguang, C., Anthony, A.J. 2013. The invasive mosquito species Aedes albopictus: current knowledge and future perspectives Trends Parasitol., 29(9): 460–468.

Boreham, P. F, Garrett-Jones, C. 1973. Prevalence of mixed blood meals and double feeding in a malaria vector (*Anopheles sacharovi Favre*). Bull World Health Organ. 48(5):605-14.

Bozizic-Lothrop, B., Vujız, A. 1996. Fauna of mosquitoes (Diptera: Culicidae) of Stara Planina, Serbia. Acta entomologica Serbica, 1(1/2): 31-38.

Brugman, V. A., Hernández-Triana, L. M., Medlock, J. M., Fooks, A. R., Carpenter, S., Johnson, N. 2018. The role of *Culex pipiens* L. (Diptera: Culicidae) in virüs transmission in Europe. Int. J. Environ. Res. Public Health. 15(2): 389-397.

CDC (Centers for Disease Control and Prevention). Chikungunya virus in the United States. Atlanta. 2017. Available from www.Cdc.gov/chikungunya/geo/united-states.html

CDC (Centers for Disease Control and Prevention). Statistics and Map/Dengue. 2022.

Colpitts, TM, Conway, MJ, Montgomery, RR, and Fikrig E. (2012). West Nile Virus: biology, transmission, and human infection. Clin. Microbiol. Rev, 25: 635–648.

Coşgun Y, Bayrakdar F, Akıner MM, Gürer Giray B, Demirci B, Bedir H, Korukluoğlu G, Topluoğlu S, Kılıç S. Investigation of the presence of Zika, Dengue, Chikungunya, and West Nile virus in Aedes type mosquitoes in the Eastern Black Sea area of Turkey. Turk Hij Den Biyol Derg, 2023; 80(1): 101 – 108.

Cranston, P.S., Ramsdale, C.D., Snow, K.R. & White, G.B. (1987) Keys to the Adults, Male Hypopygia, Fourth-Instar Larvae and Pupae of the British Mosquitoes (Culicidae) with Notes on their Ecology and Medical Importance. Fresh Water Biological Association Scientific Publication, No.48, Cumbria, 152 pp.

Değirmenci, B., Akar, T., Özsoy, S., Ozdemir, M., Özdemir, B., & Demirel, B. (2016). The first fatal dengue virus infection case in Turkey: Autopsy findings. Romanian Journal of Legal Medicine, 24, 277-280.

Detinova, T. S., Smelova, V. A. 1973. Medical importance of mosquitoes (Culicidae, Diptera) from the fauna of the Soviet Union. Med. Parazitol. 42(4): 455-471.

Engler, O, Savini, G, Papa, A, Figuerola, J, Groschup, MH, Kampen, H, vd. (2013). European surveillance for West Nile virus in mosquito populations. Int. J. Environ. Res. Public Health, 10: 4869–4895.

Ergünay K, Günay F, Öter K, Kasap ÖE, Örsten S, Akkutay AZ, Erdem H, Özkul A, Alten B, (2013). Arboviral Surveillance of Field-Collected Mosquitoes Reveals Circulation of West Nile Virus Lineage 1 Strains in Eastern Thrace, Turkey. Vector-Borne and Zoonotic Diseases, 13: 744-752.

Ergünay K, Günay F, Öter K, Kasap ÖE, Örsten S, Akkutay AZ, Erdem H, Özkul A, Alten B, (2013). Arboviral Surveillance of Field-Collected Mosquitoes Reveals Circulation of West Nile Virus Lineage 1 Strains in Eastern Thrace, Turkey. Vector-Borne and Zoonotic Diseases, 13: 744-75.

Ergünay, K., Litzba, N., Brinkmann, A., Günay, F., Sarıkaya, Y., Kar, S., Örsten, S., Öter, K., Domingo, C., Erisoz Kasap, Ö., Özkul, A., Mitchell, L., Nitsche, A., Alten, B., & Linton, Y. M. (2017). Co-circulation of West Nile virus and distinct insect-specific flaviviruses in Turkey. *Parasites & vectors*, *10*(1), 149.

Ergünay, K., Saygan, M. B., Aydoğan, S., Menemenlioğlu, D., Turan, H. M., Ozkul, A., & Us, D. (2010). West Nile virus seroprevalence in blood donors from Central Anatolia, Turkey. *Vector borne and zoonotic diseases*, *10*(8), 771–775.

European Center for Disease Prevention and Control, 2018. Epidemiological update: West Nile virus transmission season in Europe, 2018. Stockholm: ECDC; 2018.

European Center for Disease Prevention and Control, 2019. Epidemiological update: West Nile virus transmission season in Europe, 2019. Stockholm: ECDC; 2019b.

European Centers for Disease Prevention and Control, 2020. Epidemiological update: West Nile virus transmission season in Europe, 2020. Stockholm: ECDC; 2020.

European Centre for Disease Prevention and Control. Zika. In: ECDC. Annual epidemiological report for 2018. Stockholm: ECDC; 2019a.

Franklinos, L. H. V, Jones, K. E., Redding, D. W., Abubakar, I. (2019) The effect of global change on mosquito-borne disease. *The Lancet Infectious Diseases*, 19 (9), e302-e312.

Gabinaud, A. 1975. Ecologie de deux *Aedes* halophile*s* du littoral méditerranéen français Aedes (Ochlerotatus*) caspius* (Pallas, 1771), *Aedes (Ochlerotatus) detritus* (Haliday, 1833) (Nematocera − Culicidae). Utilisation de la végétation comme indicateur biotique pour l'établissement d'une carte écologique. Application en dynamique des populations. PhD Thesis (manusc.), Academie de Montpellier, Universite des Sciences et Techniques du Languedoc, Montpellier, 451 pp.

Gatt, P., Deeming, J.C., & Schaffner, F. (2009). First record of Aedes (Stegomyia) albopictus (Skuse) (Diptera: Culicidae) in Malta. *European Mosquito Bulletin, 27*, 56-64.

Gómez, M., Martinez, D., Muñoz, M., & Ramírez, J. D. (2022). Aedes aegypti and Ae. albopictus microbiome/virome: new strategies for controlling arboviral transmission? *Parasites & vectors*, *15*(1), 287.

Gould EA, Higgs S (2009). Impact of climate change and other factors on emerging arbovirus diseases. Trans R Soc Trop Med Hyg, 103:109-121.

Gratz NG (2004). Critical review of the vector status of Aedes albopictus. Medical and Veterinary Entomology 18: 215–27

Guntay, O., Yikilmaz, M. S., Ozaydin, H., Izzetoglu, S., & Suner, A. (2018). Evaluation of Pyrethroid Susceptibility in *Culex pipiens* of Northern Izmir Province, Turkey. *Journal of arthropod-borne diseases*, *12*(4), 370–377.

Gutsevich AV, Monchadskii AS, Shtakelberg AA (1974). Fauna of the U.S.S.R. Diptera. Volume 3, No.4 Mosquitoes Family Culicidae. Jerusalem: KeterPublishing House.

Guz N, Cagatay NS, Fotakis EA, Durmusoglu E, Vontas J. (2020) Detection of diflubenzuron and pyrethroid resistance mutations in Culex pipiens from Muğla, Turkey. *Acta Trop*. 203: 105294.

Günay F (2015). Türkiye sivrisinek faunası üzerine DNA barkodlama yöntemiyle moleküler analizler. Doktora Tezi, Hacettepe Üniversitesi Fen Bilimleri Enstitüsü. 120 p.

Günay, F., Alten, B., Simsek, F., Aldemir, A., Linton, Y.M. 2015. Barcoding Turkish *Culex* mosquitoes to facilitate arbovirus vector incrimination studies reveals hidden diversity and new potential vectors. Acta Trop. 143:112–20.

Habirov Z, Kadamov D, Iskandarov F, Komilova S, Cook S, McAlister E, et al. Malaria and the Anopheles mosquitoes of Tajikistan. J Vec Ecol. 2012;37:419–27.

Hannoun C, Panthier R, Mouchet J, Eouzan JP (1964). Isolement en France du virus West Nile à partir de malades et du vecteur Culex modestus Ficalbi. C.R Acad Sci D., 259: 4170–4172.

Hayes EB, Sejvar JJ, Zaki SR, Lanciotti RS, Bode AV and Campbell GL (2005). Virology, pathology, and clinical manifestations of West Nile virus disease. Emerg. Infect. Dis, 11: 1174–1179.

Hemingway J (1992). Insecticide resistance gene frequencies of Anopheles sacharovi populations of Cukurova plain., Adana province, Turkey. Medical and Veterinary Entomology 6: 4342-348.

Hemingway J, Ranson H. Insecticide resistance in insect vectors of human disease. Annu Rev Entomol 2000; 45:371-91

Kalaycioglu H, Korukluoglu G, Ozkul A, Oncul O, Tosun S, Karabay O (2012). Emergence of West Nile virus infections in humans in Turkey, 2010 to 2011. Euro Surveill, 2012: 17(21):20182.

Kamgang, B., Nchoutpouen, E., Simard, F., Christophe, P. 2012. Notes on the blood-feeding behavior of Aedes albopictus (Diptera: Culicidae) in Cameroon. Parasit. Vectors., 5:57-61.

Kanojia, P.C., Paingankar, M. S., Patil, A. A., Gokhale, M. D., Deobagkar, D.N. 2010. Morphometric and allozyme variation in *Culex tritaeniorhynchus* mosquito populations from India. Journal of Insect Science. 10 (1): 138-146.

Kasap H, kasap M, Aleptekin D, Luleyap U, Herath PRJ (2000). Insecticide resistance in Anopheles sacharovi favor in southern Turkey. Bull. WHO. 78 (5);687-692

Kasap, H., Kasap, M., Mimioğlu, M. M., Aktan, F. 1981. Çukurova ve Çevresinde Sivrisinek ve Malaria Üzerine Araştırmalar. Doğa Bilim Dergisi, 5: 141-150.

Kılıçarslan, E., Öztürk, M., Beriş, F. Ş., Demirtaş, R. & Akıner, M. M. (2022). Monitoring and distribution of kdr and ace-1 mutation variations in Culex pipiens L., 1758 (Diptera: Culicidae) in artificial sites and agricultural fields in the central and eastern Black Sea Region of Türkiye. Turkish Journal of Entomology, 46 (3), 343-358.

Kraemer, M.U.G., Sinka, M.E, Duda, K.A., Mylne, A.Q.N., Shearer, F.M., Barker, C.M. 2015. The global distribution of the arbovirus vectors Aedes aegypti and Ae. Albopictus. Elife, 4:1–18.

Pierrick Labbé, Jean-Philippe David, Haoues Alout, Pascal Milesi, Nicole Pasteur, et al..Evolution of resistance to insecticide in disease vectors. Genetics and evolution of infectious diseases, Academic press, Elsevier, 2017, 28pp.

Lacey L. A. (2007). Bacillus thuringiensis serovariety israelensis and Bacillus sphaericus for mosquito control. *Journal of the American Mosquito Control Association*, *23*(2 Suppl), 133–163.

Lambert, M., Pasteur, N., Rioux, J., Delabre-Belmonte, A., Balard, Y. 1990. *Aedes caspius* (Pallas, 1771) et *Ae. dorsalis* (Meigen, 1830) (Diptera: Culicidae). Analyses Morphologique et Genetique de Deux Populations Sympatriques. Preuves de L'isolement reproductif. Annales de la Societe entomologique de France, 26(3): 381-398.

Lambrechts, L., Scott, T.W., Gubler, D.J. 2010. Consequences of the Expanding Global Distribution of Aedes albopictus for Dengue Virus Transmission. PLoS Negl Trop Dis., 4 (5): e646.

Longbottom, J., Browne, A.J., Pigott, D.M., Sinka, M.E., Golding, N., Hay, S.I., Moyes, C.L., Shearer, F.M. 2017. Mapping the spatial distribution of the Japanese encephalitis vector, *Culex tritaeniorhynchus* Giles, 1901 (Diptera: Culicidae) within areas of Japanese encephalitis risk. Parasites & Vectors. 10: 148-155.

Lustig Y, Hindiyeh M, Orshan L, Weiss L, Koren R, Katz-Likvornik S. et al. (2015). Fifteen years of mosquito surveillance reveals high genetic diversity of West Nile Virus in Israel. J. Infect. Dis, 213: 1107–1114.

Lüleyap, Ü., Kasap, H. 2000. "Sıtma vektörü *Anopheles sacharovi*'de fizyolojik insektisit direnci", Turkish Journal of Biology, 24, 437-460.

Mayer SV, Tesh RB, Vasilakis N (2017) The emergence of arthropod-borne viral diseases: A global prospective on dengue, chikungunya and zika fevers. Acta Trop, 166: 155-63.

Merdic, E. 2004. Checklist of mosquitoes (Diptera: Culicidae) of Croatia. European Mosquito Bulletin, 17:8-13.

Merdivenci, A. 1984. Türkiye Sivrinekleri (Yurdumuzda Varlığı Bilinen Sivrineklerin Biyo – Morfolojisi, Biyo – Ekolojisi, Yayılışı ve Sağlık Önemleri). İstanbul Üniversitesi, Cerrahpaşa Tıp Fakültesi Yayınları, pp 340, İstanbul.

Miller, R. H., Masuoka, P., Klein, T. A., Kim, H.C., Somer, T., Grieco, J., 2012. Ecological Niche Modeling to Estimate the Distribution of Japanese Encephalitis Virus in Asia. PLoS Negl Trop Dis. 6 (6): e1678.

Öncü C, Brinkmann A, Günay F, Kar S, Öter K, Sarıkaya Y, Nitsche A, Linton Y-M, Alten B, Ergünay K. 2018. West Nile virus, Anopheles flavivirus, a novel flavivirus as well as Merida-like rhabdovirus Turkey in field-collected mosquitoes from Thrace and Anatolia. Infect Genet Evol. 57:36–45.

Öter K, Gunay F, Tuzer E, Linton YM, Bellini R, Alten B (2013). First record of Stegomyia albopicta in Turkey determined by active ovitrap surveillance and DNA barcoding. Vector Borne Zoonotic Diseases 13 (10): 753-61.

Özbay D, Kara M, Tuğcu D, Hançerli Törün S, Sütçü M, Çalışkan E, et al. A case of dengue fever complicated with trombophlebitis in a child. J Pediatr Inf 2019;13(1):e28-e31

Özbilgin, A., Topluoglu, S., Islek, E., Mollahaliloglu, E., Erkoc, Y. 2011. Malaria in Turkey: Successful control and strategies for achieving elimination, Acta Tropica, 120:15-23.

Özer N, Ergunay K, Şimsek F, Kaynaş S, Alten B, Çağlar SS, Ustaçelebi S (2007). West Nile Virus studies in the Sanliurfa province of Turkey. Journal of Vector Ecology, 32: 202-206.

Özkul A, Ergunay K, Köysüren A, Alkan F, Arsava EM, Tezcan S, Emekdaş G, Hacıoğlu S, Turan M, Us D (2013). Concurrent occurrence of human and equine West Nile virus infections in Central Anatolia, Turkey: the first evidence for circulation of lineage 1 viruses. International Journal of Infectious Diseases, 17: 546–551.

PAHO (Pan American Health Organization). (2022) Epidemiological Update for Dengue and other Arboviruses. Available from https://ais.paho.org/ha_viz/Arbo/Arbo_Bulletin_2022.asp?env=pri

Patsoula, E., Samanidou-Voyadjoglou, A., Spanakos, G., Kremastinou, J., Nasioulas, G., Vakalis, N. C. 2007. Molecular characterization of the *Anopheles maculipennis complex* during surveillance for the 2004 Olympic Games in Athens. Med. Vet. Entomol. 21(1):36-43.

Petersen LR, Brault AC and Nasci RS (2013). West Nile virus: review of the literature. JAMA, 310: 308–315.

Pichler, V., Caputo, B., Valadas, V., Micocci, M., Horvath, C., Virgillito, C., Akiner, M., Balatsos, G., Bender, C., Besnard, G., Bravo-Barriga, D., Bueno-Mari, R., Collantes, F., Delacour-Estrella, S., Dikolli, E., Falcuta, E., Flacio, E., García-Pérez, A. L., Kalan, K., Kavran, M., … Della Torre, A. (2022). Geographic distribution of the V1016G knockdown resistance mutation in Aedes albopictus: a warning bell for Europe. *Parasites & vectors*, *15*(1), 280.

Ramsdale CD, Snow K. 2000. Distribution of the genus Anopheles in Europe. Eur Mosq Bull 7:1–26.

Ramsdale, C. D., P. R. J. Herath and G. Davidson. 1980. Recent developments of insecticide resistance in some Turkish anophelines. J. Trop. Med. Hyg. 83:11-19.

Ramsdale, C.D., Alten, B., Çaglar, S.S., Özer, N. 2001. A revised, annotated checklist of the mosquitoes (Diptera: Culicidae) of Turkey. The European Mosquito Bulletin, 9: 18-28.

Romi, R., Boccolini, D., Hovanesyan, I., Grigoryan, G., D, iLuca M, Sabatinell, G. 2002. *Anopheles sacharovi* (Diptera: Culicidae): a reemerging malaria vector in the Ararat Valley of Armenia. J Med Entomol. 39(3):446-50.

Schaffner F, Mathis A. Dengue and dengue vectors in the WHO European region: past, present, and scenarios for the future. The Lancet Infectious Diseases. 2014;14(12):1271-80.

Schaffner, F., Angel, G., Geoffroy, B., Hervy J. P, Rhaiem A, J. B. 2001. The mosquitoes of Europe (CD ROM). Montpellier, France.

Ser, O., & Cetin, H. (2019). Investigation of Susceptibility Levels of *Culex pipiens* L. (Diptera: Culicidae) Populations to Synthetic Pyrethroids in Antalya Province of Turkey. *Journal of arthropod-borne diseases*, *13*(3), 243–258.

Serter D. Present status of arbovirus sero-epidemiology in the Aegean region of Turkey. Zbl Bakt 1980 (S9): 155-61.

Sinka, M.E., Bangs, M.J., Manguin, S., Coetzee, M., Mbogo CM, Hemingway J. 2010. The dominant Anopheles vectors of human malaria in Africa, Europe and the Middle East: occurrence data, distribution maps and bionomic precis. Parasit Vectors. 3:117-125.

Soliman DE, Farid HA, Hammad RE, Gad AM, Bartholomay LC. 2016. Innate cellular immune responses in Aedes caspius (Diptera: Culicidae) mosquitoes. J Med Entomol. 53(2):262–267.

Taskin BG, Dogaroglu T, Kilic S, Dogac E, Taskin V. (2015) Pesticide biochemistry and physiology, seasonal dynamics of insecticide resistance, multiple resistance, and morphometric variation in field populations of Culex pipiens. *Pestic Biochem Physiol*. 129: 14– 27.

Tezcan S, Kızıldamar S, Ulger M, Aslan G, Tiftik N, Ozkul A, Emekdaş G, Niedrig M, Ergünay K. Flavivirus seroepidemiology in blood donors in Mersin province, Turkey. Mikrobiyol Bul. 2014; 48:606-617.

Turell, M. J., O'Guinin M. L., Dohm, D. J., Jones, J.W. 2001. Vector competence of North American mosquitoes (Diptera:Culicidae) for West Nile Virus. J.Med.Entomol. 38: 130–134.

Uyar Y, Aktaş E, Yağcı Çağlayık D, Ergönül O, Yüce A. An imported dengue Fever case in Turkey and review of the literature. Mikrobiyol Bul 2013; 47(1): 173-80.

Vinogradova, E.B. 2000. *Culex pipiens* Mosquitoes: Taxonomy, Distribution, Ecology, Physiology, Genetics, Applied Importance and Control, Pensoft Publishers, Sofia, Bulgaria, 250 pp.

Violaris, M., Vasquez, M.I., Samanidou, A., Wirth, M.C., Hadjivassilis, A. 2009. The mosquito fauna of the Republic of Cyprus: a revised list. J Am Mosq Control Assoc. 25(2):199-202.

Wang, G., Li, C., Guo, X., Xing, D., Dong, Y., Wang, Z., Zhang, Y., Liu, M., Zheng, Z., Zhang, H., Zhu, X., Wu, Z., & Zhao, T. (2012). Identifying the main mosquito species in China based on DNA barcoding. *PloS one*, *7*(10), e47051.

WHO (World Health Organisation). (2022) World malaria report 2022.

WHO. Global insecticide use for vector-borne disease control, a 10 year assessment (2000-2009). 2011.

Wilson, J.J. Sevarkodiyone, S.P. 2015. Host Preference of Blood Feeding Mosquitoes in Rural Areas of Southern Tamil Nadu, India. Academic Journal of Entomology 8 (2): 80-83.

World Health Organisation (WHO), 2013. Republic of Turkey Ministry of Health, World Health Organization and the University of California, San Francisco Global Health Group. Eliminating Malaria : Case-study 5. The long road to malaria elimination in Turkey. Geneva, Switzerland.

World Health Organization, "World Malaria Project 2012," 2012.

Yavaşoglu, S. İ., Yaylagül, E. Ö., Akıner, M. M., Ülger, C., Çağlar, S. S., & Şimşek, F. M. (2019). Current insecticide resistance status in Anopheles sacharovi and Anopheles superpictus populations in former malaria endemic areas of Turkey. *Acta tropica*, *193*, 148–157.

Yavaşoğlu SI. First report on mild insecticide resistance in newly established Aegean Aedes albopictus populations of Turkey. Turk J Zool 2021; 45: 223-34.

Yavaşoğlu, S. İ., & Şimşek, F. M. (2022). Allele Specific Polymerase Chain Reaction (AS-PCR) Assay to Detect Knockdown and Acetylcholinesterase Mutations in *Anopheles superpictus*. *Turkısh Journal of Parasitology*, *46*(4), 307–311.

Yavaşoğlu, S. İ., Bursalı, F., & Şimşek, F. M. (2022). Detection of L1014F knockdown resistance mutation in Culex tritaeniorhynchus populations. *Pesticide biochemistry and physiology*, *188*, 105229.

Yurttas, H., Alten, B. 2006. Geographic differentiation of life table attributes among *Anopheles sacharovi* (Diptera: Culicidae) populations in Turkey. J. Vector Ecol. 31(2):275-8

Chapter 5

A Computational Study on a Versatile Material with Promising Applications in Various Fields

Ahmet KUNDURACIOĞLU[1]

[1] Asist. Prof. Dr. .;Bursa Uludag University Mustafakemalpasa Voc. College, org. Agriculture Dept.. ahmettkunduracioglu@gmail.com or akunduracioglu@uludag.edu.tr
ORCID No: 0000-0002-6421-9912

ABSTRACT

In this study, a very versatile molecule with the IUPAC name (7R)-3-[(5-methyl-1,3,4-thiadiazol-2-yl)sulfanylmethyl]-8-oxo-7-[[2-(tetrazol-1-yl) acetyl]amino]-5-thia-1-azabicyclo[4.2.0]oct-2-ene-2-carboxylic acid (MTSTA) has been investigated via computational methods. SPARTAN'14 a computational chemistry software was used in these studies with HF and DFT methods in the level of EDF2 and B3LYP. The calculated bond lengths, bond angles and torsion angles have been tabulated and depicted. Also, Mulliken charges, NMR spectra and other properties have been examined.

Keywords: Cephalosporin Antibiotics, Spectroscopic Properties, Molecular Structure, HOMO&LUMO, Computational Chemistry.

INTRODUCTION

In recent years, the exploration of novel materials with exceptional properties has been a focal point of scientific research. Among these materials. The compound with the IUPAC name (7R)-3-[(5-methyl-1,3,4-thiadiazol-2-yl)sulfanylmethyl]-8-oxo-7-[[2-(tetrazol-1-yl)acetyl]amino]-5-thia-1-azabicyclo[4.2.0]oct-2-ene-2-carboxylic acid (MTSTA) is a complex chemical compound with significant pharmaceutical potential. Its intricate molecular structure encompasses diverse functional groups and heterocyclic components, making it a compound of interest in medicinal chemistry and drug discovery. (Barupal&Fiehn, 2019)

The Class of Cephalosporin Antibiotics

This compound belongs to the class of cephalosporin antibiotics, which are widely used for their antibacterial properties. Cephalosporins exhibit a broad spectrum of activity against various bacterial strains by interfering with the synthesis of bacterial cell walls. They target specific enzymes involved in cell wall biosynthesis, inhibiting bacterial growth and reproduction. (Chen et al., 2018)

The title compound (MTSTA) possesses a unique chemical structure that contributes to its antibacterial effects. The presence of the 5-methyl-1,3,4-thiadiazol-2-yl and tetrazol-1-yl moieties in the side chain adds to its pharmacological activity and potential therapeutic applications.

Understanding the properties, synthesis, and biological activities of this compound is crucial in the development of new antibiotics and the treatment of bacterial infections. Further exploration of its structure-activity relationships and mechanisms of action can lead to the discovery of more effective and targeted antibacterial agents. (Murakami et al.1981)

Computational Studies on the Class of Cephalosporin Antibiotics

Computational studies have played a significant role in advancing our understanding of the Class of Cephalosporin Antibiotics, a group of widely used antibacterial agents. Through computational techniques and simulations, researchers have gained valuable insights into the structural properties, mechanisms of action, and drug design aspects of these antibiotics.

One area of computational research involves the elucidation of the three-dimensional structures of cephalosporin antibiotics. Using computational modeling approaches such as molecular dynamics simulations and quantum mechanical calculations, researchers have been able to predict and refine the molecular structures of these compounds. These studies provide insights into

the conformational flexibility, stability, and intermolecular interactions that play a crucial role in their biological activity.(Mittal et al., 2019, Mittal&Awasthi, 2019)

Furthermore, computational studies have shed light on the mechanisms of action of cephalosporins. By employing molecular docking, molecular dynamics simulations, and quantum mechanical calculations, researchers have explored how these antibiotics interact with their biological targets, typically enzymes involved in cell wall synthesis. Computational approaches have helped in understanding the binding modes, energetics, and dynamics of the antibiotic-target interactions, providing valuable information for the development of more potent and selective antibiotics.

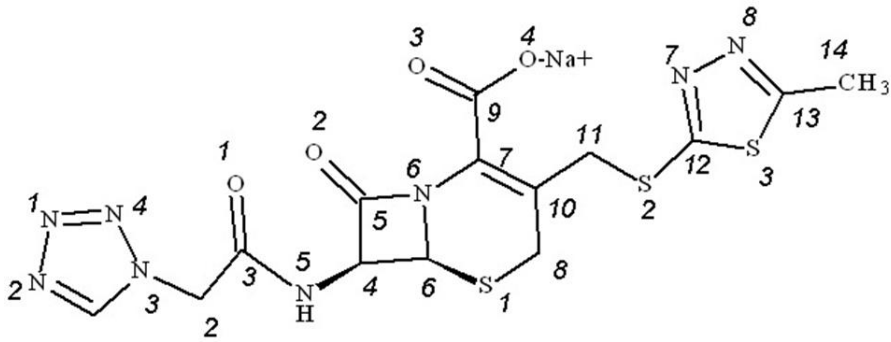

Figure 1. Molecular formula and Labeling of the Atoms in MTSTA

Computational studies have also been instrumental in identifying structure-activity relationships (SAR) within the cephalosporin class. By systematically modifying the chemical structure of these antibiotics and performing virtual screening studies, researchers have gained insights into the key structural features that contribute to their antibacterial activity. This knowledge has facilitated the rational design and optimization of cephalosporin derivatives with enhanced efficacy, improved pharmacokinetic properties, and reduced resistance development. (Awastiet al.,2022)

Moreover, computational approaches have been utilized to explore the resistance mechanisms and develop strategies to overcome bacterial resistance to cephalosporin antibiotics. Through the analysis of bacterial resistance enzymes (e.g., beta-lactamases) and the study of resistance-conferring mutations, computational methods have provided insights into the structural basis of resistance and guided the design of novel inhibitors that can restore the activity of cephalosporins against resistant strains.

In conclusion, computational studies have significantly contributed to our understanding of the Class of Cephalosporin Antibiotics. By providing insights into their structures, mechanisms of action, SAR, and resistance mechanisms, computational approaches have facilitated the rational design and optimization of these antibiotics. Through the integration of computational and experimental studies, the development of more effective and targeted cephalosporin antibiotics is continuously advancing, offering new solutions in the fight against bacterial infections.

EXPERIMENTAL STUDIES

Computational Details:

Spartan is a powerful computational chemistry software widely used by researchers and scientists in the field of molecular modeling and simulations. Developed by Wavefunction Inc., Spartan offers a range of tools and capabilities that facilitate the study of molecular structures, properties, and reactions. (Hehre, 2014)

One of the key features of Spartan is its user-friendly interface, which allows researchers to easily set up and run various calculations. The software supports a wide range of computational methods, including molecular mechanics, semi-empirical methods, and quantum mechanical calculations. It also provides a diverse set of visualization tools, enabling users to analyze and interpret results effectively.

Spartan offers extensive capabilities for studying molecular properties, such as geometries, energies, electronic structures, and spectroscopic properties. It enables researchers to perform tasks such as molecular docking, drug design, and optimization of reaction pathways. The software also supports the calculation of molecular properties in solution and can simulate complex systems using molecular dynamics simulations. (Hehre, 2014a, Hehre, 2014b)

Overall, Spartan computational software provides a comprehensive suite of tools and features that empower researchers to explore and understand molecular systems. Its versatility, user-friendly interface, and wide range of computational methods make it an invaluable tool in various fields, including pharmaceutical research, materials science, and chemical engineering.

In this study SPARTAN'14 was used with HF and DFT (EDF2 and B3LYP) methods using 3-21G, 6-31G* basis sets. All calculations were carried on according to ground state in vacuum media. Calculations were arranged primarily to examine the compound from three aspects: molecular structure, electronic properties, and spectroscopic data. (Kunduracioglu, 2021)

Molecular Structure

The bond lengths, bond angles, and dihedral angles form the molecular structure of any compound.Understanding the molecular structure of compounds is essential in elucidating their chemical properties and behaviors. The arrangement of atoms, as characterized by bond lengths, bond angles, and dihedral angles, plays a critical role in determining a molecule's overall shape and reactivity. In this article, we delve into the experimental aspect of exploring molecular structure, focusing on the measurement and analysis of these geometric parameters.

Experimental techniques such as X-ray crystallography, neutron diffraction, and spectroscopic methods provide valuable insights into the structural features of molecules. X-ray crystallography, for example, utilizes the diffraction patterns obtained from crystalline samples to determine the precise positions of atoms and their connectivity within the crystal lattice. This information enables the determination of accurate bond lengths and bond angles.Silverstein et al., 2005)

Similarly, spectroscopic methods, including infrared (IR) and nuclear magnetic resonance (NMR) spectroscopy, offer valuable data on molecular structure. IR spectroscopy provides information about bond vibrations and can be used to infer bond lengths and angles based on characteristic absorption frequencies. NMR spectroscopy, on the other hand, provides insights into the connectivity of atoms within a molecule and can aid in determining dihedral angles. Jensen, 2017)

The experimental determination of bond lengths, bond angles, and dihedral angles provides essential information for validating and refining theoretical models and computational predictions. These parameters are crucial in understanding the stability, reactivity, and intermolecular interactions of compounds. Moreover, they form the foundation for studying molecular dynamics, conformational analysis, and structure-activity relationships in various scientific disciplines, including chemistry, biochemistry, and material science.

Table 1. Calculated Bond Lengths Of MTSTA

BONDS	HF-321G	EDF2 6-31G*	B3LYP 6-31G*	BONDS	HF-321G	EDF2 6-31G*	B3LYP 6-31G*
C5,C4	1.549	1.541	1.549	**N4,N3**	1.406	1.351	1.359
C2,C3	1.527	1.535	1.542	**N3,N2**	1.281	1.291	1.295
C4,C6	1.580	1.564	1.571	**N2,N1**	1.384	1.348	1.355
C7,C9	1.506	1.515	1.523	**N7,N8**	1.429	1.363	1.373
C10,C11	1.510	1.494	1.501	**N1,C1**	1.344	1.343	1.348
C13,C14	1.498	1.488	1.496	**N4,C1**	1.302	1.314	1.318
C3,O1	1.214	1.218	1.221	**N5,C3**	1.355	1.358	1.364
O2,C5	1.218	1.220	1.223	**N5,C4**	1.429	1.426	1.433
O3,C9	1.257	1.256	1.259	**N6,C6**	1.472	1.457	1.463
O4,C9	1.264	1.260	1.264	**N6,C5**	1.359	1.366	1.371
C1,H1	1.061	1.079	1.080	**N6,C7**	1.404	1.398	1.406
H3,C2	1.077	1.089	1.090	**N7,C12**	1.284	1.304	1.306
H2,C2	1.081	1.094	1.095	**N8,C13**	1.279	1.296	1.299
H5,C4	1.077	1.092	1.092	**N1,C2**	1.454	1.449	1.457
H4,N5	1.001	1.016	1.017	**S3,C13**	1.743	1.758	1.766
H6,C6	1.076	1.093	1.094	**S1,C6**	1.803	1.819	1.829
H8,C8	1.084	1.096	1.097	**S1,C8**	1.830	1.841	1.851
H7,C8	1.081	1.093	1.094	**S2,C11**	1.836	1.859	1.870
H9,C11	1.078	1.091	1.092	**S2,C12**	1.750	1.751	1.760
H10,C11	1.076	1.089	1.090	**S3,C12**	1.742	1.753	1.761
H13,C14	1.080	1.091	1.093	**Na1,O3**	2.195	2.241	2.253
H11,C14	1.084	1.094	1.096	**Na1,O4**	2.359	2.336	2.344
H12,C14	1.084	1.094	1.096				

Bond lengths are tabulated on Table 1. As seen from the table O3-Na1 bond is shorter then O4-Na1. But the difference is not as big as expected. Most dramatical change is seen in C-O bonds: C3-O1, C5-O2 bonds are almost equal, but O3-C9 bond is markedly longer than first two. And as expected, O4-C9 bond is prominently the longest. N7-N8 bond is longer than other N-N bonds.

Table 2. Calculated Bond Angles Of MTSTA

Angle	HF-321G	EDF2 6-31G*	B3LYP 6-31G*	Angle	HF-321G	EDF2 6-31G*	B3LYP 6-31G*
N4,C1,N1	110.13	108.92	109.05	**C10,C7,C9**	125.53	127.67	127.75
C1,N1,N2	107.29	107.61	107.56	**C7,C9,O4**	117.29	116.87	116.83
N1,N2,N3	106.90	106.70	106.67	**C7,C9,O3**	116.70	115.79	115.85
N2,N3,N4	110.20	110.98	111.01	**C7,C10,C11**	120.60	119.39	119.44
N3,N4,C1	105.48	105.79	105.71	**C10,C11,S2**	110.99	112.12	112.55
N2,N1,C2	120.85	121.18	121.24	**C11,S2,C12**	100.29	100.48	100.79
N1,C2,C3	111.95	114.37	114.52	**C12,S3,C13**	87.29	86.36	86.26
C1,N1,C2	131.82	131.12	131.12	**S2,C12,S3**	120.25	120.56	120.22
C3,N5,C4	121.07	121.41	121.59	**S3,C13,N8**	114.17	113.19	113.31
O1,C3,C2	121.27	120.12	120.00	**S3,C13,C14**	122.46	122.99	122.87
O1,C3,N5	124.08	124.71	124.69	**C13,N8,N7**	112.21	113.80	113.72
C4,N5,C3	121.07	121.41	121.59	**N8,N7,C12**	112.57	113.38	113.26
C6,N6,C5	96.45	95.52	95.58	**N7,C12,S3**	113.75	113.27	113.44
N5,C4,C5	115.07	115.69	115.93	**H1,C1,N4**	125.71	126.66	126.58
N5,C4,C6	119.39	119.38	119.42	**H3,C2,H2**	109.91	108.75	108.82
C4,C6,N6	86.15	87.61	87.58	**H4,N5,C3**	119.96	119.14	119.19
C2,C3,N5	114.62	115.14	115.26	**H4,N5,C4**	118.94	119.40	119.20
O2,C5,N6	131.81	133.11	133.15	**H5,C4,N5**	109.42	107.93	107.98
O2,C5,C4	136.40	134.85	134.89	**H5,C4,C6**	112.56	113.02	112.93
S2,C12,N7	125.99	126.16	126.34	**H6,C6,C4**	115.99	115.49	115.50
C4,C6,S1	115.81	117.44	117.55	**S1,C6,N6**	109.53	111.00	110.98
C6,S1,C8	95.67	94.14	94.35	**H8,C8,H7**	107.39	106.18	106.38
S1,C8,C10	115.23	115.55	115.75	**H9,C11,H10**	110.33	109.92	109.75
C8,C10,C7	123.42	123.70	123.79	**H13,C14,H11**	109.10	108.80	108.85
C10,C7,N6	120.85	120.23	120.26	**H11,C14,H12**	108.54	107.77	107.79
C7,N6,C5	128.76	131.19	131.18	**H12,C14,H13**	109.11	108.84	108.88

Bond angles are shown in the Table 2. According to the table the CSC bonds vary in a range far from each other, with different values such as 95, 100, and 87. This is because S1 and S3 are ring atoms while S2 atom is on a chain. The same is true for angles containing N. C3N5C4 is about 121° while C5N6C6 is 95°. As the same, C4C6N6 is about 87° while other CCN bonds are about 120°.

In short, an angle changes according to the geometric part to which it belongs. (Kunduracioglu, 2021)

Table 3. Calculated Dihedral (torsion) Angles Of MTSTA

Bonds	HF-321G	EDF2 6-31G*	B3LYP 6-31G*	Bonds	HF-321G	EDF2 6-31G*	B3LYP 6-31G*
C1,N1,N2 ,N3	-0.06	0.09	0.10	**C6,N6, C7,C10**	-14.26	-9.40	-10.14
N4,N3, N2,N1	0.28	0.22	0.20	**N6,C7, C10,C8**	5.55	1.81	2.00
N2,N1, C2,C3	-78.86	-70.37	-71.72	**N6,C6, S1,C8**	-52.42	-52.78	-52.31
N1,C2, C3,O1	-135.00	-138.14	-138.43	**C10,C8, S1,C6**	48.73	49.12	48.32
N1,C2, C3,N5	46.75	43.95	43.74	**C8,C10, C11,S2**	-93.81	-86.43	-88.14
C2,C3, N5,C4	-177.75	-178.44	-179.08	**C10,C11 S2,C12**	100.96	100.61	101.36
O1,C3, N5,C4	4.06	3.76	3.20	**C11,S2, C12,S3**	164.38	168.36	167.00
N5,C4, C5,O2	-45.48	-50.63	-50.88	**S3,C12, N7,N8**	-0.15	-0.19	-0.18
C4,C6, N6,C5	8.18	4.93	5.05	**C12,S3, C13,N8**	0.50	0.38	0.44
O2,C5, N6,C6	165.53	170.52	170.83	**C12,S3, C13,C14**	-179.58	-179.64	-179.62
O2,C5, N6,C7	14.79	16.99	16.98				

Table 3 exhibits the torsion angles of the molecule MTSTA. The spatial position of a molecule is an important property of its geometry. Especially in cyclic compounds, or in compounds containing rings, the buckling angle gains great importance. There are 3 separate rings in the MTSTA molecule. While the rings 1 and 3 of these rings are mostly planar, it is seen that the ring number 2, which contains S, is bent between 15-80 degrees around S2.

Mulliken Charge Distribution

Like other compounds, MTSTA's atoms have different electronegativities. Electron distribution is not homogenous on the molecule for this reason. The more an atom is electronegative, the more electrons it gathers up. different partial charges on each atom occur because of this heterogeneity. The electron-rich parts of the molecule are partially negatively charged, and the electron-poor parts are partially positively charged. Therefore, electron-rich regions are more

susceptible to electrophilic attacks, while electron-poor regions are more susceptible to nucleophilic attacks. The Mulliken charge distribution is therefore of particular importance in predicting potential reaction mechanisms that the molecule is involved(Jensen, 2016). ESPMap determines the distance at which a given positive charge can interact with and bind to the molecule. Molecular ESP is calculated via equation 1 (Peter et al., 2011).

$$Vr = \sum_A \frac{Z_A}{R_A - r} - \int \frac{\rho(r')}{(r' - r)} dr' \quad (1)$$

The calculated Mulliken charge values are exhibited in Table 4 for MTSTA which are also depicted as figure2 as colors. Also Figure 3 exhibits these values as graphics.

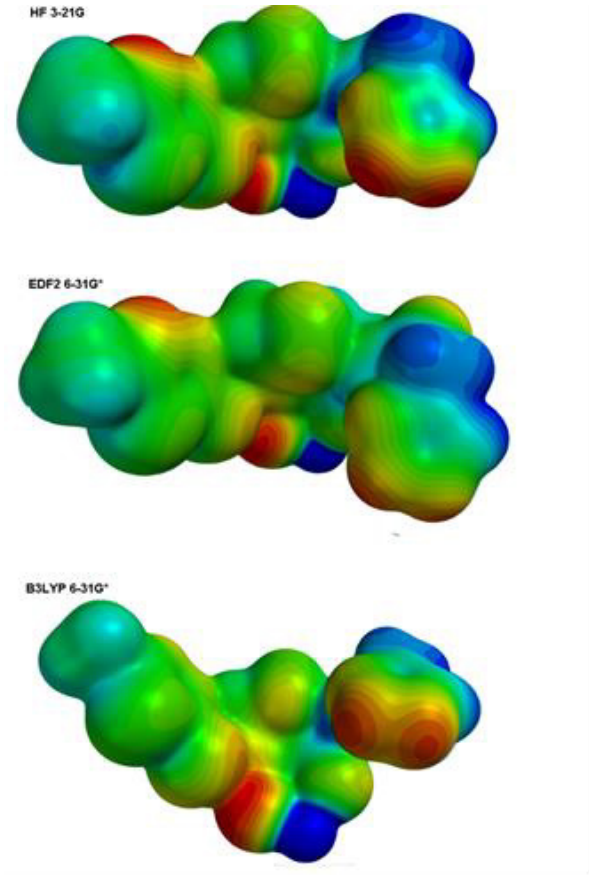

Figure 2. Electrostatic Potential Map Of MTSTA

At a glance the most important points are briefly:

- All O atoms have negative charge as expected. And their charges don't differ dramatically.
- Although all N atoms have negative charges their values differ according to position and neighborhood. N5 and N6 those are chain atoms, have bigger negative charge than the N atoms of the rings.
- S atoms have positive charges, but their values differ due to their positions too.
- C atoms are divided into two parts, C1, C3, C5, C7, C9 and C13 have positive charges and the others have negative. Also their charge values remarkebly change according to their positions.

Table 4. Calculated Mulliken Charges Of atoms in MTSTA

Atom	HF-321G	EDF2 6-31G*	B3LYP 6-31G*	Atom	HF-321G	EDF2 6-31G*	B3LYP 6-31G*
N1	-0.698	-0.236	-0.247	**O1**	-0.614	-0.485	-0.489
N2	-0.032	-0.091	-0.088	**O2**	-0.663	-0.517	-0.522
N3	-0.051	-0.074	-0.072	**O3**	-0.674	-0.535	-0.543
N4	-0.419	-0.302	-0.303	**O4**	-0.678	-0.532	-0.540
N5	-0.923	-0.587	-0.595	**S1**	0.249	0.128	0.125
N6	-0.959	-0.456	-0.468	**S2**	0.395	0.239	0.236
N7	-0.427	-0.283	-0.283	**S3**	0.420	0.237	0.235
N8	-0.363	-0.252	-0.254	**Na1**	0.565	0.550	0.553
C1	0.485	0.256	0.263	**H1**	0.325	0.212	0.205
C2	-0.245	-0.285	-0.262	**H2**	0.313	0.232	0.225
C3	0.885	0.598	0.605	**H3**	0.296	0.216	0.209
C4	-0.132	-0.110	-0.094	**H4**	0.422	0.391	0.388
C5	1.017	0.632	0.640	**H5**	0.332	0.228	0.223
C6	-0.104	-0.140	-0.128	**H6**	0.281	0.205	0.198
C7	0.286	0.284	0.279	**H7**	0.327	0.239	0.235
C8	-0.644	-0.537	-0.519	**H8**	0.263	0.202	0.195
C9	0.794	0.471	0.491	**H9**	0.291	0.224	0.217
C10	-0.029	0.124	0.118	**H10**	0.295	0.226	0.219
C11	-0.624	-0.537	-0.516	**H11**	0.241	0.187	0.180
C12	-0.137	-0.087	-0.087	**H12**	0.241	0.187	0.180
C13	0.060	0.105	0.105	**H13**	0.270	0.204	0.197
C14	-0.635	-0.532	-0.507				

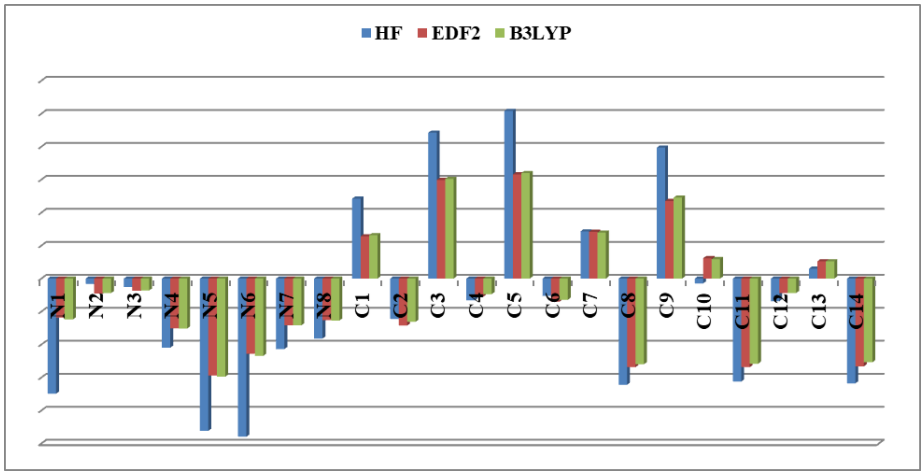

Figure 3a. Calculated Mulliken Charges Of The Atoms in MTSTA

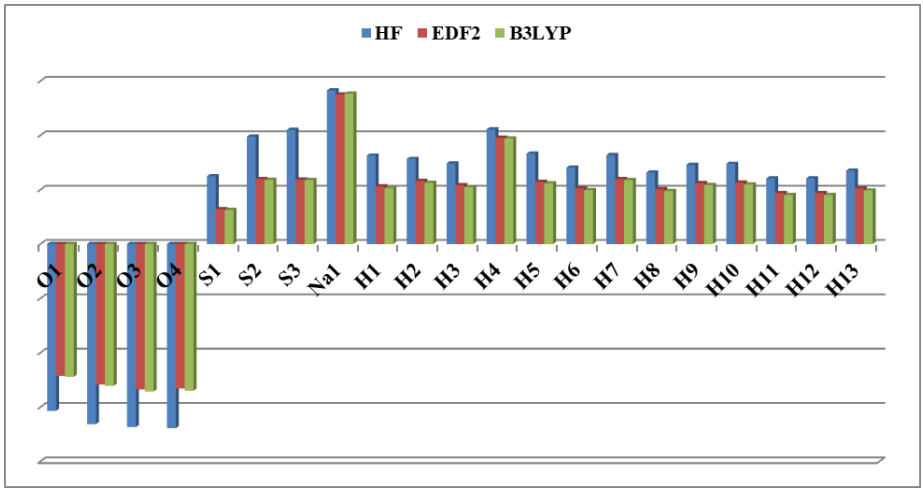

Figure 3b. Calculated Mulliken Charges Of The Atoms in MTSTA

Molecular Orbital Energies Of MTSTA

HOMO (Highest Occupied Molecular Orbital) shows the highest energy level at which an electron exist around the molecule. Just opposite, LUMO (Lowest Unoccupied Molecular Orbital) refers to the lowest energy level with no electrons. The gap between HOMO and LUMO is crucial for charge transfers that affect chemical reactions. The molecules with large energy gap are expected to be chemically inactive and they are called hard molecules. HOMO-LUMO levels also determine the basicity or acidity of a certain molecule.

Table 5. Molecular Orbital Energies Of MTSTA

Molecular Orbitals	HF-321G	EDF2 6-31G*	B3LYP 6-31G*
LUMO+1	2.00	-1.20	-1.10
LUMO	0.70	-1.40	-1.30
HOMO	-8.80	-5.80	-6.00
HOMO-1	-9.30	-6.00	-6.20
HOMO-2	-9.90	-6.40	-6.60
HOMO-3	-10.40	-6.50	-6.70
HOMO-4	-10.90	-6.80	-7.00
HOMO-5	-10.90	-6.90	-7.10
HOMO-6	-11.00	-7.00	-7.20
HOMO-7	-11.20	-7.40	-7.60
HOMO-8	-11.60	-7.60	-7.80
HOMO-9	-11.80	-7.70	-7.80

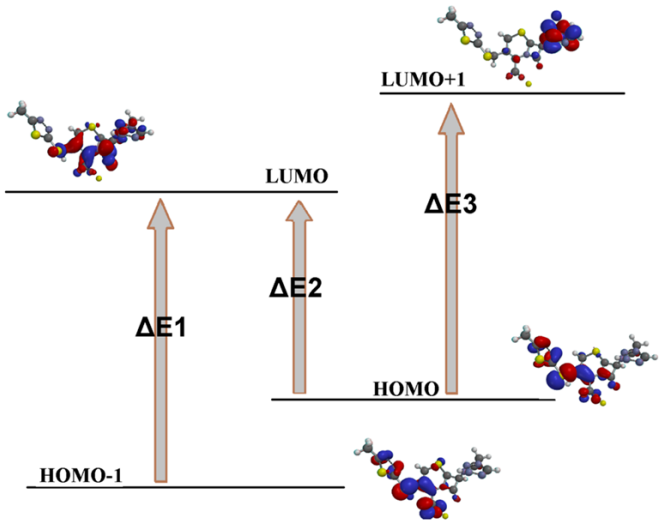

Figure 4. Electron transfers and Corresponding E values for MTSTA

In the molecule MTSTA the energy gap between HOMO&LUMO is 9.50/4.40/4.90 (lets say about 5.0) which means our molecule can be supposed to be a "soft" molecule (Table 6). The larger the gap is, the higher kinetic stability the molecule has. Molecule's hardness and softness can be calculated via equation 2a and 2b (Sahin et al., 2015, Pearson, 2005).

$$\eta=(\text{ELUMO}-\text{EHOMO}) \quad (2a)$$

$$S=1/\eta \quad (2b)$$

NMR Spectra

NMR is one of the most used and practical method for understanding the structure of a molecule. Chemical Shift values of the atoms, especially the H atoms reveal the neighborhood and bonding of atoms in a molecule quite clearly.

In the molecule MTSTA chemical Shift values are as tabulated in table 7.

Table 7. Calculated NMR Shift Values for Atoms in MTSTA

Atom	HF-321G	EDF2 6-31G*	B3LYP 6-31G*	Atom	HF-321G	EDF2 6-31G*	B3LYP 6-31G*
C1	140.41	144.84	147.35	**H1**	9.28	8.37	7.91
C2	46.56	51.02	51.95	**H2**	5.50	5.43	4.94
C3	159.53	167.24	165.72	**H3**	4.81	4.83	4.36
C4	53.96	58.83	59.88	**H4**	5.26	6.92	6.65
C5	168.50	163.98	169.09	**H5**	5.81	6.39	5.41
C6	46.99	58.29	58.89	**H6**	4.32	5.15	4.92
C7	121.41	134.22	134.34	**H7**	3.62	4.58	4.04
C8	19.27	25.95	26.64	**H8**	2.72	3.53	3.36
C9	178.55	170.75	175.65	**H9**	3.51	4.70	4.23
C10	115.18	117.40	119.12	**H10**	3.67	4.19	3.82
C11	30.61	35.97	37.30	**H11**	2.66	2.71	2.50
C12	166.12	175.21	173.55	**H12**	2.66	2.71	2.50
C13	153.70	163.61	164.84	**H13**	2.66	2.71	2.50
C14	15.67	15.55	16.34				

According to the values:

- Terminal H atoms have appeared as 2.66, 2.71, 250 ppm according to the method.The molecules structure with lots of Ns and Ss gave this result.
- H1which belongs to tetrazole ring is the most acidic proton of the molecule with shift values at 9-8 ppm.
- Mostly Shift values for the H atoms have found to be bigger than other molecules. Because molecule has a number of S, N and O atoms.
- The value about 15 ppm refers terminal C atom (C14)

- The biggest shift values belong to the C1,C5, C7, C9, C10, C12 and C13. These Cs are surrounded by N atoms, and double bonds.

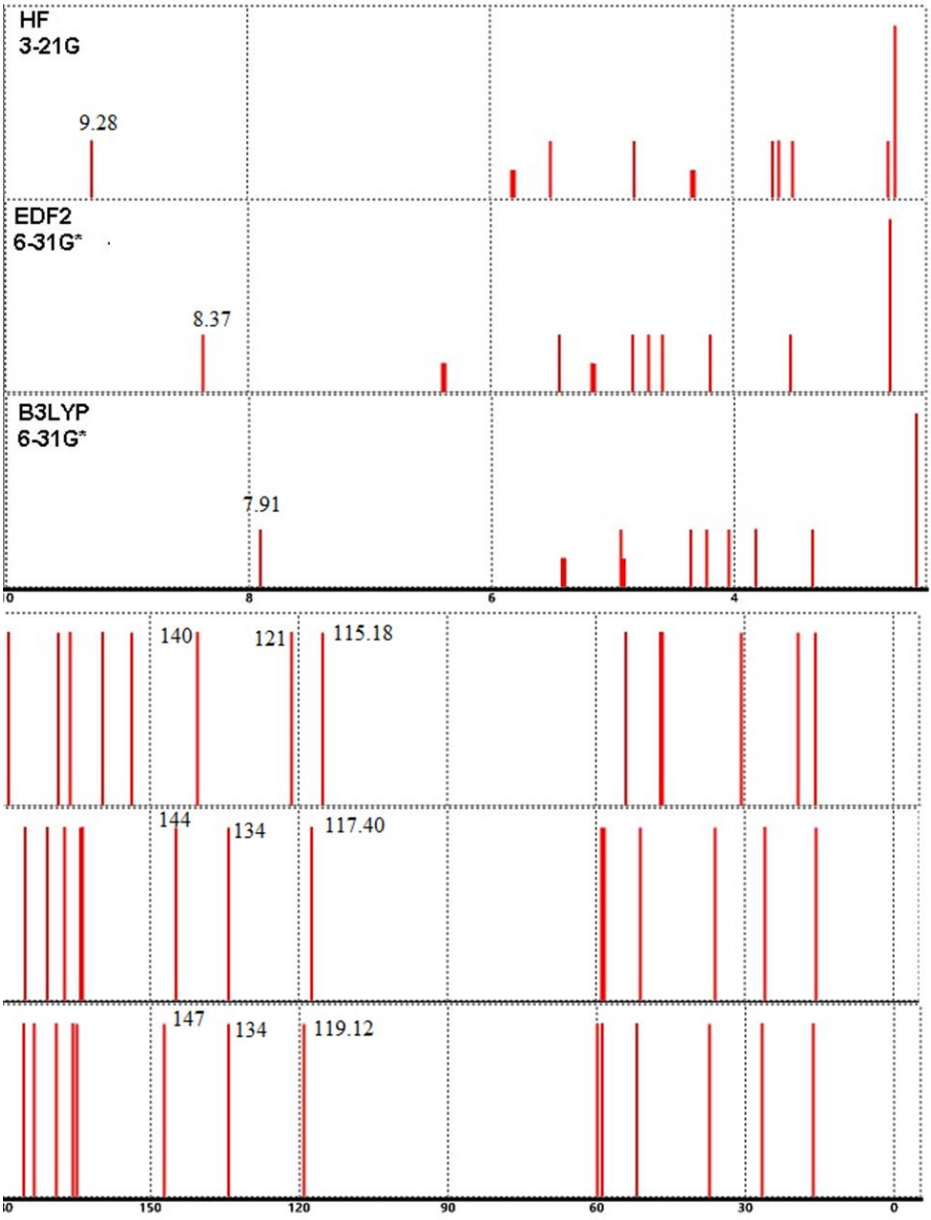

Figure 4. Calculated 1H and 13C NMR Spectra for MTSTA

CONCLUSIONS

In conclusion, the compound MTSTA (5-Methyl-1,3,4-thiadiazol-2-yl-sulfanylmethyl-8-oxo-7-[[2-(tetrazol-1-yl)acetyl]amino]-5-thia-1-azabicyclo[4.2.0]oct-2-ene-2-carboxylic acid) holds great promise in the field of medicinal chemistry and drug discovery. Through its unique structural features and diverse functional groups, MTSTA exhibits potential as an antibacterial agent, particularly as a cephalosporin antibiotic.

The computational studies conducted on MTSTA have provided valuable insights into its molecular properties, mechanisms of action, and structure-activity relationships. Researchers have been able to visualize and analyze its three-dimensional structure, gaining a deeper understanding of its shape, stability, and interactions with biological targets. These computational approaches have also elucidated the key factors contributing to its antibacterial activity, paving the way for the design and optimization of more potent derivatives.

Furthermore, the studies on MTSTA have highlighted its potential applications in the treatment of bacterial infections. Its interactions with enzymes involved in cell wall synthesis, along with its structural modifications, offer avenues for overcoming bacterial resistance and developing novel cephalosporins with improved efficacy and reduced resistance development.

Moving forward, further experimental investigations and clinical trials are warranted to validate the findings from computational studies and assess the pharmacological potential of MTSTA. Additionally, future research should focus on exploring its toxicity profile, pharmacokinetics, and formulation strategies to facilitate its translation into therapeutic applications.

In conclusion, MTSTA represents an exciting prospect in the quest for new antibiotics. The integration of computational analysis with experimental studies has shed light on its molecular characteristics and potential applications. With continued research and development, MTSTA holds the promise of addressing the challenges posed by antibiotic resistance and making a significant impact in the field of infectious disease treatment.

REFERENCES

Awasthi B. P., Lee H, &Jeong B. S.(2022) Synthesis of Pyridoxine-Derived Dimethylpyridinols Fused with Aminooxazole, Aminoimidazole, and Aminopyrrole. Molecules. Mar 23;27(7):2075. doi: 10.3390/molecules27072075. PMID: 35408475; PMCID: PMC9000659.

Barupal D. K.& Fiehn O. (2019) Generating the Blood Exposome Database Using a Comprehensive Text Mining and Database Fusion Approach. Environ Health Perspect. Sep;127(9):97008. doi: 10.1289/EHP4713. Epub 2019 Sep 26. PMID: 31557052; PMCID: PMC6794490.

Chen, Y., Ai, L., Guo, P. Huang, H., Wu, Z., Liang X. &Liao, K., (2018) Molecular characterization of multidrug resistant strains of Acinetobacter baumannii isolated from pediatric intensive care unit in a Chinese tertiary hospital. BMC Infect Dis 18, 614. https://doi.org/10.1186/s12879-018-3511-0

Becke A. D., (1993), Density-functional thermochemistry. III. The role of exact exchange, Jounal of Chemical Physics 98, 5648-5652.

Erdogdu Y., Güllüoğlu M.&Kurt M., (2009), DFT, FT-Raman, FT-IR and NMR studies of 2-fluorophenylboronic acid, Journal of Raman Spectroscopy, 40(11), 1615-1623,

Hehre, W., J., (2014) SPARTAN'14, , Wavefunction Inc. Irvine CA, USA

Hehre W. J., (2014), "SPARTAN'14 Tutorial and User's Guide", Wavefunction, Inc.

Jensen F., (2017), Introduction to Computational Chemistry, Wiley

Kunduracıoğlu, A. (2021). (4-Carbamoylphenyl)Boronic Acid: A DFT Study On The Structural And Spectral Properties . Caucasian Journal of Science , 8 (2) , 209-223 . DOI: 10.48138/cjo.972212

Lee C., Yang W.& Parr R.G., (1998), Development of the Colle-Salvetti correlation-energy formula into a functional of the electron density, Physical Review B - Condensed Matter and Materials Physics 37 785-799

Mittal, R., Kumar, A., & Awasthi, S. K. (2021). Practical scale up synthesis of carboxylic acids and their bioisosteres 5-substituted-1 H-tetrazoles catalyzed by a graphene oxide-based solid acid carbocatalyst. RSC advances, 11(19), 11166-11176.

Mittal, R., & Awasthi, S. K. (2019). Recent advances in the synthesis of 5-substituted 1H-tetrazoles: A complete survey (2013–2018). Synthesis, 51(20), 3765-3783.

Murakami K, Takasuka M, Motokawa K,& Yoshida T. (1981) 1-Oxacephalosporins: enhancement of beta-lactam reactivity and

antibacterial activity. J Med Chem. Jan;24(1):88-93. doi: 10.1021/jm00133a018. PMID: 6451699.

Pearson R. G., (2005), Chemical hardness and density functional theory, Chemical Science Journal, 117(5), 369-377,

Şahin Z. S., Kaya Kantar G., Şaşmaz S.,& Büyükgüngör O., (2015), Synthesis, molecular structure, spectroscopic analysis, thermodynamic parameters and molecular modeling studies of (2-methoxyphenyl)oxalate, Journal of Molecular Structucture, 1087, 104-112.

Silverstein R.M., Webster F.X., &Kıemle D.J., (2005), Spectrometric Identification of Organic Compounds 7th Ed. John Wiley Sons INC.

Chapter 6

Synthesis and Characterization of Waugh Type $[MnMo_9O_{32}]^{6-}$ Cluster with the $[M(en)_3]^{n+}$ Cation (M=Cr, Mn, Co, Ni)

Hülya AVCI ÖZBEK[1]

[1] Arş. Gör. Dr.; Manisa Celal Bayar University Faculty of Sciences & Liberal Arts Department of Chemistry. hulya.avci@cbu.edu.tr. ORCID ID: https://orcid.org/0000-0003-1508-2558

ABSTRACT

Four new Waugh-type polyoxometalates $[Co(en)_3]_2[MnMo_9O_{32}]\cdot 15H_2O$ (**1**), $[Ni(en)_3]_3[MnMo_9O_{32}]\cdot 15H_2O$ (**2**), $[Cr(en)_3]_2[MnMo_9O_{32}]\cdot 15H_2O$ (**3**), $[Mn(en)_3]_3[MnMo_9O_{32}]\cdot 15H_2O$ (**4**) have been synthesized and characterized by FT-IR spectroscopy, ICP-MS, elemental and thermogravimetric analysis.

Keywords: Manganese, Molybdenum, Polyoxometalate, Waugh-type.

INTRODUCTION

Polyoxometalates (POMs) are molecular early metal oxide anions based on high valence transition metals (M usually Mo, W, V). In recent years, the outstanding chemical and physical properties of POMs (acidity, redox activity, photoactivity, etc.) have attracted the attention of chemists and materials scientists due to their applications in important fields such as biology, catalysis, medicine, materials chemistry and topology (Avcı Özbek et al., 2021:1794; Cao et al., 2021:129797; Fang et al., 2022: 2100827; Mousavi et al., 2022:110074; Streb et al., 2019: 20170177; Wang et al., 2015:4893).

Most POM clusters can be divided into several types, such as Keggin $[XM_{12}O_{40}]^{n-}$ (X = As, Ge, P, Si, M = Mo, V, W) (Chen et al., 2019:22270; Ruiz-Bilbao et al., 2022:2428), Dawson $[X_2M_{18}O_{62}]^{6-}$ (X = As, Ge, P, Si, M = Mo) (Yaqub et al., 2022:149), Anderson $[XM_6O_{18}]^{n-}$ (X = Al, I, M Te, = Mo, W) (Chen et al., 2017:15331; Avcı Özbek, 2023:315) Silverton $[XM_{12}O_{42}]^{n-}$ (Wan et al., 2021:2172; Zhao et al., 2021: 615595), Waugh $[XM_9O_{32}]^{n-}$ (Gong et al., 2016:834; Liang et al., 2014: 1735; Tan et al., 2009:10940; Tan et al., 2012:1111; Zammel et al. 2015:1693) and Lindqvist $[M_6O_{19}]^{n-}$ (M = Mo, Nd, Ta, W) (Li et al., 2020:10944; Zhao et al., 2021:121). Among these various polyoxometalates, Waugh-type has gained greater importance in recent studies because it has multiple coordination active centers (Cheng et al., 2008:977). It is interesting to note that since Waugh first prepared the $[MnMo_9O_{32}]^{6-}$ heteropolyanion in 1954 and named it the Waugh-type structure (Figure 1.), it is the only Waugh-type heteropolyanion that has been structurally characterised so far (Waugh et al., 1954:438).

Figure 1. Waugh-type structure in polyhedral representation (Omwoma et al., 2014:58)

There are currently a number of well-defined and characterized compounds based on the $[MnMo_9O_{32}]^{6-}$ cluster anion, some of which show activity in catalytic reactions, such as: The catalytic activity of $H_{12}[MnMo_9O_{32}(KO)_6]$ in the dehydration of cyclohexanol was determined in the study of Wu et al. (Wu et al., 2007:213). The compound $K_{0.5}(NH_4)_{5.5}[MnMo9O_{32}]\cdot 6H_2O$ has been

studied in homogeneous phenol hydroxylation and 30% hydrogen peroxide was used as oxidant (Lin et al., 2000:113). NiMo catalysts were prepared using Waugh-type NiMo heteropolymers as active phase precursors and their activity in the reaction of hydrodesulfurization of dibenzothiophene was investigated (Liang et al., 2014:1735).

In this work four new Waugh-type polyoxometalates $[Co(en)_3]_2[MnMo_9O_{32}]\cdot 15H_2O$ (**1**), $[Ni(en)_3]_3\ [MnMo_9O_{32}]\cdot 15H_2O$ (**2**), $[Cr(en)_3]_2\ [MnMo_9O_{32}]\cdot 15H_2O$ (**3**), $[Mn(en)_3]_3\ [MnMo_9O_{32}]\cdot 15H_2O$ (**4**) have been synthesized and characterized by FT-IR spectroscopy, ICP-MS, elemental and thermogravimetric analysis.

EXPERIMENTAL

Materials and Methods

- All chemicals used in this study were all of analytical grade purchased from commercial sources and used without purification.
- $K_3(NH_4)_3[MnMo_9O_{32}]$ was synhthesized as described by literature and characterized by FT-IR (Zammel et al. 2022:3687).
- C, H and N elemental analyses were performed on a LECO-932 CHNS elemental analyser.
- Ni, Co, Cr, Cu, Mn and Mo were determined by ICP-MS Agilent Technology 7700.
- The FT-IR spectra were obtained on a Perkin Elmer LR 64912 C spectrometer in the range 400-4000 cm^{-1} with KBr pellet.
- Thermogravimetric analysis (TGA) was performed on a Hitachi Exstar TG/DTA 7300 instrument under flowing N_2 with a heating rate of 10 ^oC/min at 25 and 800 ^oC.

Synthesis of Compounds

$[Co(en)_3]_2[MnMo_9O_{32}]\cdot 15H_2O$ (1)

Two solutions were prepared separately. Solution 1: $K_3(NH_4)_3[MnMo_9O_{32}]$ (0.176 g, 0.1 mmol) was dissolved in hot water (15 mL) under stirring. Solution 2: $CoCl_2\cdot 6H_2O$ (0.475 g, 2 mmol) was dissolved in water (5 mL) and 0.4 mL ethylenediamine (6 mmol) was added. Solution 2 added to the solution 1. The resulting mixture was kept at 60 ^oC and acidified with concentrated H_2SO_4. The pH value of the mixture was adjusted to approximately 2.00. Afterwards the mixture stirred 1-2 h at this temperature and then filtered, The product washed with H_2O and finally dried under a vacuum at 50 ^oC. Yield: 60%. FT-IR (KBr

pellets): υ = 485 (m), 674 (m), 794 (m), 897 (m), 936 (m), 1104 (m), 1056 (s), 1118 (m), 1151 (m), 1284 (m), 1320 (m), 1365 (m), 1397 (m), 1460 (s), 1588 (m), 1629 (m), 3435 (w) cm^{-1}. Elem. Anal. Calcd. $C_{12}H_{78}N_{12}Co_2MnMo_9O_{47}$ (2179,06 g/mol): C, 6.61, N, 7.71, H, 3.61, Mo, 39.63, Mn, 2.52, Co, 5.41. found: C, 6.11, N, 6.83, H, 2.60, Mo, 37.51, Mn, 1.78, Co, 5.11. TGA (loss of 15 H_2O): calcd. 12.40 %, found 12.74%.

$[Ni(en)_3]_3[MnMo_9O_{32}]\cdot 15H_2O$ (2)

Two solutions were prepared separately. Solution 1: $K_3(NH_4)_3[MnMo_9O_{32}]$ (0.176 g, 0.1 mmol) was dissolved in hot water (15 mL) under stirring. Solution 2: $NiCl_2\cdot 6H_2O$ (0.635 g, 2.67 mmol) was dissolved in water (5 mL) and 0.54 mL ethylenediamine (8 mmol) was added. Solution 2 added to the solution 1. The resulting mixture was kept at 60 ºC and acidified with concentrated H_2SO_4. The pH value of the mixture was adjusted to approximately 2.00. Afterwards the mixture stirred 1-2 h at this temperature and then filtered, The product washed with H_2O and finally dried under a vacuum at 50 ºC. Yield: 20%. FT-IR (KBr pellets): υ = 427 (m), 491 (m), 539 (m), 592 (m), 680 (m), 892 (m), 931 (s), 1030 (s), 1102 (m), 1147 (m), 1280 (m), 1323 (m), 1467 (m), 1508 (m), 1582 (m), 1629 (m), 3437 (w) cm^{-1}. Elem. Anal. Calcd. $C_{18}H_{102}N_{18}Ni_3MnMo_9O_{47}$ (2417,57 g/mol): C, 8.94, N, 10.43, H, 4.25, Mo, 35.72, Mn, 2.27, Ni, 7.28. found: C, 8.76, N, 9.88, H, 4.47, Mo, 35.27, Mn, 1.82, Ni, 6.47. TGA (loss of 15 H_2O): calcd. 11.18 %, found 11.13%.

$[Cr(en)_3]_2[MnMo_9O_{32}]\cdot 15H_2O$ (3)

This compound was prepared similarly to **1**, with $CrCl_3\cdot 6H_2O$ instead of $CoCl_2\cdot 6H_2O$.Yield: 70%. FT-IR (KBr pellets): υ = 517 (m), 868 (m), 1053 (m), 1128 (m), 1288 (m), 1371 (m), 1401 (m), 1452 (m), 1507 (m), 1622 (m), 3400 (w) cm^{-1}. Elem. Anal. Calcd. $C_{12}H_{78}N_{12}Cr_2MnMo_9O_{47}$ (2165,19 g/mol): C, 6.66, N, 7.76, H, 3.63, Mo, 39.88, Mn, 2.54, Ni, 4.80. found: C, 6.39, N, 7.95, H, 3.99, Mo, 39.00, Mn, 1.54, Ni, 3.79. TGA (loss of 15 H_2O): calcd. 12.40 %, found 12.34%.

$[Mn(en)_3]_3[MnMo_9O_{32}]\cdot 15H_2O$ (4)

This compound was prepared similarly to **2**, with $MnCl_2\cdot 2H_2O$ instead of $NiCl_2\cdot 6H_2O$.Yield: 25%. FT-IR (KBr pellets): υ = 537 (m), 595 (m), 755 (m), 820 (m), 857 (m), 930 (m), 1068 (m), 1114 (m), 1368 (m), 1508 (m), 1623 (m), 3414 (w) cm^{-1}. Elem. Anal. Calcd. $C_{18}H_{102}N_{18}Mn_4Mo_9O_{47}$ (2406,30 g/mol): C, 8.98, N, 10.48, H, 4.27, Mo, 35.88, Mn, 9.13. found: C, 8.88, N, 8.75, H, 4.17, Mo, 34.91, Mn, 9.00. TGA (loss of 15 H_2O): calcd. 11.23 %, found 11.52%.

RESULTS AND DISCUSSIONS

Compounds $[Co(en)_3]_2$ $[MnMo_9O_{32}]\cdot 15H_2O$ (**1**), $[Ni(en)_3]_3$ $[MnMo_9O_{32}]\cdot 15H_2O$ (**2**), $[Cr(en)_3]_2$ $[MnMo_9O_{32}]\cdot 15H_2O$ (**3**), $[Mn(en)_3]_3$ $[MnMo_9O_{32}]\cdot 15H_2O$ (**4**) were synthesized by using $K_3(NH_4)_3[MnMo_9O_{32}]$, $CoCl_2\cdot 6H_2O$/ $NiCl_2\cdot 6H_2O$/ $CrCl_3\cdot 6H_2O$/ $MnCl_2\cdot 2H_2O$ and ethylenediamine (Figure 2). The pH is an important factor in the formation of Waugh-type compounds. For 1-4, the best pH is 2. The measured elemental analyses (C, H, N) and ICP-MS (Mo, Mn, Co, Ni, Cr) data of the new compounds **1-4** are in good agreement with the computed values. In addition, experimental elemental analysis results and other spectroscopic data (FT-IR and TGA) support the structures of the compounds. Thus, the structures of these newly synthesised compounds were found to be similar to the previously reported compounds (Gavrilova et al., 2005:427; Kaziev et al., 2007:840; Lin et al., 2000:113; Quinones et al., 2007:412; Tan et al., 2000:1418).

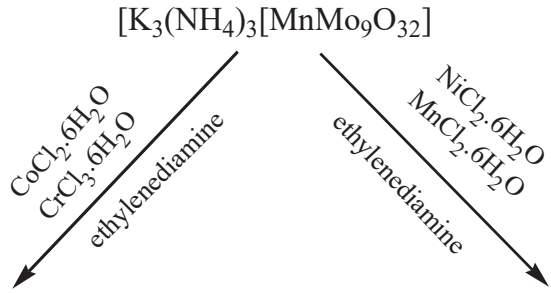

$[Co(en)_3]_2[MnMo_9O_{32}]\cdot 15H_2O$ **(1)** $[Ni(en)_3]_3[MnMo_9O_{32}]\cdot 15H_2O$ **(2)**

$[Cr(en)_3]_2[MnMo_9O_{32}]\cdot 15H_2O$ **(3)** $[Mn(en)_3]_3[MnMo_9O_{32}]\cdot 15H_2O$ **(4)**

Figure 2. Synthesis of **1-4**

As shown in Figure 3, the FT-IR spectra of **1-4** show similar adsorption peaks, indicating the similar chemical bonds. Compounds **1-4** show characteristic FT-IR bands with the POMs in the $[MnMo_9O_{32}]^{6-}$ structure in the literature. At 857-936 cm^{-1}, vibrations of terminal Mo=O bonds appear as a doublet. The bands in the region of 421-595 cm^{-1} can be attributed to vibrations of Mo-O-Mo bridges. The adsorption band at 542 (**1**), 539 (**2**, **3**), 537 (**4**) cm^{-1} is assigned to Mn-O respectively. The NH_2 and CH_2 vibrations in the ethylenediamine ligand can be attributed to the peaks at 1700-1400 cm^{-1}. The FT-IR spectra also show bands at 3400-3435 cm^{-1} associated with the vibrational modes of water molecules and hydroxyl groups. The data obtained

from FT-IR analyses are in agreement with previously reported studies (Gavrilova et al., 2005:427; Kaziev et al., 2007:840; Lin et al., 2000:113; Quinones et al., 2007:412).

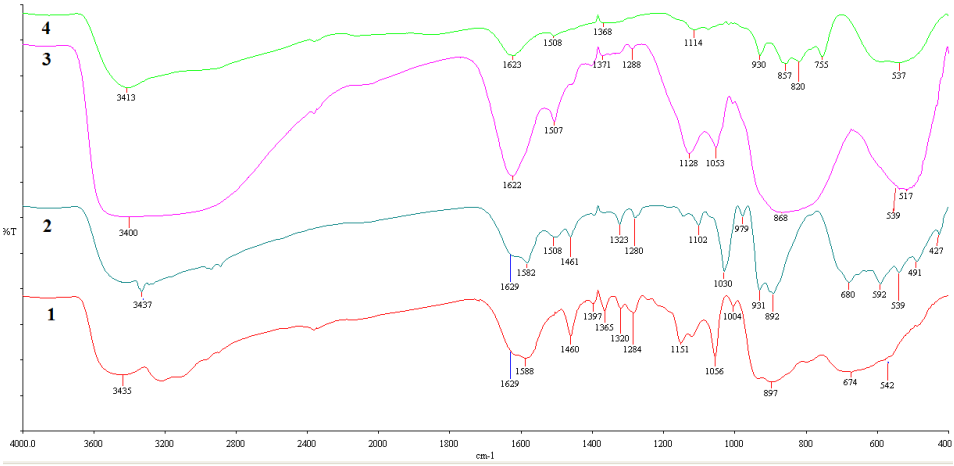

Figure 3. FT-IR spectra of **1-4**

The thermogravimetric analyses (TGAs) have been studied in the temperature range from 25 to 800 °C as shown in Figure 4. In the thermogram of **1,** the mass loss of 12.74% in the range of 47-180 °C is associated with the release of 15 water molecules. In **2**, a loss of 11.13% in the temperature range of 41-205 °C is attributed to the removal of 15 water molecules. Compound **3** lost 12.34% of its mass at the temperature range of 44-180 °C, which is assigned to the loss of 15 water molecules. In **4**, the weight loss of 11.52% in the range from 51 to 216 °C is associated with 15 water molecules. The data obtained as a result of TGA analyses are in agreement with both theoretical values (Table 1) and previously reported studies (Gavrilova et al., 2005:427; Kaziev et al., 2007:840; Quinones et al., 2007:412; Tan et al., 2000:1418).

Table 1. TGA analysis results for **1-4**

Compound	Losses Part	Calculated (%)	Experimental (%)	Temperature range (°C)
1	15 H_2O	12.40	12.74	47-180
2	15 H_2O	11.18	11.13	41-205
3	15 H_2O	12.40	12.34	44-180
4	15 H_2O	11.23	11.52	51-216

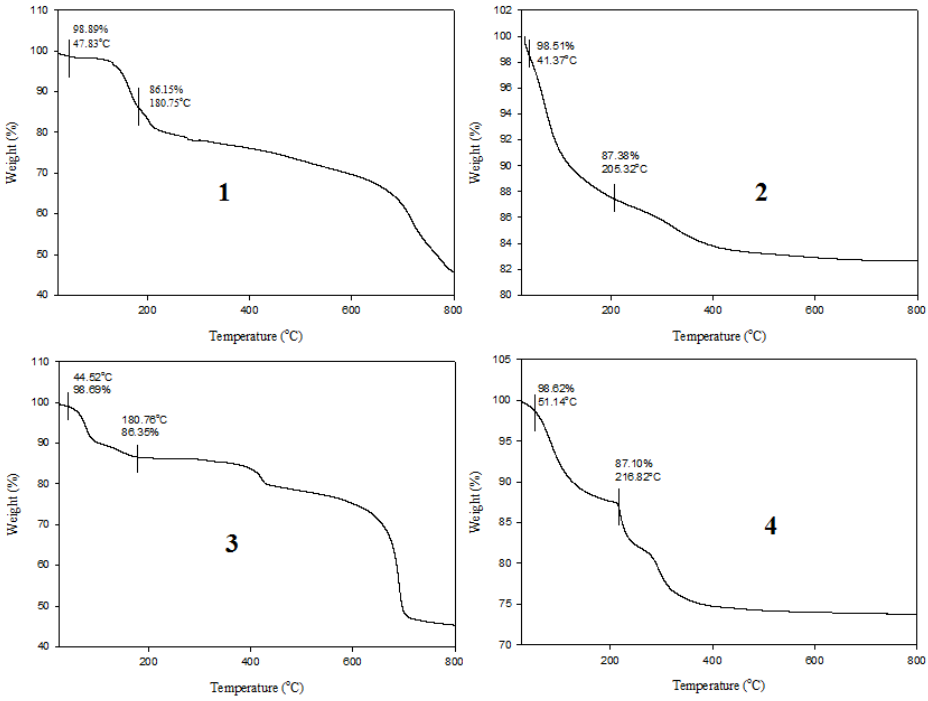

Figure 4. TGA thermograms of **1-4**

CONCLUSION

This paper reports synthesis and characterization of four new Waugh-type polyoxoanion $[MnMo_9O_{32}]^{6-}$ with the $[M(en)_3]^{n+}$ cation (M=Cr, Mn, Co, Ni). Their structures were identified using elemental analysis, FT-IR, ICP-MS and TGA.

REFERENCES

Avcı Özbek, H., Erden Kopar, E., Demirhan, F. (2021). Synthesis, structure, and antimicrobial properties of mixed-metal organometallic polyoxometalates $[Cp^*_2M_5VO_{17}]^-$ (M = Mo, W). Journal of Coordination Chemistry. 74(11), 1794-1809.

Avcı Özbek, H. (2023). Synthesis and Characterization of New Anderson-Type Polyoxometalates: $[M((1,10\text{-phen})(OH)_x]_3[Cr(OH)_6Mo_6O_{18}]\cdot 16H_2O$ (M=Cr, Mn, Co, Ni, Cu; x=1,2). Journal of the Turkish Chemical Society Section A: Chemistry, 10(2), 315-324.

Cao, X., Liu, J., Wang, Y. (2021). Efficient green catalysis for the production of n-butyl acetate over Keggin-type $Sn_{x/4}H_{3-x}PW_{12}O_{40}$. Materials Letters, 294, 129797.

Chen, Y., Zhang, C., Yang, C., Zhang, J., Kai, Z., Fang, Q., Gao, L. (2017). Waugh type $[CoMo_9O_{32}]^{6-}$ cluster with atomically dispersed Co^{3+} derives from Anderson type $[CoMo_6O_{24}]^{3-}$ for photocatalytic oxygen molecule activation. Nanoscale, 9, 15332–15339.

Chen, Y., Tian, S., Qin, Z., Zhang, J., Cao, Y., Chu, S., Lu, L., Li, G. (2019). $[MW_{12}O_{44}]$ cluster: unprecedented central heteroatoms atomically dispersed in eight coordination state bridging 1:12 polyoxometalate family of Keggin and Silverton Nanoscale, 11, 22270-22276.

Cheng, H., Ren, Y., Liu, S., Xie, L. (2008). Syntheses, Structures and Spectroscopic Characterization of Extended Waugh-Type Polyoxometalates with Metal Ions as Linkers. Zeitschrift für anorganische und allgemeine Chemie, 634(5), 977-980.

Fang, Y., Zhang, Q., Li, F., Xu, L. (2022). Exploring Inorganic Hole Collection Materials from Mixed- Metal Dawson-Type Polyoxometalates for Efficient Organic Photovoltaic Devices. Solar RRL, 6, 2100827.

Gavrilova, L.O., Molchanov, V. N. (2005). Complexation of Heteropoly Anion $[MnMo_9O_{32}]^{6-}$ with Lanthanide Ions. Russian Journal of Coordination Chemistry, 31, (6), 401–409.

Gong, P., Li, Y., Zhai, C., Jie, L., Zhao, J. (2016). Syntheses, structural characterization and photophysical properties of two series of rareearth-isonicotinic-acid containing Waugh-type manganomolybdates. CrystEngComm, 19, 834–852.

Holguin Quinones, S., Kaziev, G.Z., Oreshkina, A.V., de Ita, A., Zavodnik, V. E., Glazunova, Y.T. (2007). Synthesis, Thermal Analysis, IR Spectra, and Crystal Structure of Ammonium 9-Molybdomanganate. Russian Journal of Coordination Chemistry, 33(6), 412–416.

Li, Y.H., Wang, Z.Y., Ma, B., Xu, H., Zang, S.Q., Mak, T. (2020) Self-Assembly of Thiolate-Protected Silver Coordination Polymers Regulated by POMs. Nanoscale, 12, 10944–10948.

Lin, S., Zhen, Y., Wang, S.M., Dai, Y.M. (2000). Catalytic activity of $K_{0.5}(NH_4)_{5.5}[MnMo9O_{32}]\cdot 6H_2O$ in phenol hydroxylation with hydrogen peroxide. Journal of Molecular Catalysis A: Chemical, 156, 113–120.

Liang, J., Liu, Y., Zhao, J., Li, X., Liu, C. (2014) Waugh-Type NiMo Heteropoly compounds as More Effective Precursors of Hydrodesulfurization Catalyst. Catalysis Letters, 144, 1735–1744.

Kaziev, G.Z., Oreshkina, A.V., Holguin Quinones, S., Zavodnik, V. E., de Ita, A., Tripol'skaya, T.A. (2007). Manganese (II) 9-Molybdomanganate (IV), $[Mn(H_2O)_4]_3\cdot[MnMo_9O_{32}]\cdot 2H_2O$:Synthesis, Thermal Analysis, IR Spectra, and Crystal Structure. Russian Journal of Coordination Chemistry, 33(11), 826–830.

Mousavi, S.M., Hashemi, S.A., Mazraedoost, S., Chiang, W.H., Yousefi, K., Arjmand, O., Ghahramani, Y., Gholami, A., Omidifar, N., Rumjit, N.P., Salari, M., Sadrmousavi-Dizaj, A. (2022). Anticancer, antimicrobial and biomedical features of polyoxometalate as advanced materials: A review study. Inorganic Chemistry Communications, 146, 110074.

Omwoma, S., Chena, W., Tsunashima R., Song, Y.F. (2014). Recent advances on polyoxometalates intercalated layered double hydroxides: From synthetic approaches to functional material applications. Coordination Chemistry Reviews, 258-259, 58-71.

Ruiz-Bilbao, E., Pardo-Almanza, M., Oyarzabal, I., Artetxe, B., Felices, L.S., García, J.A., Seco, J.M., Colacio, E., Lezama, L., Gutiérrez-Zorrilla, J.M. (2022). Slow Magnetic Relaxation and Luminescent Properties of Mononuclear Lanthanide-Substituted Keggin-Type Polyoxotungstates with Compartmental Organic LigandsInorganic Chemistry, 61:2428–2443.

Streb, C., Kastner, K., Tucher, J. (2019) Polyoxometalates in photocatalysis. Physical Sciences Reviews, 20170177.

Tan, H., Li, Y., Chen, W., Liu, D., Su, Z., Lu, Y., Wang, E. (2009). From Racemic Compound to Spontaneous Resolution: A Linker-Imposed Evolution of Chiral $[MnMo_9O_{32}]^{6-}$-Based Polyoxometalate Compounds. Chemistry: A European Journal, 15, 10940-10947.

Tan, H., Chen, W.L., Liu, D., Yan A., Wang, E. (2011). Two new compounds with microporous constructed by Waugh-type polyoxoanion and transition metal ions. Science Chine Chemistry, 54 (9), 1418–1422.

Tan, H., Li, Y., Chen, W., Yan, A., Liu, D., Wang, E. (2009). A Series of $[MnMo_9O_{32}]^{6-}$ Based Solids: Homochiral Transferred from Adjacent Polyoxoanions to One-, Two-, and Three-Dimensional Frameworks. Crystal Growth & Design, 12, 1111−1117.

Wan, R., Liu, Z., Ma, X., Li, H., Ma, P., Zhang, C., Niu, J., Wang, J. (2021). Discovery of two Na^+-centered Silverton-type polyoxometalates $\{NaM_{12}O_{42}\}$ (M = Mo, W). Chemical Communications, 57, 2172–2175.

Wang, S.S., Yang, G.Y. (2015). Recent Advances in Polyoxometalate-Catalyzed Reactions. Chemical Reviews, 115 (11), 4893-4962.

Waugh, J.L.T., Shoemaker, D.P., Pauling, L. (1954). On the Structure of the Heteropoly Anion in Ammonium 9-Molybdomananate, $(NH_4)_6MnMo_9O_{32}\cdot 8H_2O$. Acta Crystallographica, 7, 438.

Wu, D., Xu, M., Lin, S. (2007). Synthesis, crystal structure and catalytic activity of a Waugh type polyoxometalate $H_{12}[MnMo_9O_{32}(KO)_6]$. Frontiers of Chemistry China, 2(2), 213–217.

Yaqub, A., Gilani, S.R., Bilal, S., Hayat, A., Asif, A., Siddique, S.A. (2022). Efficient Preparation of a Nonenzymatic Nanoassembly Based on Cobalt-Substituted Polyoxometalate and Polyethylene Imine- Capped Silver Nanoparticles for the Electrochemical Sensing of Carbofuran. ACS Omega, 7, 149–159.

Zammel, D., Nagazi, I., Gassoumi, B., Haddad, A. (2015). Synthesis and Characterization of a Novel Waugh-Type Polyoxometalate $K_{1.5}(NH_4)_{4.5}[MnMo_9O_{32}]\cdot 4.2H_2O$. Journal of Cluster Science, 26, 1693–1706.

Zammel, D., Nagazi, I., Gassoumi, B., Haddad, A. (2022). Hirshfeld surface investigation, crystal structure, physico‑chemical studies and chemical sensor applications of $K_3(NH_4)_3[MnMo_9O_{32}]\cdot 9H_2O$. Journal of the Iranian Chemical Society,19, 3687-3696.

Zhao, Y., Sun, X., Ji, Y., Kong, H., Wang, J. (2021). A 3D Silverton-Type Polyoxomolybdate Based on $\{PrMo_{12}O_{42}\}$: Synthesis, Structure, Photoluminescence and Magnetic Properties. Frontiers in Chemistry, 9, 615595.

Zhao, M., Zhu, X.Y., Li, Y.Z., Chang, J.N., Li, M.X., Ma, L.H., Guo, X.Y. (2022). A Lindqvist‑type $[W_6O_{19}]^{2-}$ organic–inorganic compound: synthesis, characterization, antibacterial activity and preliminary studies on the mechanism of action. Tungsten, 4, 121–129.